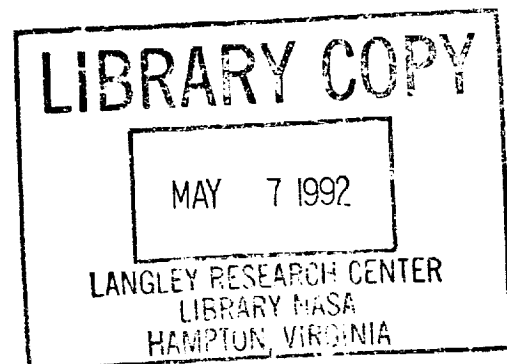


# DEVELOPMENT OF COMPOSITES TECHNOLOGY FOR JOINTS AND CUTOUTS IN FUSELAGE STRUCTURE OF LARGE TRANSPORT AIRCRAFT



## MIANNUAL TECHNICAL REPORT — NO. 2

PREPARED FOR LANGLEY RESEARCH CENTER  
CONTRACT NAS1-17701  
DRL ITEM NO. 008



Douglas Aircraft Company  
3855 Lakewood Boulevard  
Long Beach, California 90846

(NASA-CR-190175) DEVELOPMENT OF  
COMPOSITES TECHNOLOGY FOR JOINTS  
AND CUTOUTS IN FUSELAGE STRUCTURE  
OF LARGE TRANSPORT AIRCRAFT  
Semiannual Technical Report No. 2,  
1 Oct. 1984 - 31 Mar. 1985  
(Douglas Aircraft Co.) 153 p

N92-71168

Unclass

29/05 0091384

91384

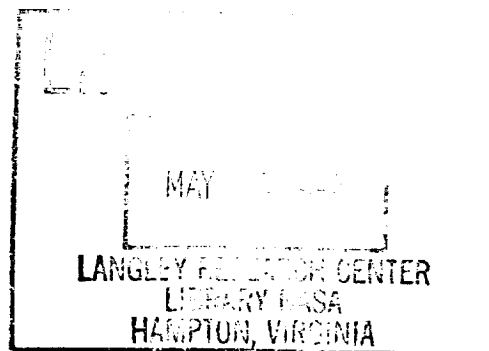
1	2	3	4	5	6	7	8	9	10	11	12	13	14	15	16	17	18	19	20	21	22	23	24	25	26	27	28	29	30	31	32	33	34	35	36	37	38	39	40	41	42	43	44	45	46	47	48	49	50	51	52	53	54	55	56	57	58	59	60	61	62	63	64	65	66	67	68	69	70	71	72	73	74	75	76	77	78	79	80	81	82	83	84	85	86	87	88	89	90	91	92	93	94	95	96	97	98	99	100	
2	1	2	3	4	5	6	7	8	9	10	11	12	13	14	15	16	17	18	19	20	21	22	23	24	25	26	27	28	29	30	31	32	33	34	35	36	37	38	39	40	41	42	43	44	45	46	47	48	49	50	51	52	53	54	55	56	57	58	59	60	61	62	63	64	65	66	67	68	69	70	71	72	73	74	75	76	77	78	79	80	81	82	83	84	85	86	87	88	89	90	91	92	93	94	95	96	97	98	99	100
3	1	2	3	4	5	6	7	8	9	10	11	12	13	14	15	16	17	18	19	20	21	22	23	24	25	26	27	28	29	30	31	32	33	34	35	36	37	38	39	40	41	42	43	44	45	46	47	48	49	50	51	52	53	54	55	56	57	58	59	60	61	62	63	64	65	66	67	68	69	70	71	72	73	74	75	76	77	78	79	80	81	82	83	84	85	86	87	88	89	90	91	92	93	94	95	96	97	98	99	100
4	1	2	3	4	5	6	7	8	9	10	11	12	13	14	15	16	17	18	19	20	21	22	23	24	25	26	27	28	29	30	31	32	33	34	35	36	37	38	39	40	41	42	43	44	45	46	47	48	49	50	51	52	53	54	55	56	57	58	59	60	61	62	63	64	65	66	67	68	69	70	71	72	73	74	75	76	77	78	79	80	81	82	83	84	85	86	87	88	89	90	91	92	93	94	95	96	97	98	99	100
5	1	2	3	4	5	6	7	8	9	10	11	12	13	14	15	16	17	18	19	20	21	22	23	24	25	26	27	28	29	30	31	32	33	34	35	36	37	38	39	40	41	42	43	44	45	46	47	48	49	50	51	52	53	54	55	56	57	58	59	60	61	62	63	64	65	66	67	68	69	70	71	72	73	74	75	76	77	78	79	80	81	82	83	84	85	86	87	88	89	90	91	92	93	94	95	96	97	98	99	100
6	1	2	3	4	5	6	7	8	9	10	11	12	13	14	15	16	17	18	19	20	21	22	23	24	25	26	27	28	29	30	31	32	33	34	35	36	37	38	39	40	41	42	43	44	45	46	47	48	49	50	51	52	53	54	55	56	57	58	59	60	61	62	63	64	65	66	67	68	69	70	71	72	73	74	75	76	77	78	79	80	81	82	83	84	85	86	87	88	89	90	91	92	93	94	95	96	97	98	99	100
7	1	2	3	4	5	6	7	8	9	10	11	12	13	14	15	16	17	18	19	20	21	22	23	24	25	26	27	28	29	30	31	32	33	34	35	36	37	38	39	40	41	42	43	44	45	46	47	48	49	50	51	52	53	54	55	56	57	58	59	60	61	62	63	64	65	66	67	68	69	70	71	72	73	74	75	76	77	78	79	80	81	82	83	84	85	86	87	88	89	90	91	92	93	94	95	96	97	98	99	100
8	1	2	3	4	5	6	7	8	9	10	11	12	13	14	15	16	17	18	19	20	21	22	23	24	25	26	27	28	29	30	31	32	33	34	35	36	37	38	39	40	41	42	43	44	45	46	47	48	49	50	51	52	53	54	55	56	57	58	59	60	61	62	63	64	65	66	67	68	69	70	71	72	73	74	75	76	77	78	79	80	81	82	83	84	85	86	87	88	89	90	91	92	93	94	95	96	97	98	99	100
9	1	2	3	4	5	6	7	8	9	10	11	12	13	14	15	16	17	18	19	20	21	22	23	24	25	26	27	28	29	30	31	32	33	34	35	36	37	38	39	40	41	42	43	44	45	46	47	48	49	50	51	52	53	54	55	56	57	58	59	60	61	62	63	64	65	66	67	68	69	70	71	72	73	74	75	76	77	78	79	80	81	82	83	84	85	86	87	88	89	90	91	92	93	94	95	96	97	98	99	100
10	1	2	3	4	5	6	7	8	9	10	11	12	13	14	15	16	17	18	19	20	21	22	23	24	25	26	27	28	29	30	31	32	33	34	35	36	37	38	39	40	41	42	43	44	45	46	47	48	49	50	51	52	53	54	55	56	57	58	59	60	61	62	63	64	65	66	67	68	69	70	71	72	73	74	75	76	77	78	79	80	81	82	83	84	85	86	87	88	89	90	91	92	93	94	95	96	97	98	99	100
11	1	2	3	4	5	6	7	8	9	10	11	12	13	14	15	16	17	18	19	20	21	22	23	24	25	26	27	28	29	30	31	32	33	34	35	36	37	38	39	40	41	42	43	44	45	46	47	48	49	50	51	52	53	54	55	56	57	58	59	60	61	62	63	64	65	66	67	68	69	70	71	72	73	74	75	76	77	78	79	80	81	82	83	84	85	86	87	88	89	90	91	92	93	94	95	96	97	98	99	100
12	1	2	3	4	5	6	7	8	9	10	11	12	13	14	15	16	17	18	19	20	21	22	23	24	25	26	27	28	29	30	31	32	33	34	35	36	37	38	39	40	41	42	43	44	45	46	47	48	49	50	51	52	53	54	55	56	57	58	59	60	61	62	63	64	65	66	67	68	69	70	71	72	73	74	75	76	77	78	79	80	81	82	83	84	85	86	87	88	89	90	91	92	93	94	95	96	97	98	99	100
13	1	2	3	4	5	6	7	8	9	10	11	12	13	14	15	16	17	18	19	20	21	22	23	24	25	26	27	28	29	30	31	32	33	34	35	36	37	38	39	40	41	42	43	44	45	46	47	48	49	50	51	52	53	54	55	56	57	58	59	60	61	62	63	64	65	66	67	68	69	70	71	72	73	74	75	76	77	78	79	80	81	82	83	84	85	86	87	88	89	90	91	92	93	94	95	96	97	98	99	100
14	1	2	3	4	5	6	7	8	9	10	11	12	13	14	15	16	17	18	19	20	21	22	23	24	25	26	27	28	29	30	31	32	33	34	35	36	37	38	39	40	41	42	43	44	45	46	47	48	49	50	51	52	53	54	55	56	57	58	59	60	61	62	63	64	65	66	67	68	69	70	71	72	73	74	75	76	77	78	79	80	81	82	83	84	85	86	87	88	89	90	91	92	93	94	95	96	97	98	99	100
15	1	2	3	4	5	6	7	8	9	10	11	12	13	14	15	16	17	18	19	20	21	22	23	24	25	26	27	28	29	30	31	32	33	34	35	36	37	38	39	40	41	42	43	44	45	46	47	48	49	50	51	52	53	54	55	56	57	58	59	60	61	62	63	64	65	66	67	68	69	70	71	72	73	74	75	76	77	78	79	80	81	82	83	84	85	86	87	88	89	90	91	92	93	94	95	96	97	98	99	100
16	1	2	3	4	5	6	7	8	9	10	11	12	13	14	15	16	17	18	19	20	21	22	23	24	25	26	27	28	29	30	31	32	33	34	35	36	37	38	39	40	41	42	43	44	45	46	47	48	49	50	51	52	53	54	55	56	57	58	59	60	61	62	63	64	65	66	67	68	69	70	71	72	73	74	75	76	77	78	79	80	81	82	83	84	85	86	87	88	89	90	91	92	93	94	95	96	97	98	99	100
17	1	2	3	4	5	6	7	8	9	10	11	12	13	14	15	16	17	18	19	20	21	22	23	24	25	26	27	28	29	30	31	32	33	34	35	36	37	38	39	40	41	42	43	44	45	46	47	48	49	50	51	52	53	54	55	56	57	58	59	60	61	62	63	64	65	66	67	68	69	70	71	72	73	74	75	76	77	78	79	80	81	82	83	84	85	86	87	88	89	90	91	92	93	94	95	96	97	98	99	100
18	1	2	3	4	5	6	7	8	9	10	11	12	13	14	15	16	17	18	19	20	21	22	23	24	25	26	27	28	29	30	31	32	33	34	35	36	37	38	39	40	41	42	43	44	45	46	47	48	49	50	51	52	53	54	55	56	57	58	59	60	61	62	63	64</																																				

**DOUGLAS AIRCRAFT COMPANY**

3855 Lakewood Boulevard Long Beach, California 90846  
TWX: 9103416842  
Telex: 674357

ACEE-34-PR-3507

30 April 1985



DRL ITEM NUMBER 008

DEVELOPMENT OF COMPOSITES TECHNOLOGY FOR  
JOINTS AND CUTOUTS IN  
FUSELAGE STRUCTURE OF LARGE TRANSPORT AIRCRAFT

SEMIANNUAL TECHNICAL REPORT - No. 2

FOR EARLY DOMESTIC DISSEMINATION

Because of its possible early commercial potential, this data, which has been developed under a U.S. Government program, is being disseminated within the United States in advance of general publication. This data may be duplicated and used by the recipient with the express limitation that it not be published. Release of this data to other domestic parties by the recipient shall be made subject to these limitations. Foreign release may be made only with prior NASA approval and appropriate export licenses. This legend shall be marked on any reproduction of this data in whole or in part. Date for general release will be three (3) years from date indicated on the document.

PREPARED FOR LANGLEY RESEARCH CENTER

CONTRACT NAS1-17701



ORIGINAL PAGE IS  
OF POOR QUALITY

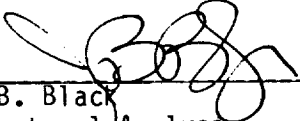


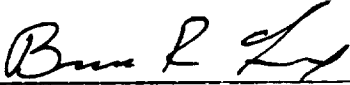
ACEE-34-PR-3507

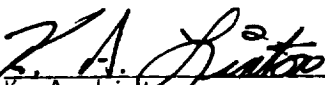
30 APRIL 1985

DRL ITEM NUMBER 008


Prepared by:

  
J. B. Black  
Structural Analysis

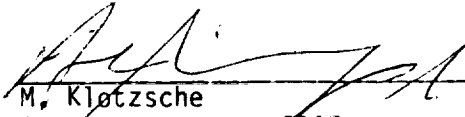
  
B. R. Fox  
Structural Design

  
K. A. Linton  
Structural Design

Approved by:

  
P. T. Sumida  
Project Manager  
Composite Fuselage Program

Approved by:

  
M. Klotzsche  
Program Manager, CRAD and  
Cooperative Technology Development

Prepared Under Contract NAS1-17701  
McDonnell Douglas Corporation

III

11 INTENTIONALLY BLANK

PRECEDING PAGE BLANK NOT FILMED



## FORWARD

This report was prepared by the Douglas Aircraft Company (DAC) of the McDonnell Douglas Corporation as part of a program to develop and demonstrate the technology required to use composites in fuselage structures of commercial and military transports by 1990. This second Semiannual Technical Report covers work accomplished between 1 October 1984 and 31 March 1985.

The program for Development of Composites Technology for Joints and Cutouts in Fuselage Structure of Large Transport Aircraft is sponsored by the National Aeronautics and Space Administration, Langley Research Center (LRC) under NASA Contract NAS1-17701. The Project Manager for DAC is Mr. P. T. Sumida. Mr. H. L. Bohon is Project Manager for NASA, LRC. The Technical Representative for NASA, LRC is Mr. A. J. Chapman.





## CONTENTS

Section		Page
1	INTRODUCTION . . . . .	1
2	SUMMARY. . . . .	5
3	DESIGN OPTIMIZATION . . . . .	7
	3.1 Design Development . . . . .	7
	Fuselage Barrel Description . . . . .	7
	Design Approach . . . . .	7
	Fuselage Barrel Design . . . . .	10
	Joints and Cutouts . . . . .	21
	Test Drawing Preparation . . . . .	32
	3.2 Design Methodology . . . . .	39
	Joints . . . . .	44
	Cutouts . . . . .	77
4	PROCESS DEVELOPMENT AND FABRICATION . . . . .	93
	4.1 Process Development . . . . .	93
	Materials . . . . .	93
	Testing . . . . .	93
	Fabrication of Group A, B and C Specimens . . . . .	99
	Fabrication and Process Verification . . . . .	102
	4.2 Tool Design and Fabrication . . . . .	106
	Shear/Interaction Panels . . . . .	106
	Demonstration Panel . . . . .	110
	4.3 Test Article Fabrication . . . . .	113
5	TECHNOLOGY DEMONSTRATION . . . . .	115
	5.1 Development Test . . . . .	115
	Group A Specimens . . . . .	115
	Group B Specimens . . . . .	125
6	REFERENCES . . . . .	129
	APPENDIX A . . . . .	A1



FIGURE		PAGE
1	PROGRAM SCHEDULE	3
2	BASELINE AIRCRAFT AND BARREL SECTION	8
3	COMPOSITE SHELL DESIGN	8
4	FUSELAGE SKIN LAYUPS	12
5	LONGERON CONFIGURATIONS	13
6	REINFORCED LONGERON LAYUPS	15
7	STATION 1109 MARGINS OF SAFETY	16
8	STATION 979 MARGINS OF SAFETY	17
9	FRAME AND SHEAR TEE	18
10	SHEAR TEE DESIGNS	18
11	INJECTION MOLDED SHEAR CLIP	20
12	FRAME/LONGERON INTERSECTION	20
13	JOINT STRENGTH POSSIBILITIES	22
14	DAMAGE TOLERANCE AT A JOINT	22
15	LONGITUDINAL SPLICE CONFIGURATION	25
16	TRANSVERSE SKIN SPLICE	25
17	TRANSVERSE SKIN/LONGERON SPLICE	26
18	LONGERON SPLICE CROSS SECTION	26
19	PASSENGER WINDOW BELT	28
20	DISCONTINUOUS LONGERON DETAILS	29
21	WINDOW KEEPER AND CONTINUOUS LONGERON	30
22	PASSENGER DOOR SUBSTRUCTURE	31
23	PASSENGER SKIN REINFORCEMENT	33
24	PASSENGER DOOR CUTOUT DETAILS	34
25	TRANSVERSE SPLICE SHEAR INTERACTION PANEL	35
26	PASSENGER WINDOW BELT SHEAR INTERACTION PANEL	36

LIST OF FIGURES (Continued)

FIGURE		PAGE
27	BEARING BYPASS CURVES FOR DOUBLE SHEAR, LAYUP #2 3/16 PROTRUDING HEAD FASTENERS	45
28	BEARING BYPASS CURVE FOR SINGLE SHEAR, LAYUP #2 3/16 PROTRUDING HEAD FASTENERS ( $\beta = .15$ )	45
29	BEARING BYPASS CURVES FOR DOUBLE SHEAR, LAYUP #3 3/16 PROTRUDING HEAD FASTENERS	46
30	BEARING BYPASS CURVES FOR DOUBLE SHEAR, LAYUP #4 3/16 PROTRUDING HEAD FASTENERS	46
31	SINGLE SHEAR BEARING DISTRIBUTION	47
32	CORRELATION OF SINGLE SHEAR BEARING BYPASS CURVE WITH TEST RESULTS	49
33	JOINT STRENGTH VERSUS BOLT SPACING FOR LAMINATE #4	50
34	JOINT STRENGTH VERSUS BOLT SPACING FOR LAMINATE #2	51
35	JOINT STRENGTH VERSUS BOLT SPACING FOR LAMINATE #3	53
36	FASTENER FLEXIBILITY MEASUREMENT	55
37	SINGLE LOAD/DEFLECTION DEVICE	58
38	DOUBLE SHEAR DEVICE	59
39	DOUBLE SHEAR DEVICE	60
40	LOAD/DEFLECTION CURVE, DOUBLE SHEAR TENSION, LAMINATE #2 (25,50,25)	61
41	LOAD/DEFLECTION CURVE, SINGLE SHEAR TENSION, LAMINATE #2 (25,50,25)	62
42	LOAD/DEFLECTION CURVE, DOUBLE SHEAR TENSION, LAMINATE #3 (60,20,20)	63
43	LOAD/DEFLECTION CURVE, DOUBLE SHEAR TENSION, LAMINATE #4 (33,33,33)	64
44	LOAD/DEFLECTION CURVE, SINGLE SHEAR TENSION, LAMINATE #2 (25,50,25), COUNTERSUNK	65
45	FINITE ELEMENT MODEL FOR DETERMINING $C_p$ and $C_{sfem}$	66
46	FINITE ELEMENT MODEL FOR A COUNTERSUNK, SINGLE SHEAR CONNECTION	69
47	COMPARISON OF TENSION AND COMPRESSION JOINTS	70
48	COMPRESSION JOINT TEST RESULTS - LAMINATE #2	71

LIST OF FIGURES (Continued)

FIGURE		PAGE
49	COMPRESSION JOINT TEST RESULTS - LAMINATE #3	72
50	COMPRESSION JOINT TEST RESULTS - LAMINATE #4	73
51	PROPOSED INTERACTION FOR DESIGN OF COMPRESSION JOINTS	76
52	UNSTIFFENED CUTOUT FINITE ELEMENT MODEL	78
53	TANGENTIAL STRESS AND ALLOWABLES FOR UNSTIFF- ENED CUTOUT PANELS SOFTENED WITH E GLASS	79
54	MARGINS OF SAFETY AT CUTOUT FOR UNSTIFFENED CUTOUT PANELS SOFTENED WITH E GLASS	80
55	TANGENTIAL STRESS AND ALLOWABLES FOR UNSTIFF- ENED CUTOUT PANELS SOFTENED WITH S2 GLASS	82
56	MARGINS OF SAFETY AT CUTOUT FOR UNSTIFFENED CUTOUT PANELS SOFTENED WITH S2 GLASS	83
57	VARIATIONS OF STRESS AND MARGIN OF SAFETY ACROSS THE WIDTH OF UNSTIFFENED CUTOUTS SOFTENED WITH S2 GLASS	85
58	STIFFENED CUTOUT FINITE ELEMENT MODEL	86
59	TANGENTIAL STRESS AND ALLOWABLES FOR STIFFENED CUTOUT PANELS SOFTENED WITH S2 GLASS	87
60	MARGIN OF SAFETY AT CUTOUT FOR STIFFENED CUTOUT PANELS SOFTENED WITH S2 GLASS	88
61	RADIAL VARIATION OF STRESS FOR STIFFENED CUTOUT PANELS SOFTENED WITH S2 GLASS	89
62	RADIAL VARIATION IN MARGIN OF SAFETY FOR STIFFENED CUTOUT PANELS SOFTENED WITH S2 GLASS	91
63	LIGHTNING STRIKE PANEL CONFIGURATION	100
64	PROCESS VERIFICATION PANEL	103
65	BONDED LONGERON TO SKIN CROSS-SECTION	105
66	11.5 x CARBON EPOXY DETAILS BONDED WITH FM-300 SHOWING SCRIM CLOTH ENDS AS DOTS	105
67	PHOTOMICROGRAPH OF LONGERON RADIUS	106
68	SHEAR TEE TOOLING APPROACH	108
69	FRAME TOOLING CONCEPT	109
70	DEMONSTRATION PANEL BONDING JIG	111
71	BONDING JIG	112

LIST OF FIGURES (Continued)

FIGURE		PAGE
72	FAST-CUT, EGGCRATE STRUCTURE DETAILS	113
73	LIGHTNING STRIKE PANEL SETUP	117
74	TEST CIRCUIT FOR LIGHTNING SIMULATION	118
75	NICKEL-COATED TEST SPECIMEN AFTER STRIKE	119
76	HIGH PEAK CURRENT COMPONENT WAVEFORM (KA vs t)	120
77	CONTINUING CURRENT COMPONENT WAVEFORM (A vs t)	120
78	AFTER STRIKE DAMAGE ON WIRE WOVEN PANEL (UNC-505-2)	121
79	AFTER STRIKE DAMAGE ON NICKEL-COATED PANEL (UNC-507-3)	122
80	AFTER STRIKE DAMAGE ON UNPROTECTED PANEL (UNC-509-3)	126
81	TYPICAL SHEAR-TEE SETUP	
82	SHEAR-TEE SPECIMEN UNDER AN 800 LB LOAD	127

LIST OF TABLES

TABLE		PAGE
I	MONOLAYER PROPERTIES	40
II	LAMINATE PROPERTIES	43
III	FASTENER FLEXIBILITY CALCULATIONS FOR TESTED LAMINATES	57
IV	PROCESS DEVELOPMENT SPECIMEN STATUS	94
V	COMPRESSION AFTER IMPACT TEST DATA (ST-1)	95
VI	OPEN-HOLE TENSION (ST-3)	95
VII	OPEN-HOLE COMPRESSION (ST-4)	96
VIII	DOUBLE CANTILEVER BEAM (ST-5)	96
IX	MATERIAL QUALITY TEST DATA, F584/IM6 TAPE	97
X	MATERIAL QUALITY TEST DATA, F584/IM6-5HS CLOTH	98
XI	SUMMARY OF PROCESS VERIFICATION TESTS	104
XII	LIGHTNING DISCHARGE TEST VALUES	124
XIII	LIGHTNING DAMAGE	124





## SECTION 1 INTRODUCTION

Secondary composite structure for civil and military transport aircraft have been successfully developed under the NASA Aircraft Energy Efficiency (ACEE) Program. The cost and weight benefits of such composite structures have been validated by the design, manufacture and test of several components and confidence in these applications has been achieved through interface with the FAA and the airlines. These programs are nearing completion and the aircraft manufacturers are beginning to incorporate composite versions of such structures in plans for future aircraft.

While composites technology for secondary structures is now considered state-of-the-art, the major payoff will come with application of composites to primary structure, which comprises about 75 percent of transport structural weight. However, to reach this milestone, a comprehensive data base is needed to assure that both technical and financial risks are acceptable before incorporating these materials into safety-of-flight structure.

As a follow-on to the ACEE program, NASA established the Advanced Composite Structures Technology (ACST) program to develop a composite primary airframe structures technology base to achieve the full potential of weight and cost savings possible for U.S. civil and military transport aircraft in the early 1990's. As part of the ACST program, three large transport aircraft manufacturers have been contracted to address long-lead-time critical technology for composite fuselage structure which has been identified by NASA, other Government agencies, and industry-sponsored programs. This Development of Composites Technology for Joints and Cutouts in Fuselage Structure of Large Transport Aircraft was initiated in March 1984.

The baseline aircraft for this program is the MD-100, an advanced version of the DC-10 , and the selected component is the forward fuselage barrel section approximately 30 feet in length. The constant section fuselage diameter is 237 inches. Frames are on a 20 inch spacing and longerons are spaced from approximately 6.5 inches to 7.5 inches. The forward fuselage barrel is of sufficient size and complexity to fully evaluate the technology issues of joints and cutouts.

The period of performance of this program is 30 months, with completion scheduled for September 1986. The program schedule is shown in Figure 1.

Technical information gathered during performance of this contract will be disseminated throughout the aircraft industry and the government. Information transfer will be accomplished through technical reports, industry briefings and technical workshops.

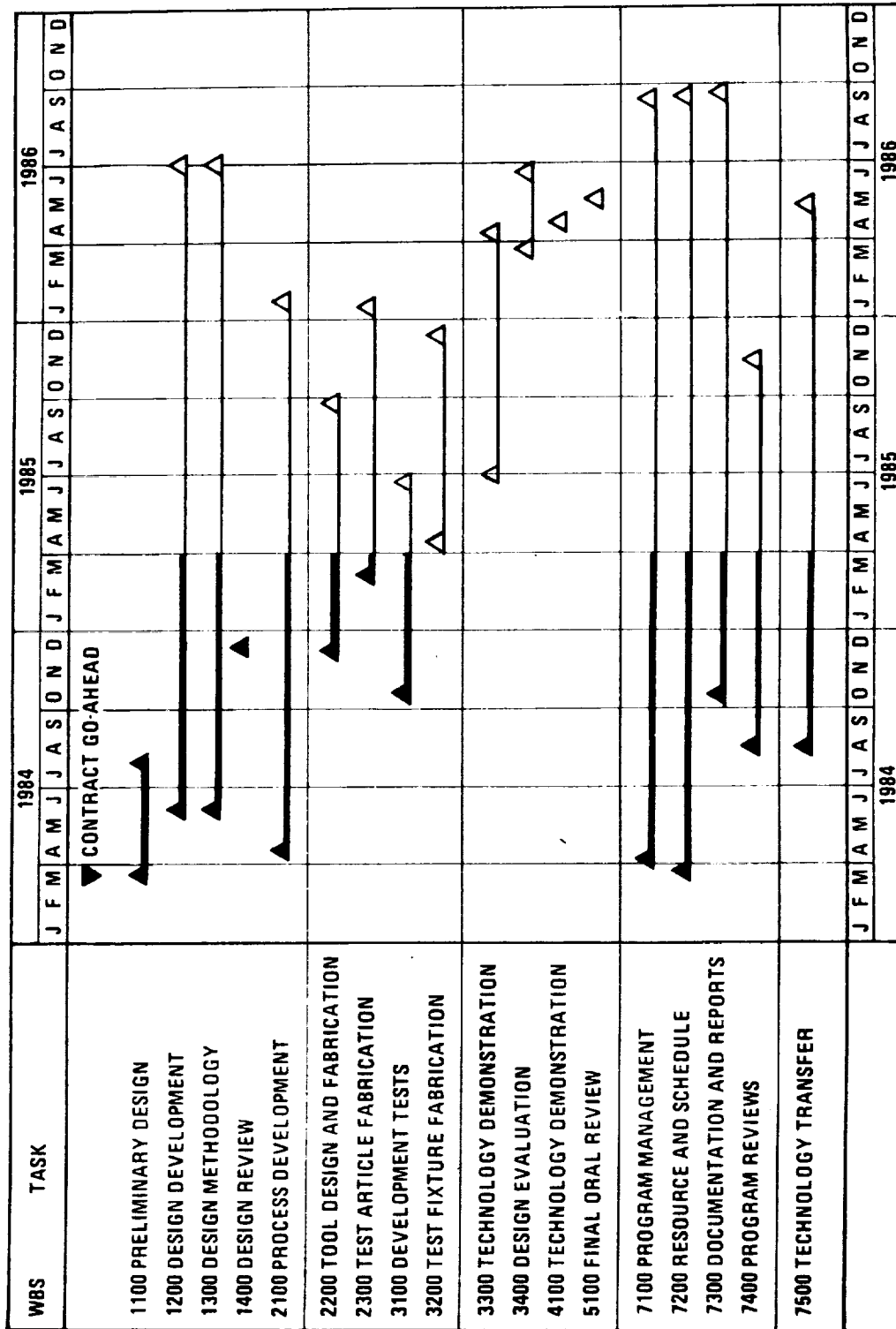


FIGURE 1. PROGRAM SCHEDULE



SECTION 2  
SUMMARY

All of the F584/IM6 tape and broadgood materials needed for the program was purchased, received and qualified for use during this reporting period. Engineering drawings for the group A and B specimens were released for fabrication. The group C drawings were started during this reporting period. In addition, the first 4' by 5' shear/interaction panel was released for fabrication.

Conceptual design activity was completed on the transverse and longitudinal splices and the window belt cutouts. Additionally, the design of the longerons, frames, and longeron-to-frame shear clips were completed. The latter structural element will be an injection molded chopped fiber/PEEK part. As a result of NASA budget reductions for fiscal 1986, the large demonstration panel activity was stopped. This effectively halted Engineering and Manufacturing R and D activity on tasks related to the demonstration panel. Design effort on the passenger door cutout was also stopped.

In Design Methodology, the primary focus was on pre-drawing release analysis of the group B, C, and D specimens and the reduction/interpretation of the group A test data. Also methodology development focused on establishing bearing/bypass relationships for multirow joint analysis, particularly with regard to compression joints.

Finite element models have been generated for the shear tee pull-off configurations, the stiffened panel, and a typical fuselage quarter bay panel. This panel was run to determine the load carried by the longeron-to-frame shear clip.

Nearly all of the group A specimens and more than one-third of the group B specimens were fabricated. The fabrication of some detail parts on the first 4' by 5' panel was started. The bonding jig for the demonstration panel, 9' by 14', was completed except for the attachment of casters. Fabrication and test of the 2' by 2' curved panel with two shear tees and a longeron for establishing and verifying manufacturing parameters was nearly completed.

Testing of the cloth and tape monolayer specimens as well as the single and double lap tension specimens was completed. Nearly all of the group A specimens have been tested including the compression after "impact" which were struck by lightning. The testing of the shear tee pull off specimens (group B) was initiated near the end of March and should be completed during April.

## SECTION 3

### DESIGN OPTIMIZATION

#### 3.1 DESIGN DEVELOPMENT

##### Fuselage Barrel Description

The subcomponent of the MD-100 selected for design development is the forward fuselage barrel just forward of the wing between fuselage stations 765 and 1129. The fuselage section is shown in Figure 2. The barrel design consists of four panels made up from discretely stiffened skins with bonded longerons and shear tees. The frames and floor beams are mechanically attached to the skin panels. A typical section of the fuselage panel is shown in Figure 3. The barrel section is joined to the nose and aft fuselage sections by mechanically fastened skin and longeron joints.

##### Design Approach

The development of technology for the design of joints and large cutouts is the prime objective of this program. However, the conceptual design of the composite barrel section required consideration of many technology issues beyond joints and cutouts. Paramount among these issues are impact resistance, damage tolerance, lightning strike protection, repairability and producibility.

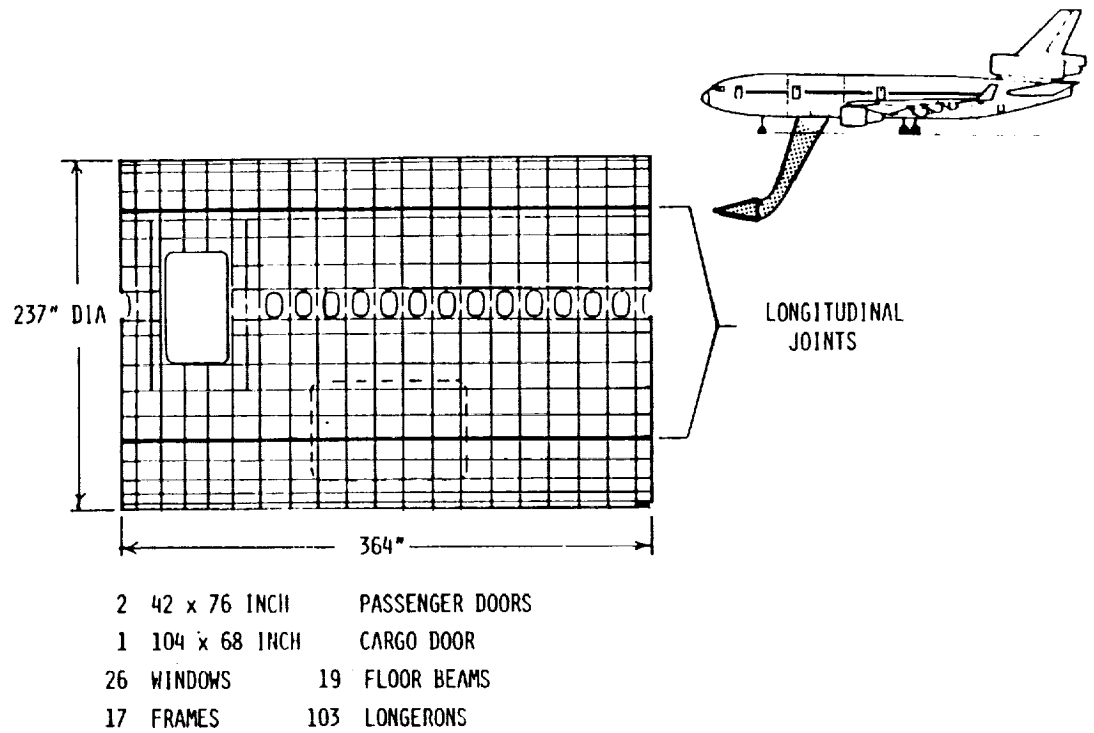


FIGURE 2 BASELINE AIRCRAFT AND BARREL SECTION

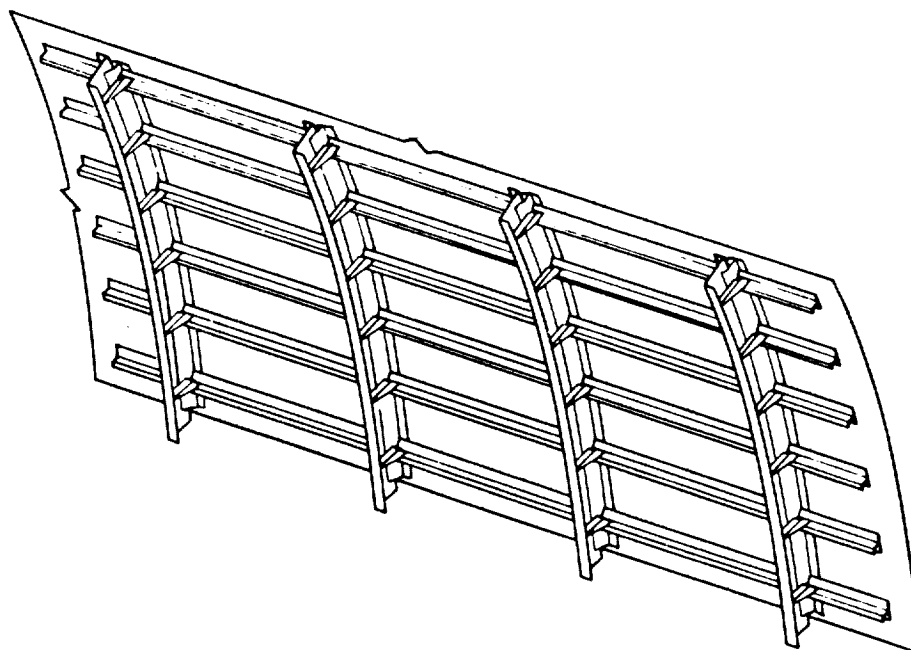


FIGURE 3 COMPOSITE SHELL DESIGN



Impact resistance has been addressed by setting a minimum skin gage and using a toughened resin system. The combination of a 0.068 skin thickness and F584 resin should be sufficient to prevent damage due to the kind of day-to-day low energy impact often experienced in service. It is extremely important for a fuselage structure to be able to absorb this type of impact without requiring constant repair. Of equal importance is the ability to operate without concern for non-visible damage. Testing of the fuselage skin layup (test CAI-A9) has indicated that the threshold of visible damage occurs at an impact energy of 4 ft. lbs. when using a 0.5 inch hemispherical steel tip for the impact device. The tests have demonstrated the ability for the damaged skin to exceed a 4500 compression micro-strain. We believe that this demonstrated level of impact resistance is adequate for the fuselage design.

Damage tolerance requirements are addressed in the fuselage design primarily by limiting the maximum permissible axial strain to 4500 micro-inches/inch and the maximum shear strain to 9000 micro-inches/inch. In addition, straps consisting of 4 plies of tape oriented in the hoop direction are incorporated in the skin at each frame station. This increases the local modulus and strength of the skin in the hoop direction by approximately 30 percent. The straps will act, to some degree, as arrestment strips for longitudinal cracks. Bonded longerons, which joggle over the straps will act as crack arresters in the transverse direction.

Four potential lightning protection systems were evaluated. These were, flame sprayed aluminum, Thorstrand on glass fiber, Cycom nickel coated carbon fiber and a cowoven fine aluminum wire system produced by Fiber-rite. The first two systems were rejected because of producibility uncertainties and weight reasons respectively. The Cycom and Fiber-rite systems were selected to be tested against each other and an unprotected panel. The test panels were painted and subjected to a simulated swept stroke strike and then compression tested. As reported in Appendix A the Fiber-rite system was clearly superior and was therefore chosen for use in the conceptual design.

Repairability has been designed into the structure from its inception. The longeron and shear tee flanges have been sized so that disbonds may be repaired with fasteners if necessary. The skin is designed for permanent bonded repairs but mechanically fastened temporary repairs are possible.

Producibility has been enhanced by extensive use of structural bonding, reducing the number of required layups to a minimum and the use of pseudo-isotropic material in areas of constantly changing orientation such as frame and shear tee webs. Injection molded structural elements are being used where practical which should result in significant cost savings.

#### Fuselage Barrel Design

The fuselage conceptual design was finalized during this reporting period. The design details are described below.

The layup pattern of each skin panel is optimized for a combination of flight and pressure loads. In the hoop direction the largest load is a consequence of a 2P pressure requirement. This sets the lower limit on the number of 90 degree plies. A minimum number of 45 degree plies are incorporated into the skin to meet the shear strength and stiffness requirements.

Since the skin is a postbuckled design, the longerons and the portion of the skin that is directly attached to the longerons takes the majority of the compression loads. Therefore, compression sets the minimum size of the longerons. Because the tension loads are in general higher than the compression loads, additional zero degree material which is necessary to carry these loads can be placed in the skin where it will be more effective for load redistribution in the event of a longeron failure. This increases the thickness of the skin which aids in impact resistance. The resulting minimum

gage skin, sized to meet the design load requirements within the imposed strain limitations is a laminate (0,90,+45,0,-45,90)s 0.068 inch thick. It is possible to use this minimum gage skin everywhere except for a small area on either side of the fuselage near the wing which must be reinforced with additional 45 degree material to meet the shear buckling limits imposed by the design criteria and at the joints. The reinforced skin near the wing and joints is a laminate (0,90,+45,0,-45,90)s 0.091 inch thick.

Straps consisting of 4 plies of tape oriented in the hoop direction are incorporated in the skin at each frame station. This is done for three reasons. The first reason is to act as crack arrestment strips even though determining the effectiveness of these arrestment strips is beyond the scope of this program. The second reason for the straps is to reduce the adverse effects of the "mouse hole" cut out discontinuity at the longeron/frame intersection. Normally this is an area of high stresses resulting from a combination of peak shear stresses and bending. The capability to mold composites is being exploited here by locating the integral hoop strap under the shear tees and longeron intersections which reinforces this area. The final reason for the hoop straps is a result of the bending behavior of the frame. The frame, shear tee and skin act together in bending, which places the neutral axis near the frame outer cap. Hoop direction fibers in the skin are much more efficient in bending than the same fibers would be in the outer frame cap.

The resulting skin is a highly efficient post buckled design which meets all strength and stiffness requirements as well as the strain and buckling limits. Skin layup schematics are shown in Figure 4.

"J" section longerons are used for structural efficiency and ease of attachment. The longeron height is set at 1.45 inches with a 0.5 inch free flange and a 2.25 inch wide base flange. The longerons are secondarily bonded to the skin with FM-300 adhesive. A four ply minimum gage longeron is used forward of station 939. Aft of station 939 a six ply longeron layup is used. These longerons are shown in Figure 5. The longerons in the keel region aft of

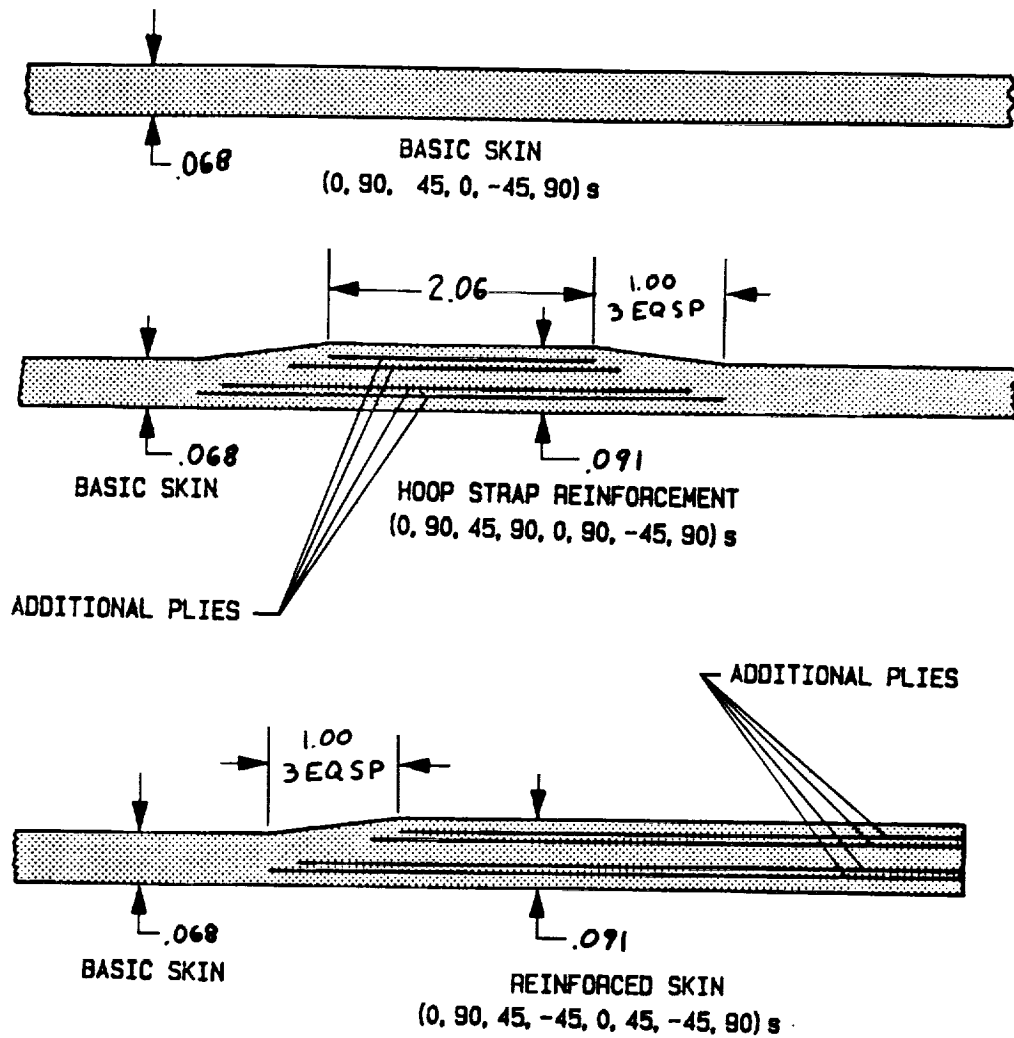
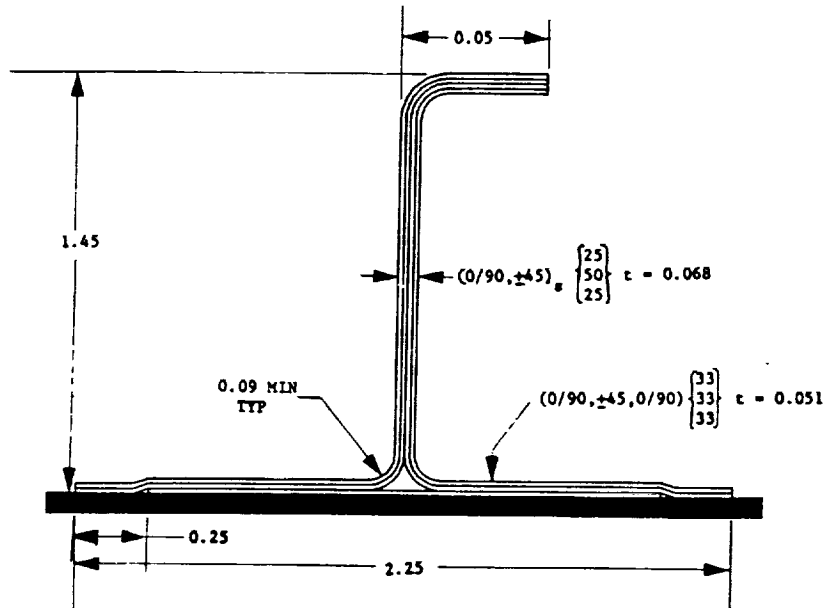


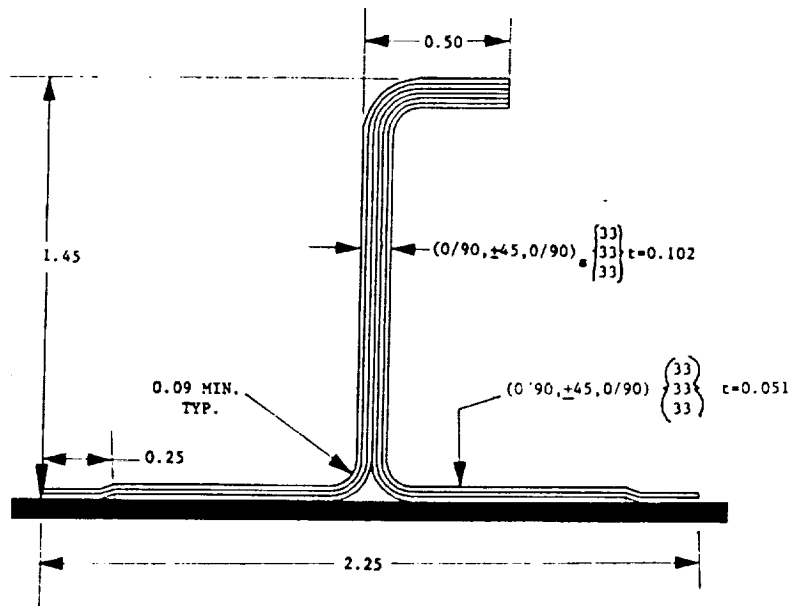
FIGURE 4 FUSELAGE SKIN LAYUPS

MINIMUM GAGE LONGERON



LOCATION: MINIMUM GAGE LONGERON, ALL LONGERONS FORWARD OF STA. 939  
AND BETWEEN LONGERONS # 25 & 35 FORWARD OF STA. 979.

BASIC LONGERON



LOCATION: CROWN REGION AFT OF STA. 939 ABOVE LONGERON # 25.  
KEEL REGION AFT OF STA. 939 BELOW LONGERON # 38.  
SIDEWALL REGION BETWEEN LONGERON # 25 & 35 AFT OF  
STA. 979.

FIGURE 5 LONGERON CONFIGURATIONS

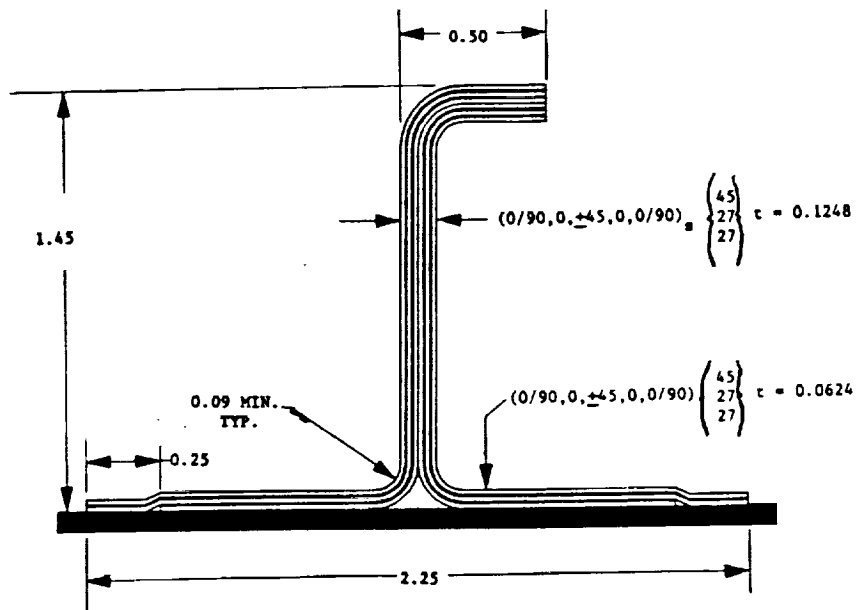
station 959 are reinforced to a 45 percent zero degree layup because of the high compressive loads in this area. The same longeron is used in the crown region aft of station 1089 in order to assist the skin in carrying the high tension loads in this area. The longerons are reinforced to 54 percent zero degree fibers at the transverse splice. These longeron layups are shown in Figure 6. Two fuselage cross sections showing longeron type, location, skin layup and calculated margins of safety are shown in Figure 7 and 8.

The basic frame design is a pseudo-isotropic "Z" section. Where necessary the caps are reinforced with additional zero degree material up to a maximum of 40 percent of the fibers in the zero direction. The webs however remain pseudo-isotropic. This is done to simplify the frame construction since the material orientation at any particular web location will not have to be controlled. A typical frame cross section, showing both minimum gage and reinforced caps is shown in Figure 9. The additional skin hoop plies at each frame station serve to make the frame more efficient in bending.

Information from the shear tee pull off tests have resulted in the selection of two shear tee designs. The first, for lightly loaded areas in the crown and keel regions of the aircraft consists of a 4 ply pseudo-isotropic web and a 4 ply base. The second design is used in the high shear transfer regions at the fuselage side walls, near the floor beams and in the vicinity of cutouts. Figure 10 shows a cross section of both shear tee configurations.

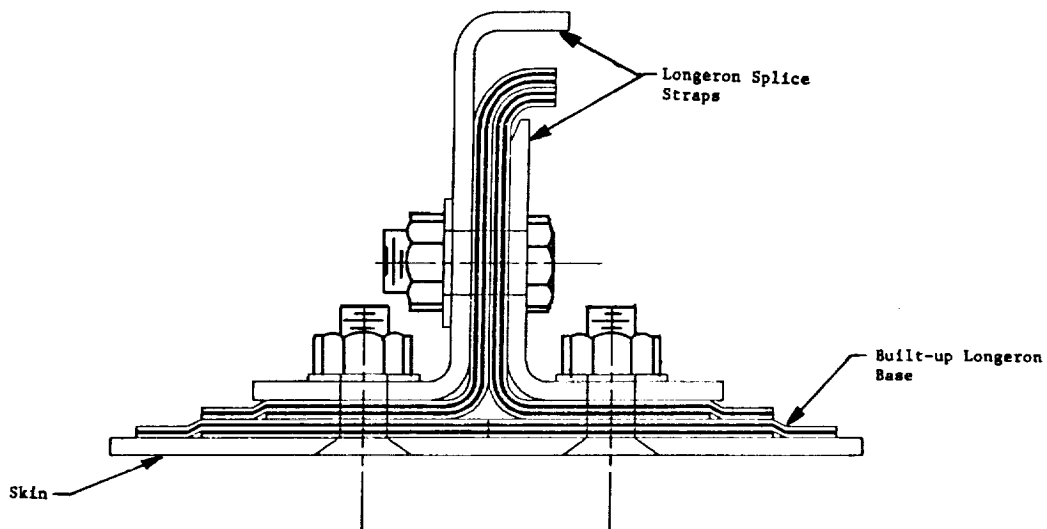
Frame to longeron clips are used at each frame-longeron intersection. The clips stabilize both the frame and the longeron and also serve to assist the shear tees in resisting pressure pillowing loads. Because the clips are identical and a large number are required it is possible that a low cost-high volume production method may be used. Test parts for the program will be injection molded with PEEK thermoplastic and 40% chopped carbon fiber. PEEK is being used because of its excellent solvent resistance and burn

SECOND REINFORCED LONGERON



LOCATION: CROWN REGION AFT OF STA. 1089 ABOVE LONGERON # 5.  
KEEL REGION AFT OF STA. 959 BELOW LONGERON # 42.

Longeron Splice Section



Location: Transverse Splices

FIGURE 6 REINFORCED LONGERON LAYUPS

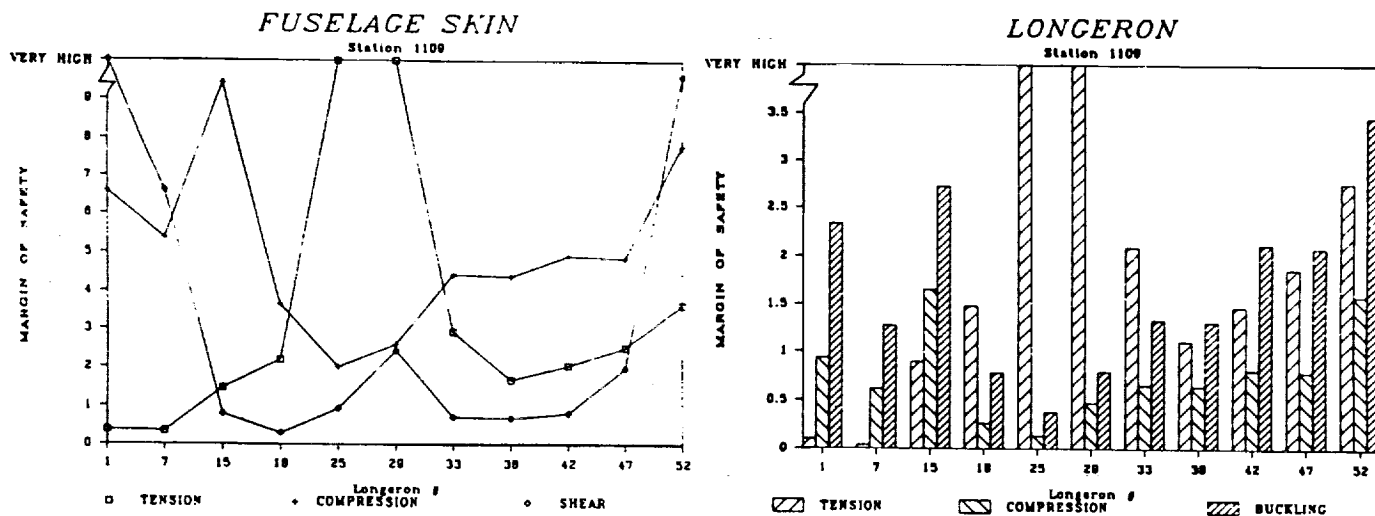
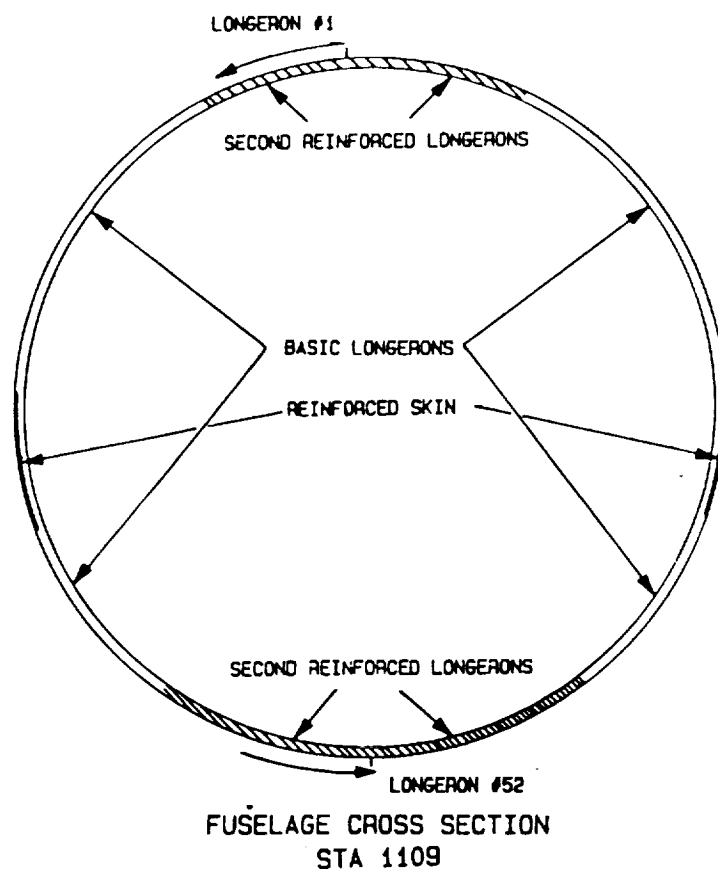


FIGURE 7 STATION 1109 MARGINS OF SAFETY



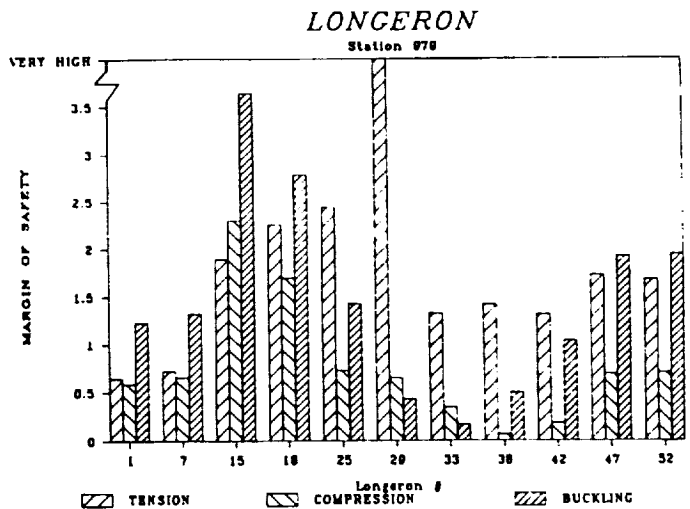
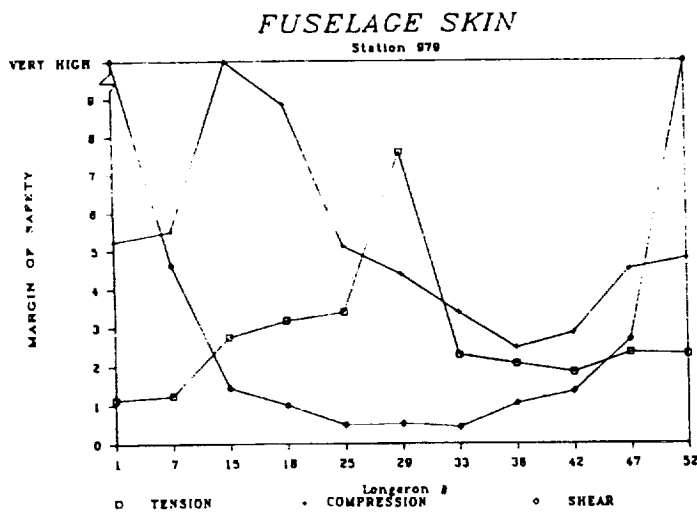
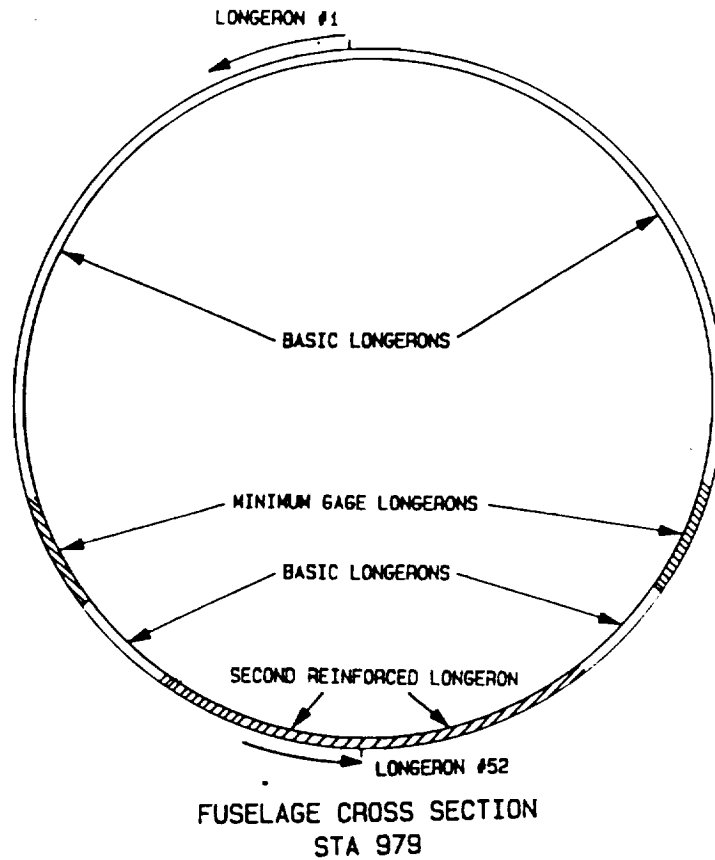


FIGURE 8 STATION 979 MARGINS OF SAFETY

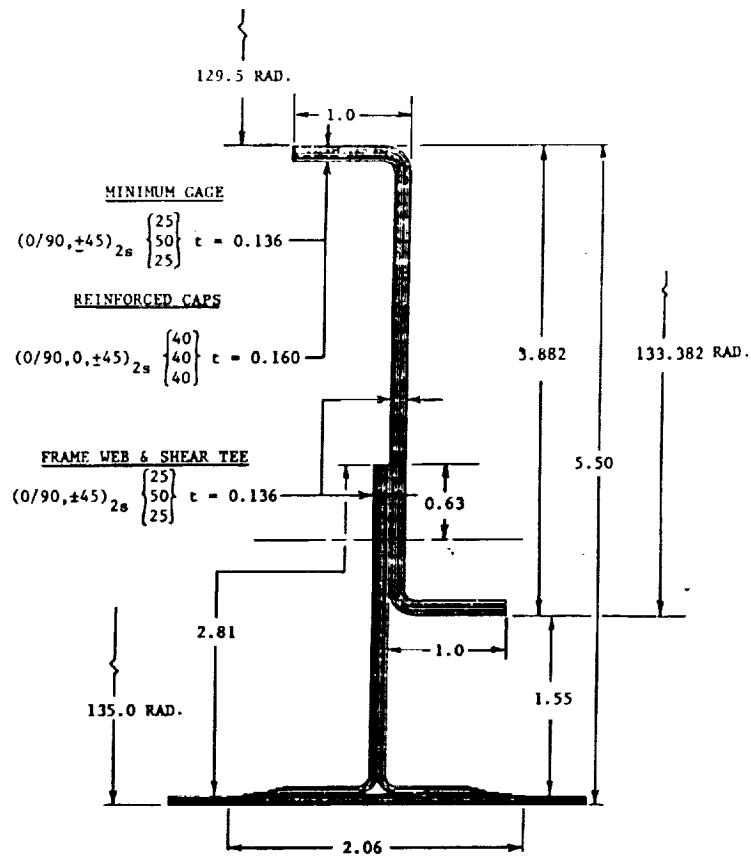


FIGURE 9 FRAME AND SHEAR TEE

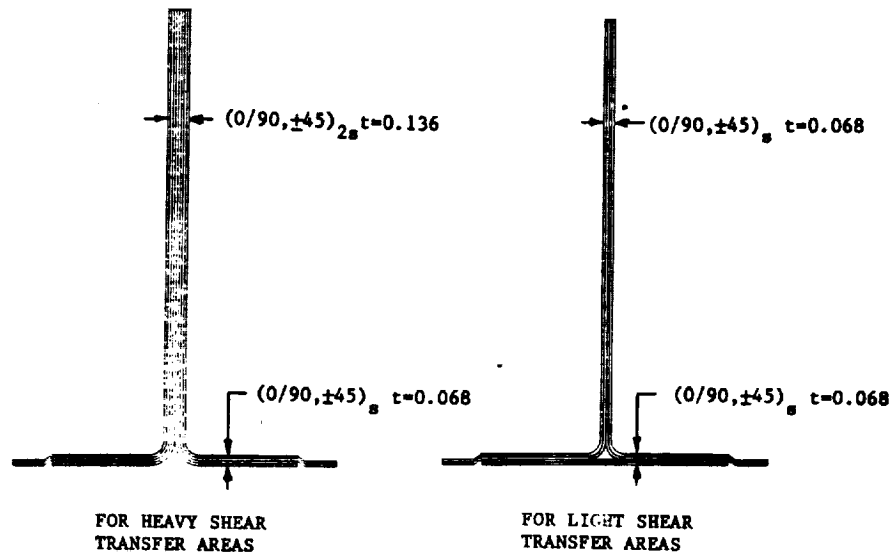


FIGURE 10 SHEAR TEE DESIGNS

characteristics. Figure 11 shows a detail of the clip design. If the parts prove to be satisfactory, they will be used in the test panels (tests C4 through D3). To our knowledge this is the first application of an injection molded part for primary structure.

The longerons and shear tees are secondarily bonded to the skin panels. The longerons have 0.22 inch high built-in joggles for the imbedded hoop straps. The skin panels are attached to the frames by the shear tees. In the mouse hole region of the shear tees, a shear clip is used to connect the longeron, shear tee, and frame together. A schematic of this arrangement is shown in Figure 12. The floor beams, struts and four skin panels are then assembled into the barrel section.

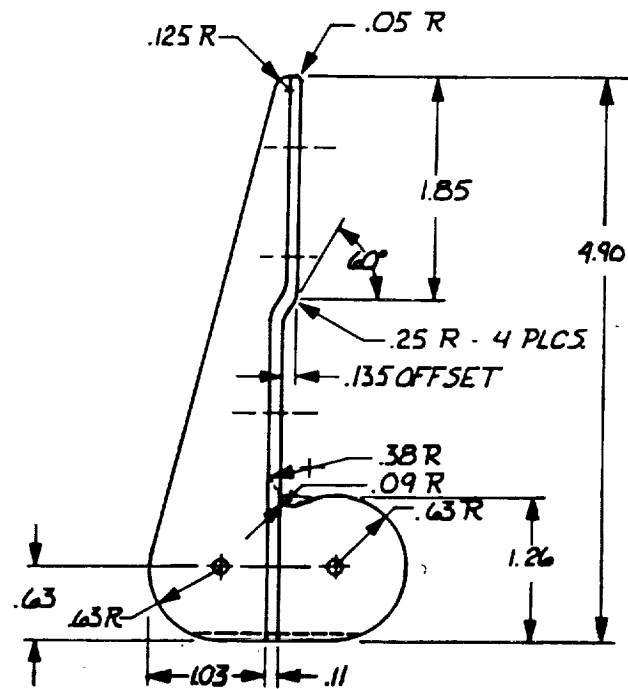


FIGURE 11 INJECTION MOLDED SHEAR CLIP

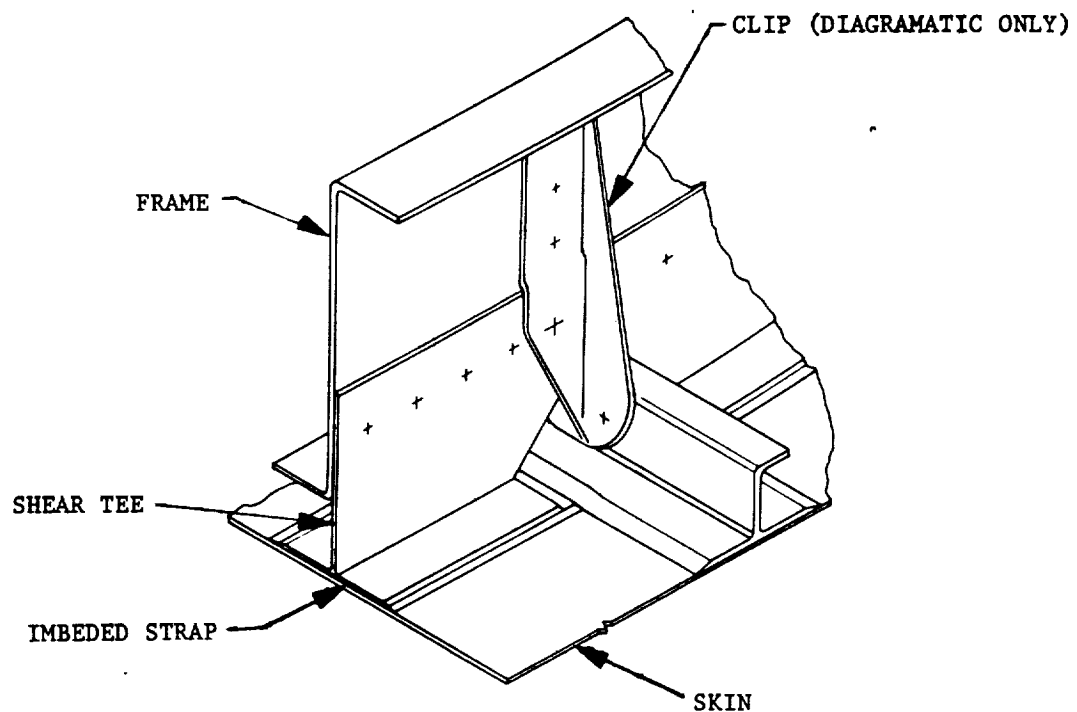


FIGURE 12 FRAME/LONGERON INTERSECTION

### Joints and Cutouts

Work is progressing on development of technology necessary for the successful design of joints and cutouts in fuselage structure. Currently, emphasis on joints is being placed on development of longitudinal and transverse skin splices and the transverse skin and longeron splice. Emphasis on cutout development is being placed on subcomponent development for analysis verification and developing the window belt and passenger door reinforcement concepts.

Before the design of a structural joint can begin, the required joint strength must first be determined. Obviously, the absolute minimum strength necessary for a joint is the ultimate design load in that location. At the other extreme the maximum strength that a joint should be designed for (in the types of structure under consideration here) is the strength of the basic panel. It is expected then that the "proper" joint strength requirement lies somewhere between the above defined lower and upper limits as shown in Figure 13. In a bonded carbon epoxy structure the basic skin tension strength can be very high, in our case almost 140 ksi. On the other hand the design loads can be comparatively low as a result of the limitations on the allowable maximum strain which were imposed for damage tolerance reasons.

Any joint strength requirement above design ultimate load is therefore a damage tolerance issue (or possibly fatigue). If damage is sustained either on or adjacent to the joint, the fasteners on both sides of the damage will be in a relatively high stress field.

If the stress is high enough the joint at that fastener will fail, enlarging the damage and forcing a failure at the next fastener. This process will continue as illustrated in Figure 14 until the joint completely unzips. The only way to completely eliminate this failure mode is to design the joint to be stronger than the basic panel strength.

## JOINT STRENGTH REQUIREMENT (HOW STRONG SHOULD A JOINT BE?)

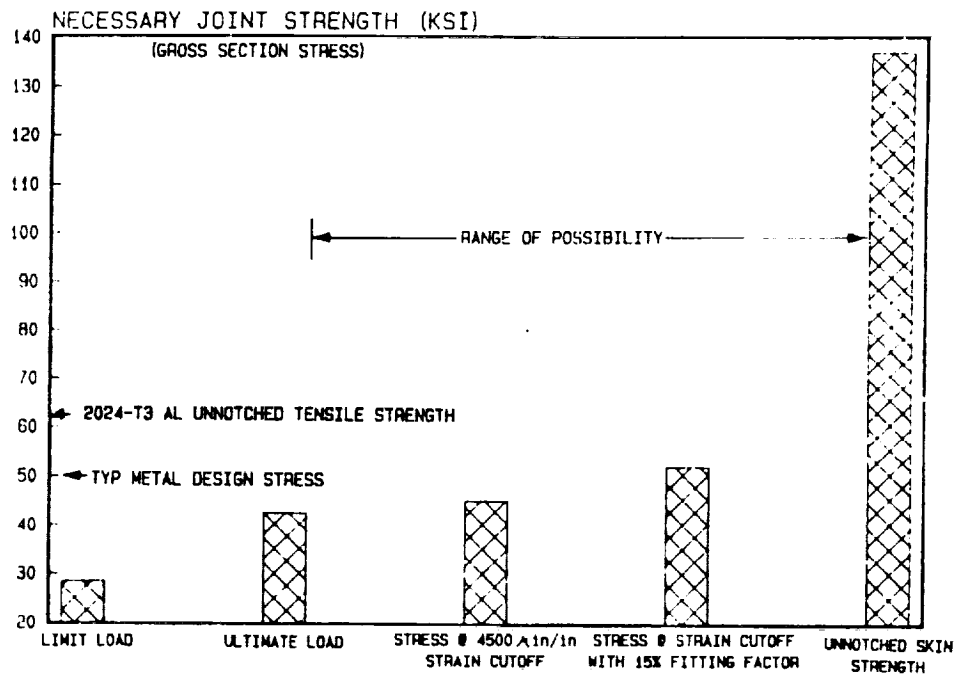


FIGURE 13 JOINT STRENGTH POSSIBILITIES

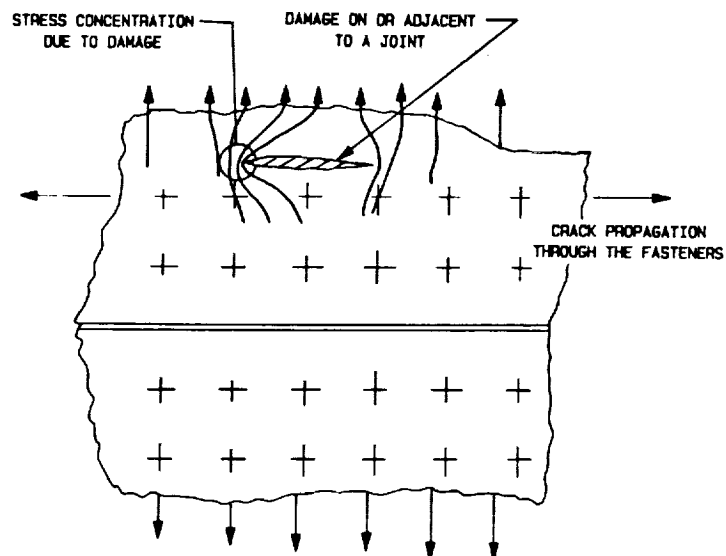


FIGURE 14 DAMAGE TOLERANCE AT A JOINT

Our damage tolerance scheme for the basic structure operates on the principle that while normal design limit strains are restricted to less than 3000 micro-inches/inch, actual local strains at damage locations could exceed 15000 micro-inches/inch prior to failure. If the joint is not capable of operating at the basic panel strains noted above, the effectiveness of our damage tolerance scheme will be reduced.

On the other hand this unzipping behavior applies to metal aircraft structure as well as composite. A typical metal fuselage joint in the MD-100 baseline aircraft is designed to a 50 KSI gross section strength, which is roughly equivalent to the net section strength of the skin panel. The unzipping can occur either in the skin or in the joint. Metal design philosophy can be used as a guide in developing composite design philosophy even though there are basic differences between the two materials. Metal structure exhibits ductile behavior at high stress levels which serves to redistribute the stress in the highly loaded portion of the structure. Composites do not exhibit this type of behavior but a composite joint can be designed so that significant bearing yield will occur before net section failure. This is somewhat analogous to ductile behavior at a joint. In the case of metal aircraft design the policy of designing the primary structure to a 50% safety factor (ultimate vs. limit load) has proven to be quite adequate. This requires that the joint strength must be capable of withstanding a 50 KSI gross section stress. To be consistent with this established aircraft design practice we have set the minimum joint strength requirement to be 15 percent greater than that required to achieve the maximum allowable strain (4500 micro-inches/inch) in the adjacent skin. The corresponding stress at this strain level, as shown in Figure 13, is higher than the typical 50 KSI design stress for a metal fuselage joint.

Additional guidelines have been set for the joint design. A limit has been set on the maximum and minimum percentage of fibers in any direction in a bolted joint. The maximum percent in the load direction is limited to 60% of the total number of fibers in the laminate. The minimum percent of fibers in any direction is limited to 20% of the laminate total.

The smallest fastener that may be used in a primary structural joint is 3/16 inch in diameter which is consistent with current metal design practice. A limit has been set on the minimum skin thickness required for countersunk fasteners. The skin must be thick enough for a minimum 0.01 inch flat under the countersink. Titanium fasteners are used for corrosion resistance. Polysulfide faying surface and fillet sealant is used for a pressure seal in the joint. The fasteners are installed wet for corrosion protection.

Longitudinal splice - The baseline longitudinal splice design has been developed. The splice is located mid bay between longerons and is a four row double shear design utilizing both internal and external splice straps as shown in figure 15. The basic 0.068 skin panel thickness is reinforced to a 0.91 inch thick pseudo-isotropic layup at the joint. The splice straps are also a 0.091 inch thick pseudo-isotropic laminate because of countersink depth requirements.

- The transverse splice is more difficult to design than the longitudinal splice since the loads from the longerons and from the skin must both be transferred across the splice. This leads to many added geometric difficulties. The longeron base must be built up so the longeron straps can clear the splice plate. The bending and axial stiffness must be kept equal to or greater than the adjacent skin panel and the load eccentricity must be minimized.

The skin is spliced by a single shear internal splice strap as shown in Figure 16. The longerons are reinforced with additional plies of zero degree material and the longeron base thickness is increased for clearance over the skin splice strap. The longerons are spliced by back-to-back "Z" and "L" section splice straps as shown in Figure 17. The longerons at the splice location and the splice straps consist of a 54 percent zero degree laminate. Base flange fasteners are 3/16 inch diameter because of edge distance constraints. Longeron web fasteners are 1/4 inch diameter to provide increased bearing area. The area between the back-to-back splice straps are stabilized with Rohacell foam as shown in Figure 18.



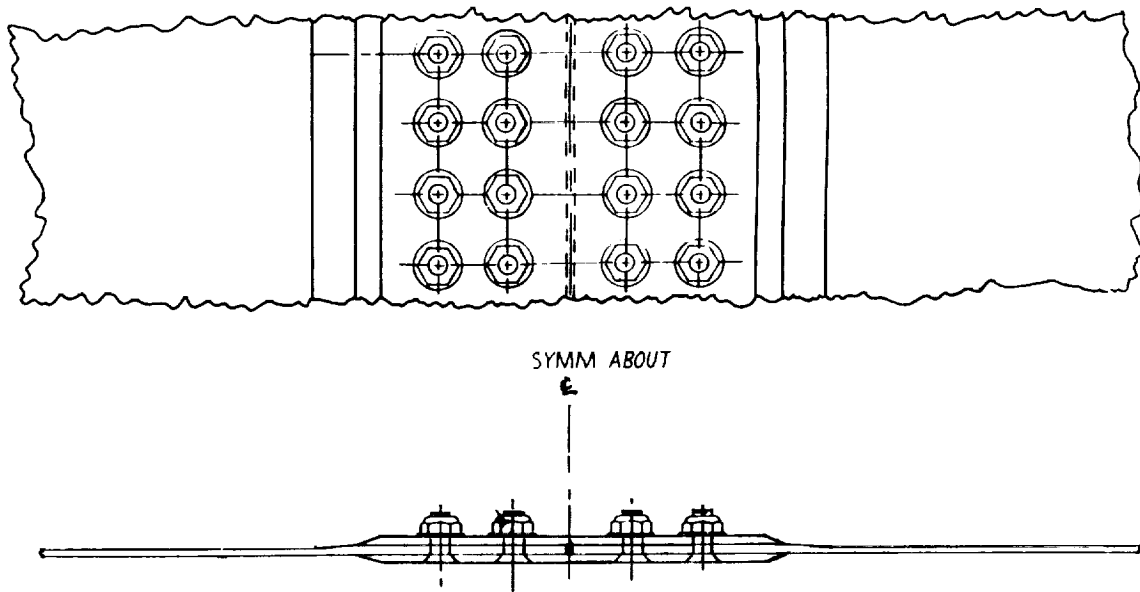


FIGURE 15 LONGITUDINAL SPLICE CONFIGURATION

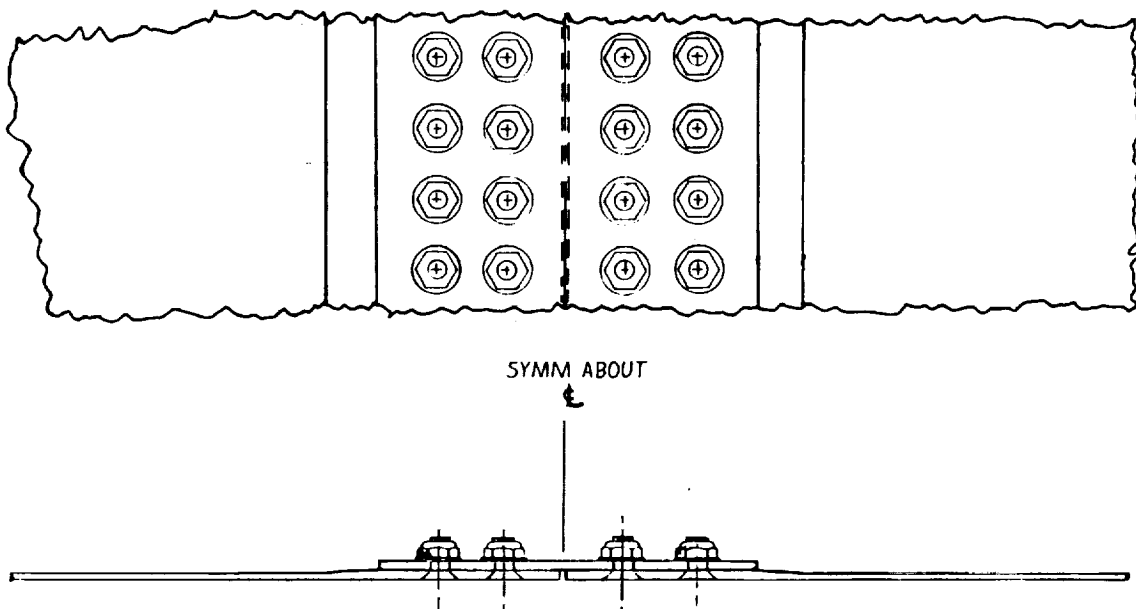


FIGURE 16 TRANSVERSE SKIN SPLICE

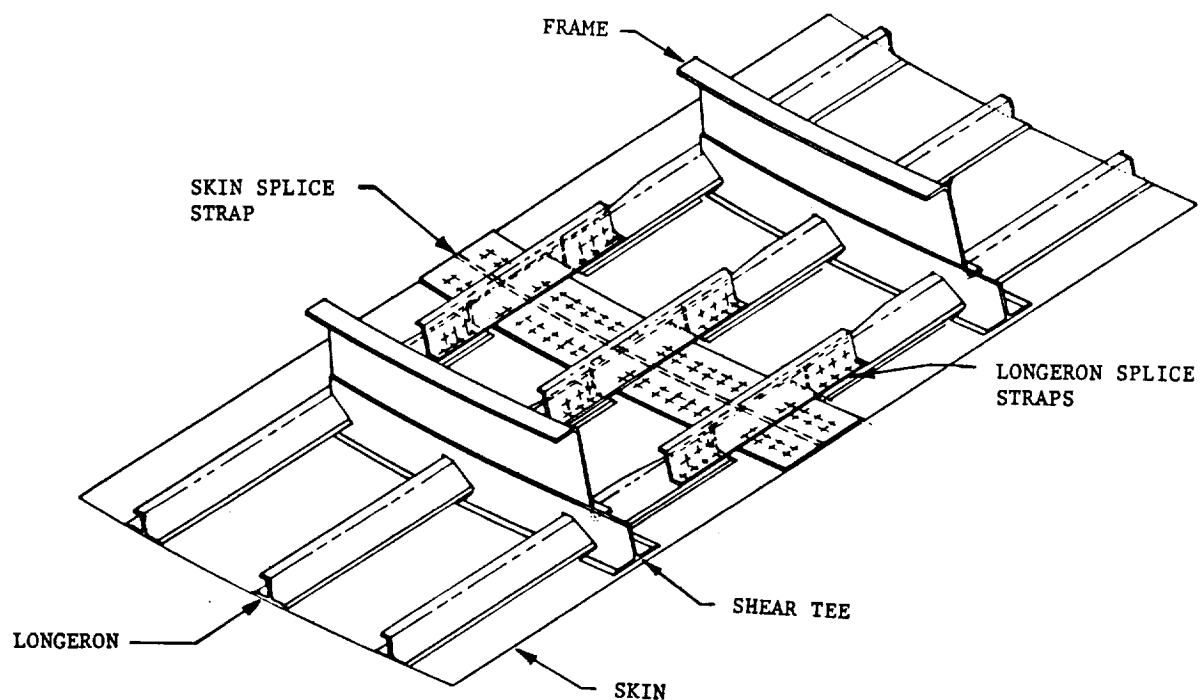


FIGURE 17 TRANSVERSE SKIN/LONGERON SPLICE

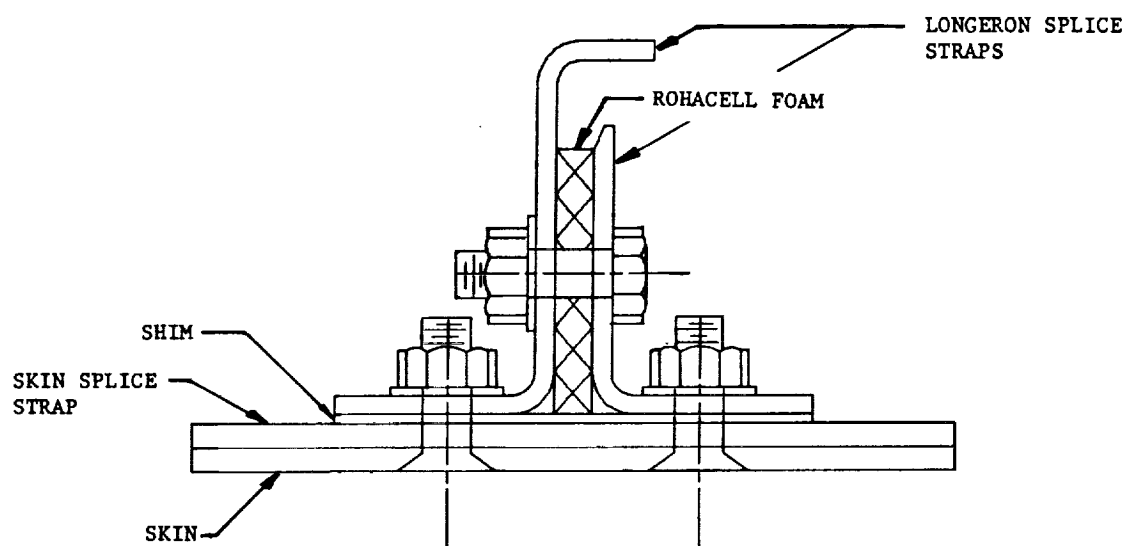


FIGURE 18 LONGERON SPLICE CROSS SECTION

The development of softening techniques for reducing the stress concentrations at the edges of cutouts is in progress. Test specimens for evaluating the behavior of softened, reinforced and unreinforced cutouts under axial and shear loading have been produced. Designs of the passenger window belt region and the structure around the passenger door have been developed.

The window belt, shown in Figure 19, lies between longerons nineteen and twenty four. Two cabin windows are located between every frame i.e., one on each side of the fuselage. The window belt is reinforced with sixty plies of tape which is built up in twenty steps between longerons nineteen to twenty and twenty four to twenty three. The window belt doubler is completely internal for aerodynamic smoothness and in order to simplify the cure tool and panel layup. The frames neck down in this region to provide increased interior room. A full depth frame is required to maintain adequate bending stiffness. For this reason discontinuous longerons are used immediately above and below the windows (longerons 20 and 23) as shown in detail A of Figure 20. The window is installed with the aid of a "window keeper" as shown in detail B of Figure 21. This is done to eliminate the interlaminar stresses that would otherwise exist if the window were allowed to bear directly against a composite skin scarf. We are investigating the potential of compression molding the window keeper. The passenger window itself is a fail safe design consisting of two separate window panes. Either the window pane or the window keeper could fail without a loss of pressure. The frame is reduced from a "Z" section to a "L" section over the window belt as shown in detail B of Figure 21. Short "butterfly" clips, shown in detail C of Figure 21, are used at longerons 19 and 24 where the frame depth is not great enough for the standard clip.

The passenger door cutout is shown in Figure 22. The door is framed with upper and lower headers and frames to form a torsionally rigid cutout support. The door pressure loads are reacted by the door stops which are attached to jamb frames and stub frames. The skin in the door region is

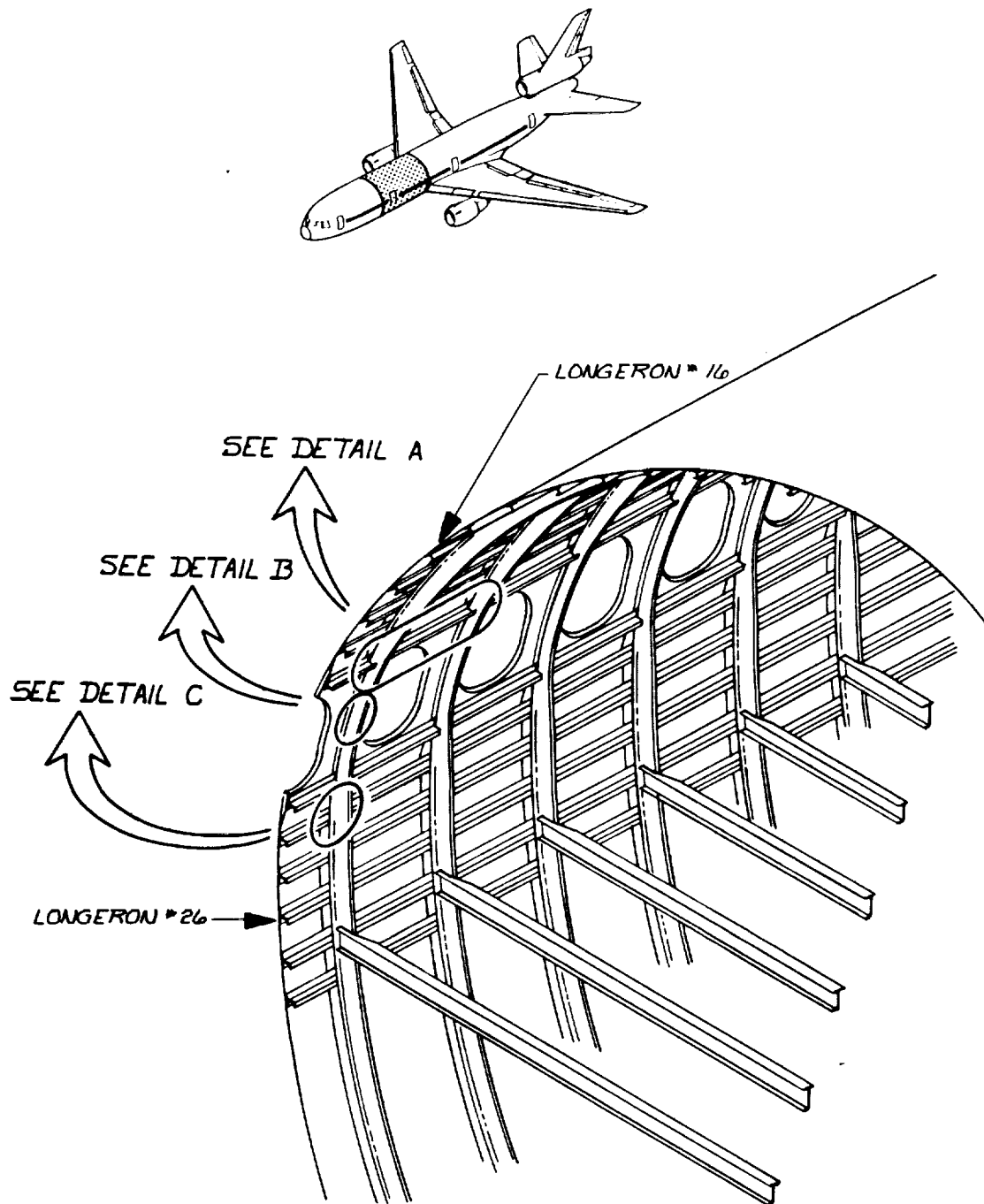
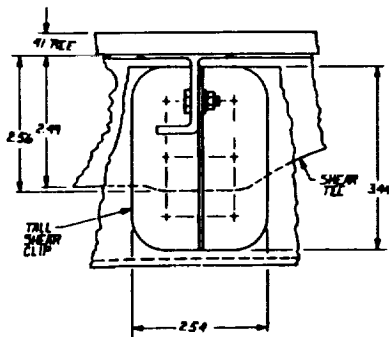
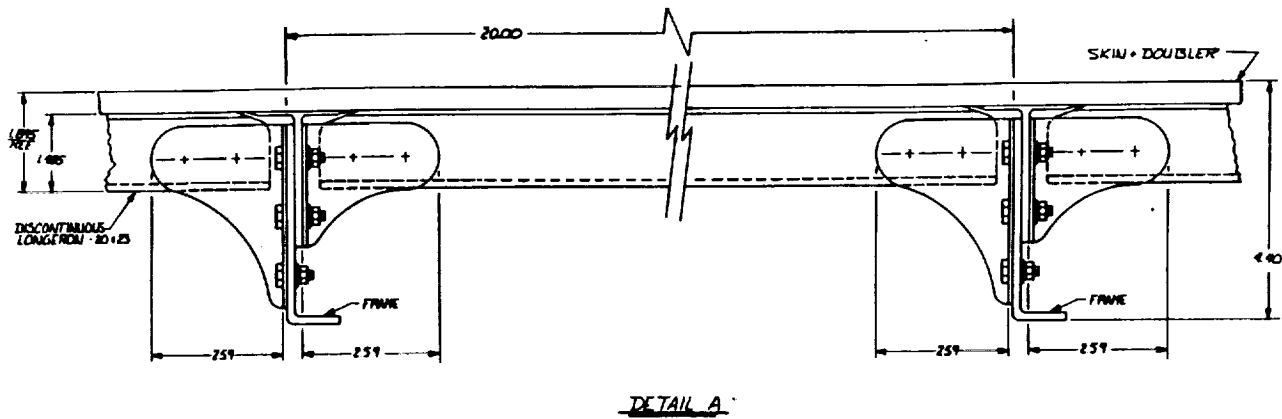
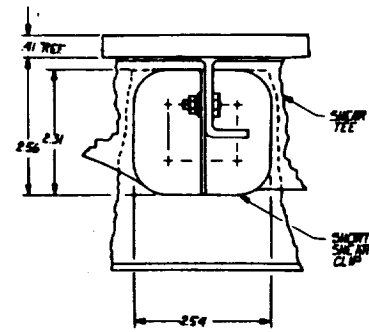


FIGURE 19 PASSENGER WINDOW BELT



LEFT SIDE VIEW  
DETAIL A



RIGHT SIDE VIEW  
DETAIL A

FIGURE 20 DISCONTINUOUS LONGERON DETAILS

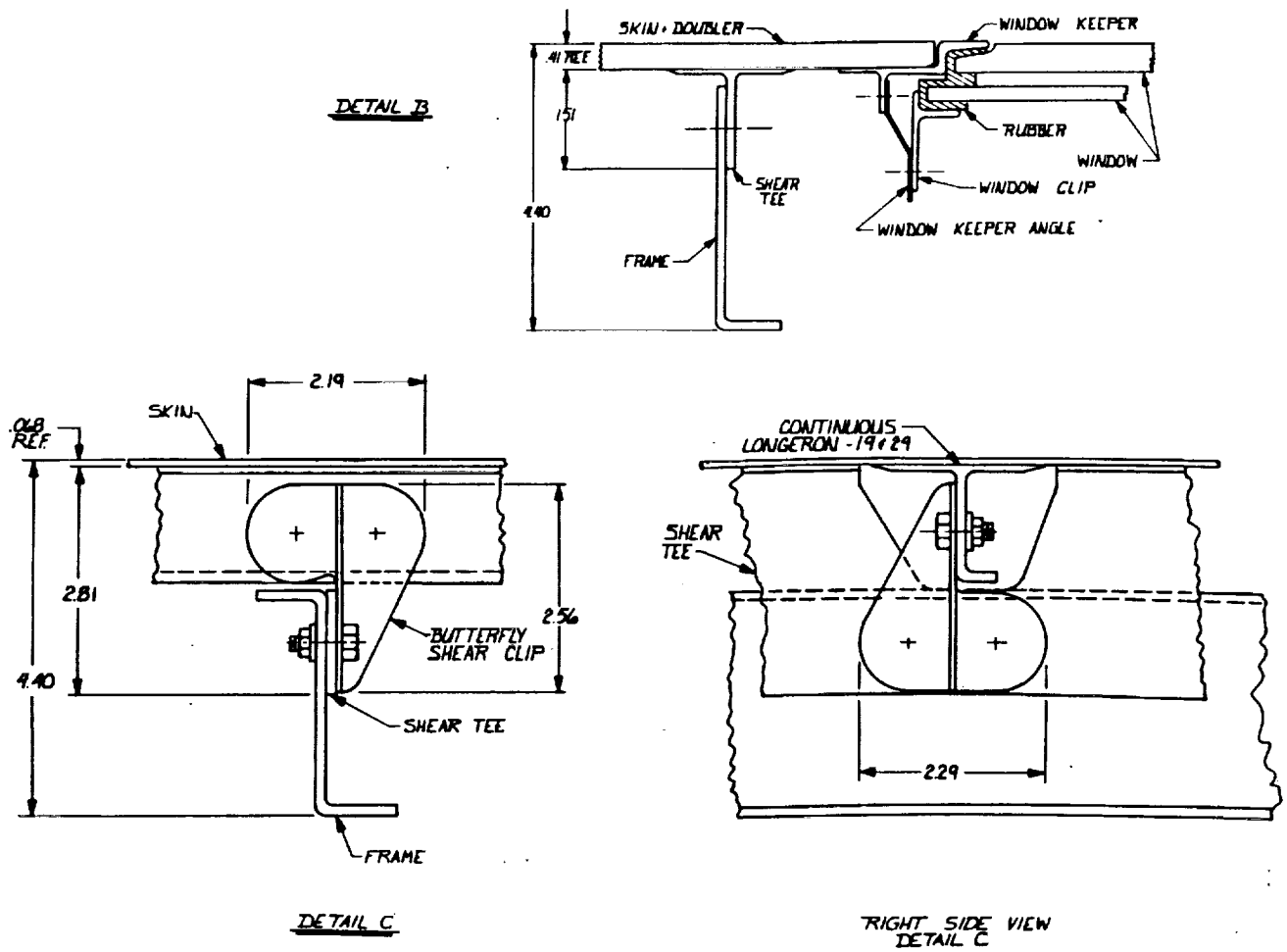
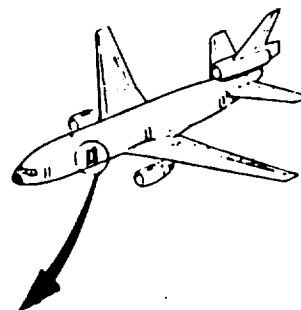
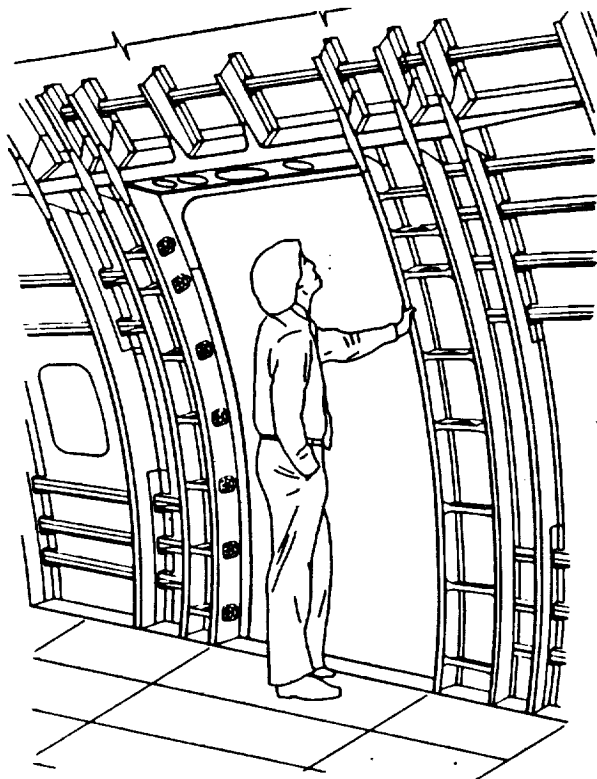


FIGURE 21 WINDOW KEEPER AND CONTINUOUS LONGERON

## PASSENGER DOOR DESIGN



## DOOR JAMB DESIGN

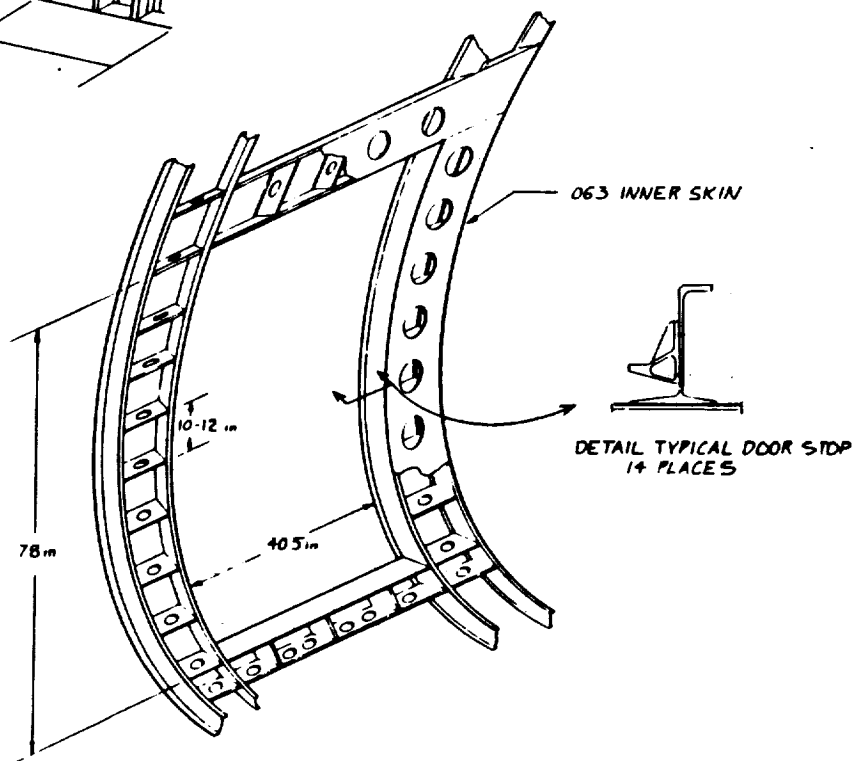


FIGURE 22 PASSENGER DOOR SUBSTRUCTURE

reinforced to a thickness of 0.228 inch as shown in Figure 23. The corners of the door cutout are reinforced further to reduce superimposed strains due to bending at the free edge. Syntactic core is being considered for this application. Door substructure details are shown in Figure 24.

### Test Drawing Preparation

Since the previous semi-annual progress report, all the Group A drawings have been completed and released. The Group B drawings have all been finished, checked, and released.

All of the Group C drawings have been released with the exception of the skin/longeron splice Z5941227. Two skin splice concepts have been developed for both the longitudinal and transverse skin joints (Z5941224 and Z5941225). These concepts will be tested against each other and the best concepts for each joint type will be selected for incorporation in the barrel design. The longeron run out test, specimen drawing Z5941226, has been released. This specimen will be tested in tension for design verification and analysis correlation. The skin/longeron splice drawing is currently being checked.

The three 4 x 5 foot shear interaction panel drawings have been completed in design. The basic panel, drawing ZJ010374 has been released to manufacturing. The transverse splice panel, drawing ZJ010375 shown in Figure 25, is a two bay panel incorporating three frames and six longerons. One bay contains a skin/longeron splice. The other bay is representative of the typical shell structure. The cutout panel, drawing ZJ010276 shown in Figure 26, represents the passenger window belt region. Two windows, three frames with cross sections appropriate to the window belt region, two discontinuous longerons, and two continuous longerons are included in the panel.



# PASSENGER DOOR REGION

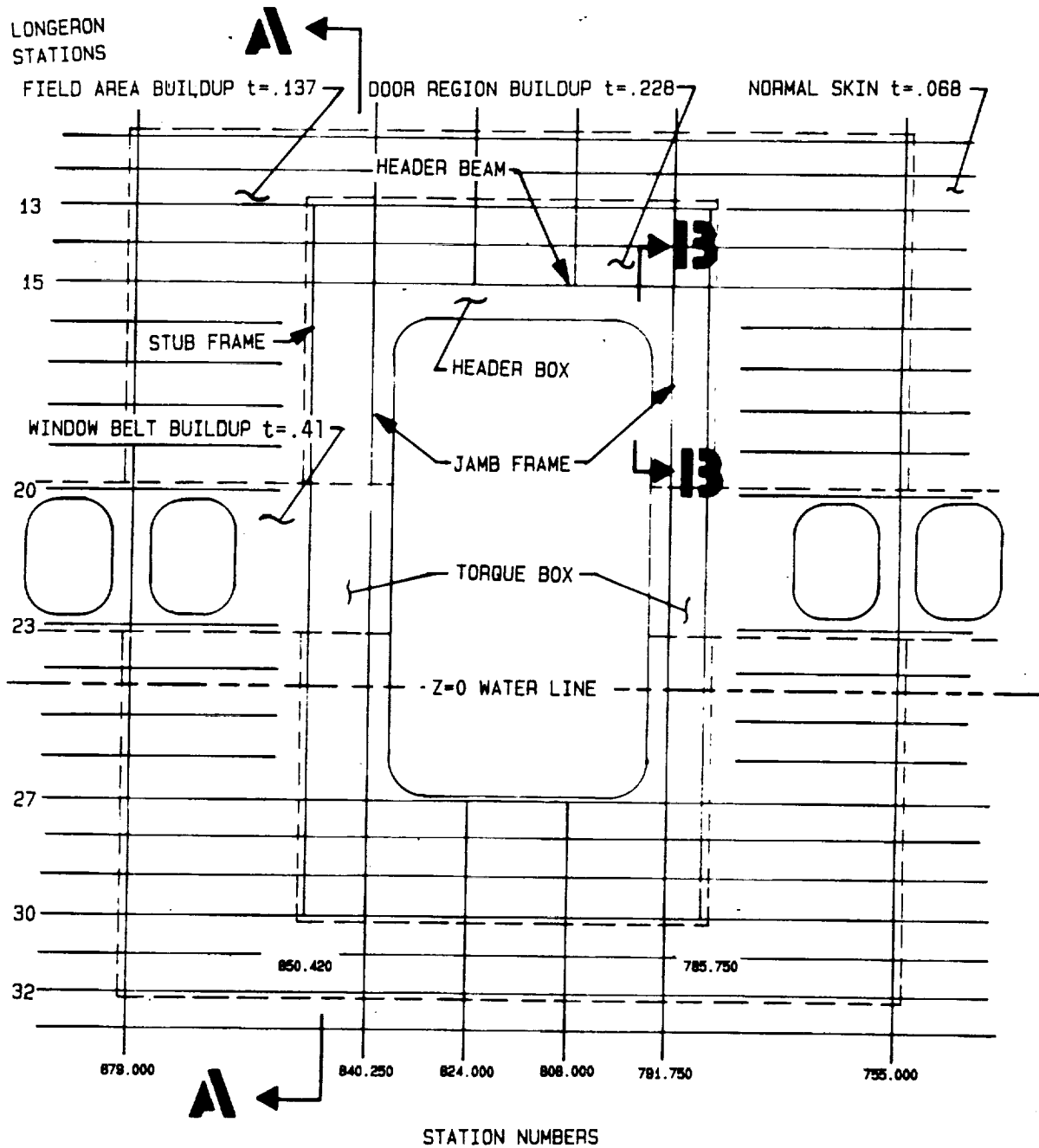


FIGURE 23 PASSENGER SKIN REINFORCEMENT

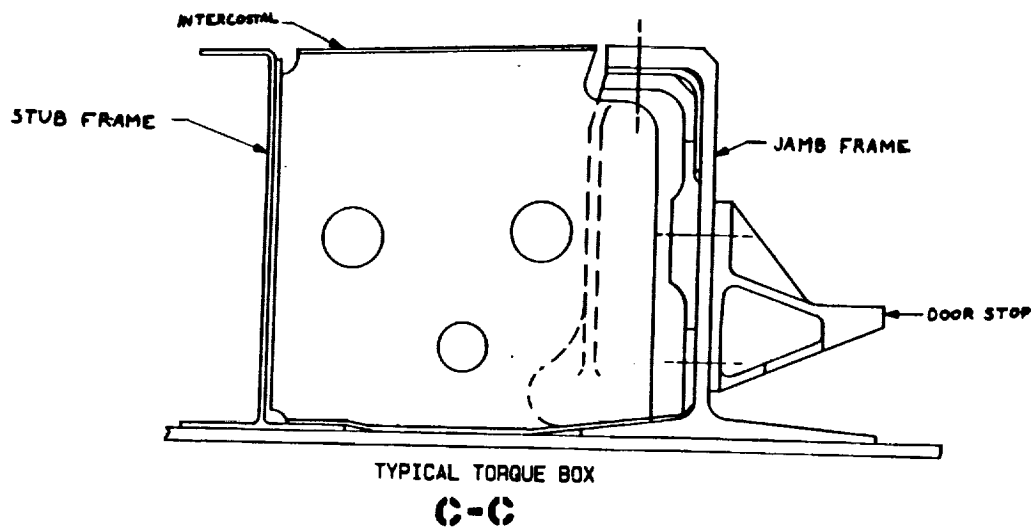
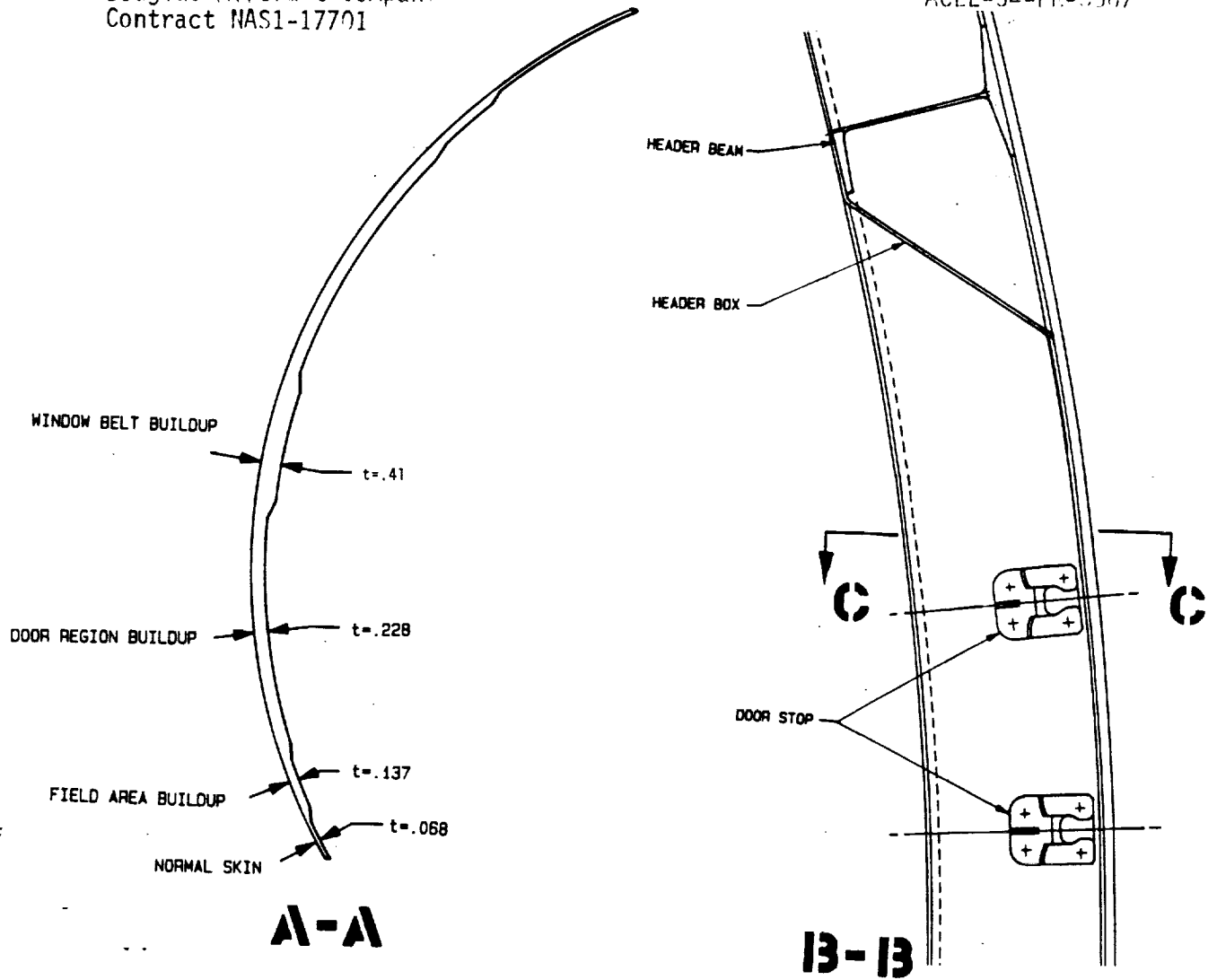


FIGURE 24 PASSENGER DOOR CUTOUT DETAILS

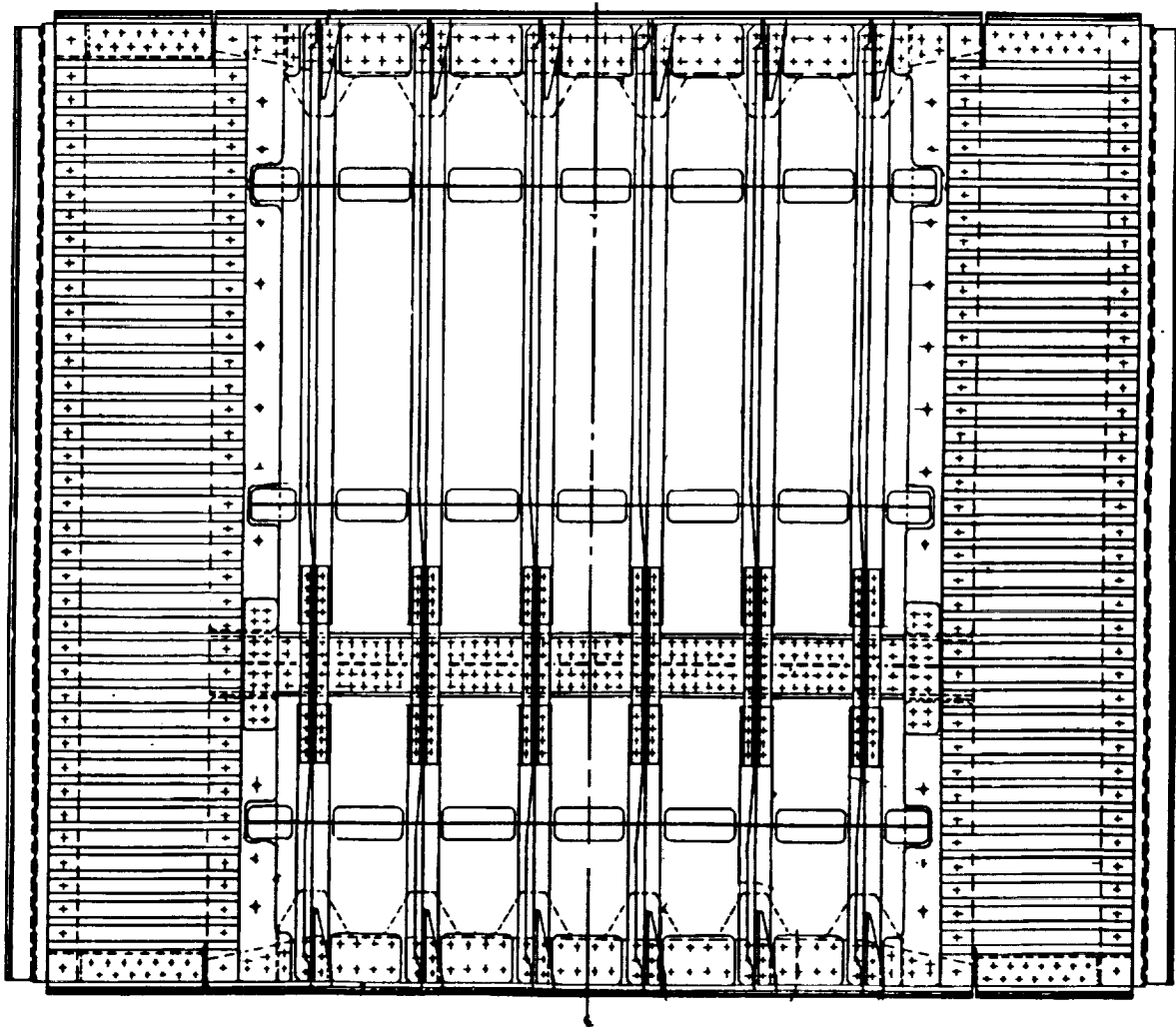


FIGURE 25 TRANSVERSE SPLICE SHEAR INTERACTION PANEL

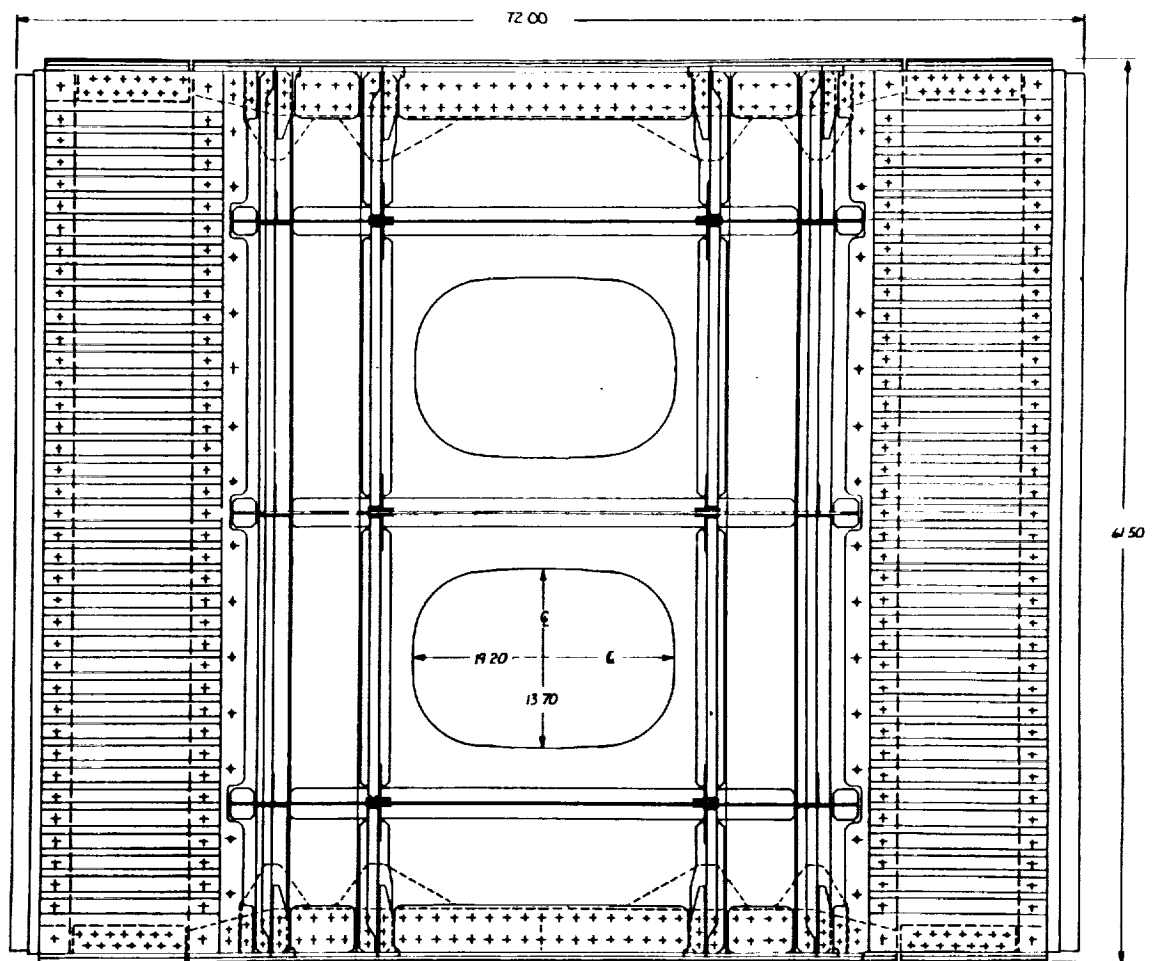


FIGURE 26 PASSENGER WINDOW BELT SHEAR INTERACTION PANEL

The basic panel drawing has been released. The other two are in the Engineering release system.

The Task Assignment drawing (TAD) for the Group B and C tests is being prepared. This document defines the procedures for each test including the test preparation, loading conditions, reaction requirements, data acquisition requirements such as strain gage and photo elastic survey locations and other test related items.



### 3.2 DESIGN METHODOLOGY

Work during the semi-annual reporting period concentrated on the analysis of the Group B and Group C test specimens and the reduction/interpretation of the Group A test results. A complete table of the Group A test results obtained to date are included as Appendix A.

The majority of the Group A testing was structured to determine basic monolayer properties, laminate allowables and stiffnesses, and joint strength data.

Table I presents the monolayer values for F584/IM6 tape and cloth as well as for 120 weave "E glass" and "S2 glass" in the F584 resin system. The F584/IM6 tape properties are all tested values as determined from the Group A test results. The F584/IM6 cloth values are likewise derived from test results with the only exceptions being the transverse properties, ( $E_T$ ,  $F_T^T$  and  $F_T^C$ ) which are assumed to be the same as the corresponding longitudinal properties, (i.e., warp and fill properties were assumed to be the same). The F584/"E glass" properties are partially derived from test results and partially estimated values. Monolayer tests were conducted for this material using specimens cut from a panel fabricated using a no-bleed procedure (as is used for the F584/IM6 tape and cloth laminates). The higher resin content of the fiberglass cloth material, however, resulted in this panel curing out at a thickness of .0061 inches per ply versus the manufacturer's specification of .0047 inches per ply. Consequently, the specimens tested lower than expected for tension modulus and tension strength, as well as for in-plane shear strength. Compression values, however, were if anything, slightly higher than expected. These tests are being rerun with specimens made from a panel which was fabricated using a bleed procedure. Values presented in Table I are simply those used for the analysis of the stiffened and unstiffened cutouts discussed later in the text. The thickness, modulus, Poisson's ratio and compressive strength are from the E glass test data. Shear modulus and shear strength (resin dominated properties) are from F584/IM6

TABLE I MONOLAYER PROPERTIES

MATERIAL	$t_{nom}$ (in)	$E_L$ (MSI)	$E_T$ (MSI)	$\nu_{LT}$	$G_{LT}$ (MSI)	$F_L^t$ (Ksi)	$F_L^c$ (Ksi)	$F_T^t$ (Ksi)	$F_T^c$ (ksi)	$F_{SH}$ (Ksi)
F584/IM6 Tape	.0057	23.0	1.25	.33	.7	343.4	202.7	7.1	37.4	20.2
F584/IM6 Cloth	.0170	10.1	10.1*	.071	.55	142.8	86.4	142.8*	86.4*	16.7
F584/"E Glass"	.0061	2.1	2.1*	.18	.7*	51.0*	65.3	51.0*	65.3*	16.7*
F584/"S Glass"	.0061*	3.6*	3.6*	.18*	.7*	120.0*	150.0*	120.0*	150.0*	16.7*

\*Estimated Property



tape and cloth test results. The tension strength is an estimated value based on data from MIL-HDBK-17. Properties for the F584/"S2 glass" are all estimated based on the E glass numbers and the relative strengths of the E glass and S2 glass fibers as reported by the manufacturer.

Table II presents laminate properties for four basic layup patterns used throughout the fuselage design. Most values are derived from the Group A test results. Calculated values (denoted by asterisks) were obtained from STRENGTH, a Douglas computer code which calculates elastic and strength properties from monolayer data. Assumed values (denoted by plusses) are based on the assumption that laminates with equal number of 0's and 90's will have equal longitudinal (X) and transverse (Y) in-plane properties. The omitted C values for layup #1 stem from the lack of any joint testing for this layup; all joints are intended to be made through the "padded up skin" (layup #2). The omitted loaded hole C factor for layup #3 is a result of the absence of any loaded hole test specimen for this laminate which failed in net section tension. (See test results in Appendix A for the narrow double lap tension specimens).

Tested moduli and strength values presented in Table II were generally in good agreement (within 10%) with the values predicted by STRENGTH. Exceptions include the tensile modulus and tensile strength for laminate #1 (14% and 17% low respectively), and the compressive strength for laminate #4 (13% high). Nevertheless, there exists a certain amount of doubt about the accuracy of the unnotched tension specimen results. These specimens were "dogboned" in an attempt to avoid failures at the grips (of the test machine), however none of these specimens actually failed at the minimum cross-section. These specimens have been redesigned, fabbed and are awaiting testing.

Bearing "yield" and ultimate strengths were determined from double lap tension (DLT) specimens with a W/D of 6. The "onset of nonlinearity" was estimated from the load/deflection plots for each of these specimens (see Figures 41-44) and the average of these values assumed to be the bearing

"yield" strength. The maximum load obtained by these specimens, (which as can be seen from the load/deflection plots was after considerable hole deformation), divided by the bearing area is given as the ultimate bearing strength.

C factors presented in Table II were calculated from the unloaded hole tension (ULT) and double lap tension (DLT) specimen results using the tensile strengths determined from the suspect unnotched tension specimens. When the data from the redesigned specimens is available, the C factors will be adjusted accordingly. Loaded hole C factors were obtained from specimens with a width to bolt diameter ratio (W/D) of 3, unloaded hole values from specimens with a W/D of 4. It has been shown that both the W/D ratio and the absolute hole size can affect the effective C factor. Caution must therefore be exercised if using these values for W/D ratios or bolt sizes which deviate significantly from those tested.

The most suprising value given in Table II is the unloaded hole C factor for laminate #3 of zero, implying the lack of any stress concentration whatsoever. A low C factor for such a high percentage zero's (or low percentage 45's and 90's) laminate can best be explained by envisioning the specimen as three "strips" (2 on either side of the hole and the 3rd "interrupted" by the hole), tied together by a very "soft" shear connection. The limiting case of such an analogy, where the shear stiffness of the connection goes to zero, would in fact result in the absence of any stress concentration. Examination of the failed unloaded hole tension specimens for layup #3 reveal longitudinal splitting along the edge of the hole and a large amount of delamination. This suggests the possibility of non-catastrophic "failures" having occurred below the ultimate failure load, serving to "decouple" the laminate and thus eliminate the stress concentration. If this is the case, then it is not even proper to speak of a C factor for this laminate, as the failure mode has changed from that for which the theory was developed. Likewise it seems quite possible that the interaction between bearing and bypass loads might take on a different form for this laminate.

TABLE II LAMINATE PROPERTIES

LAYUP ±0°/±45°/±90° APPLICATION			PROPERTIES												
			E <sub>x</sub> (MSI)	E <sub>y</sub> (MSI)	ν <sub>xy</sub>	G <sub>xy</sub> (MSI)	F <sub>x</sub> <sup>tu</sup> (KSI)	F <sub>x</sub> <sup>cu</sup> (KSI)	F <sub>y</sub> <sup>tu</sup> (KSI)	F <sub>y</sub> <sup>cu</sup> (KSI)	F <sub>sh</sub> (KSI)	F <sub>bry</sub> (KSI)	F <sub>bru</sub> (KSI)	C <sub>Th</sub>	C <sub>uh</sub>
#1	33/33/33 12 ply tape	Basic Skin	8.6	8.6+	.205	2.4*	113.0	84.0	113.0+	84.0+	43.0*	-	-	-	-
#2	25/50/25 16 ply tape	Skin Pad-up	8.0	8.0+	.33	3.3*	118.4	78.0	118.4+	78.0+	58.0*	110000	167000	.31	.29
#3	60/20/20 20 ply tape & cloth	H1-Load longeron at splices	12.1	6.2*	.25	1.5*	168.2	106.0	84.0*	54.0*	28.0*	90000	140000	-	0.0
#4	33/33/33 6 ply cloth	Basic longeron	8.3	8.3+	.18	1.9*	114.4	80.7	114.4+	80.7+	35.0*	91000	147000	.33	.20

\* Calculated Value  
+ Assumed Value

Layup Patterns: #1 (0,90,45,0,-45,90)<sub>s</sub> t<sub>nom</sub> = .0684  
#2 (0,90,45,-45,0,45,-45,90)<sub>s</sub> t<sub>nom</sub> = .0912  
#3 (0/90,0,0,±45,0,0,0/90)<sub>s</sub> t<sub>nom</sub> = .1476  
#4 (0/90,±45,0/90)<sub>s</sub> t<sub>nom</sub> = .1020

### Joints

Bearing bypass curves for uniaxial tension have been generated from the Group A test results for laminates #2, #3 and #4 and are presented as Figures 27 through 30. These curves are calculated for a W/D ratio of 4 and 3/16 inch diameter protruding head fasteners. Curves for both single and double shear are given for laminate #2.

Comparison of the unloaded hole strengths from the curves with the "ULT" specimen test results presented in Appendix A will reveal that these points are simply average test values, as the tests were conducted at a W/D of 4. The loaded hole tests, on the other hand were conducted at a W/D ratio of 3. The assumption is made that the loaded hole C factor is the same for width to diameter ratios of 3 and 4. The fact that it is impossible to directly obtain  $C_{1h}$  for a W/D of 4 for these laminates is evidenced by the presence of a "bearing cutoff" on each of their bearing/bypass curves. In other words, if the double lap tension (DLT) specimens had been tested at a W/D of 4, they would have failed in bearing rather than net section tension.

As was pointed out in the discussion of the laminate properties presented in Table II, no loaded hole C factor was determined for laminate #3. This again, was because this laminate is bearing critical even at a width to diameter ratio of 3. In the absence of a test result, Figure 29 presents the bearing bypass curve for laminate #3 assuming limits on  $C_{1h}$  of 0.0 and .25. The crosshatched area illustrates the portion of the strength envelope which is affected by this assumption.

The single shear curve for laminate #2 (Figure 28) was developed using an extension of the theory used to predict load/deflections slopes for single shear joints. With this methodology the moment induced by the eccentricity of a single shear joint is considered to be reacted partly by the nut and head of the bolt (bearing against the outer faces of the joint members), and partly by a nonuniform bearing stress distribution through the thickness of each member (see Figure 31). The fraction of the moment

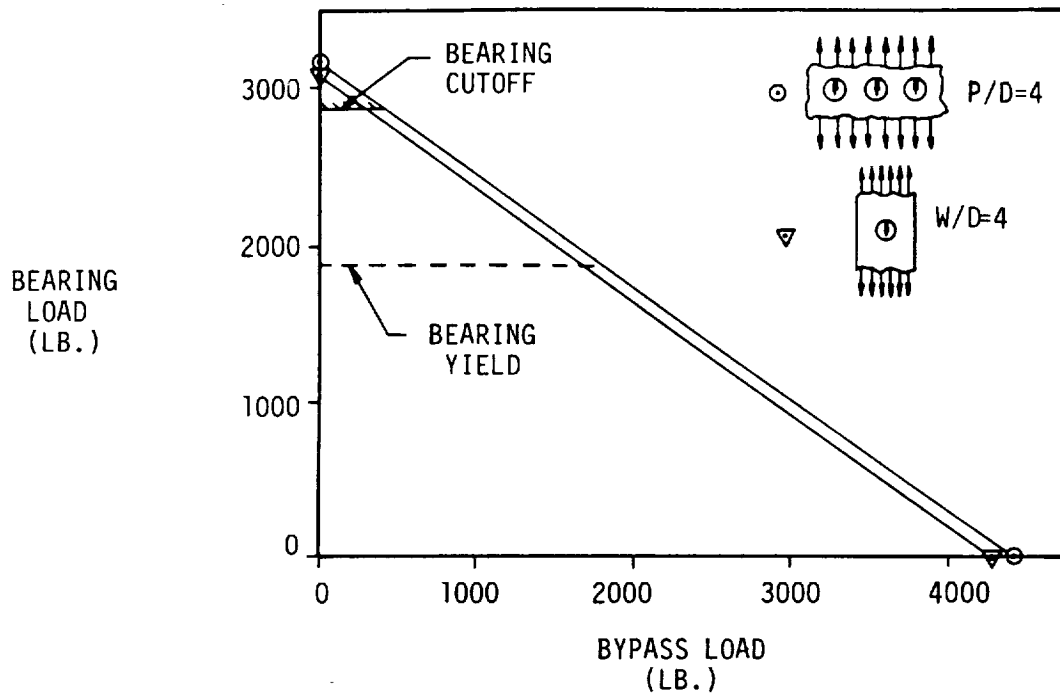


FIGURE 27. BEARING BYPASS CURVES FOR DOUBLE SHEAR, LAYUP #2  
3/16 PROTRUDING HEAD FASTENERS

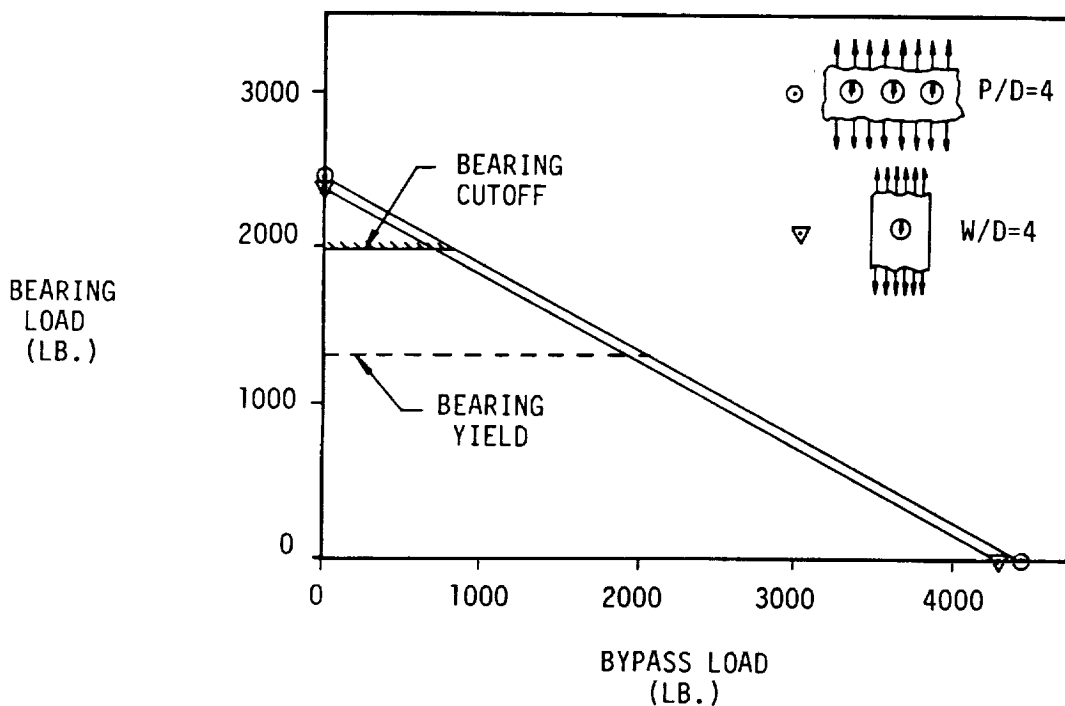


FIGURE 28. BEARING BYPASS CURVES FOR SINGLE SHEAR, LAYUP #2  
3/16 PROTRUDING HEAD FASTENERS ( $\beta = .15$ )

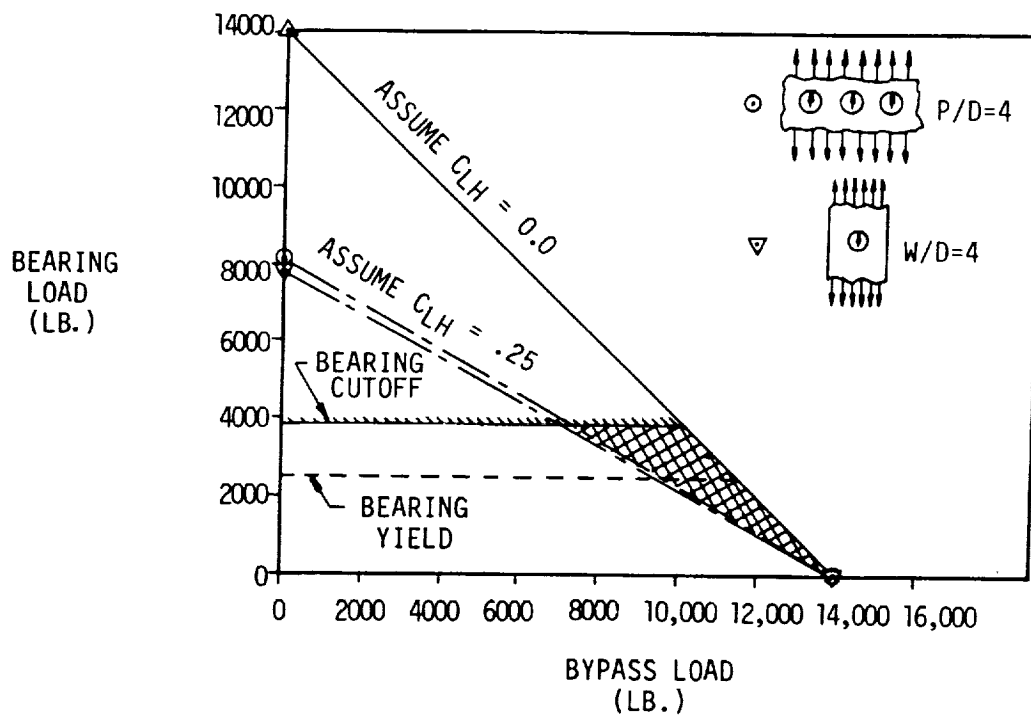


FIGURE 29. BEARING BYPASS CURVES FOR DOUBLE SHEAR, LAYUP #3  
3/16 PROTRUDING HEAD FASTENERS

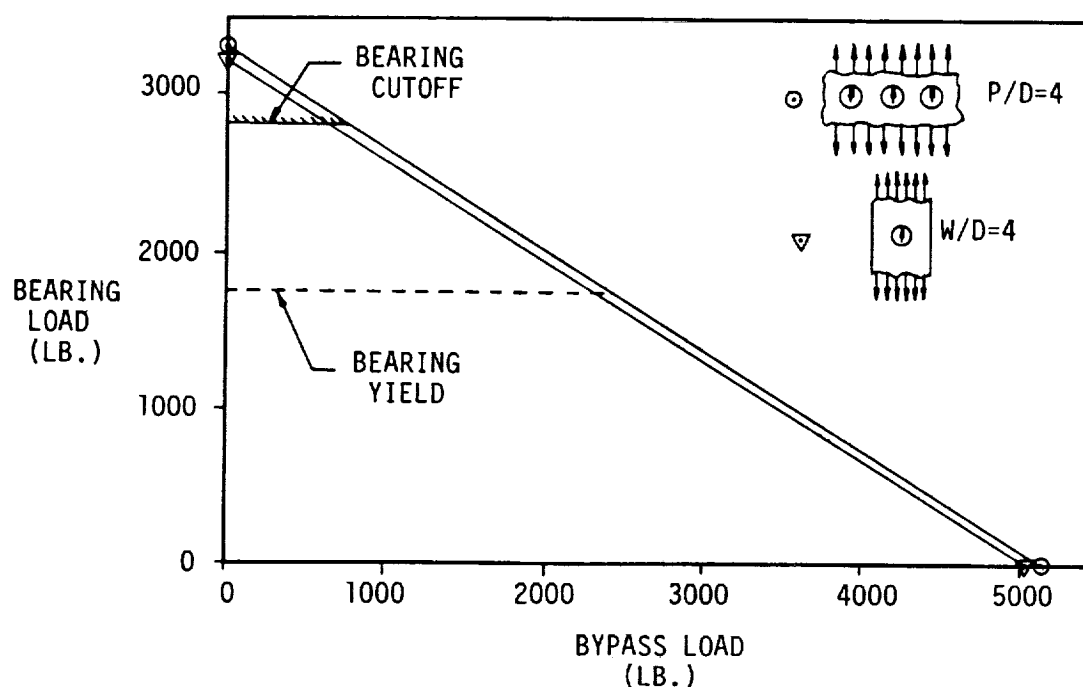


FIGURE 30. BEARING BYPASS CURVES FOR DOUBLE SHEAR, LAYUP #4  
3/16 PROTRUDING HEAD FASTENERS

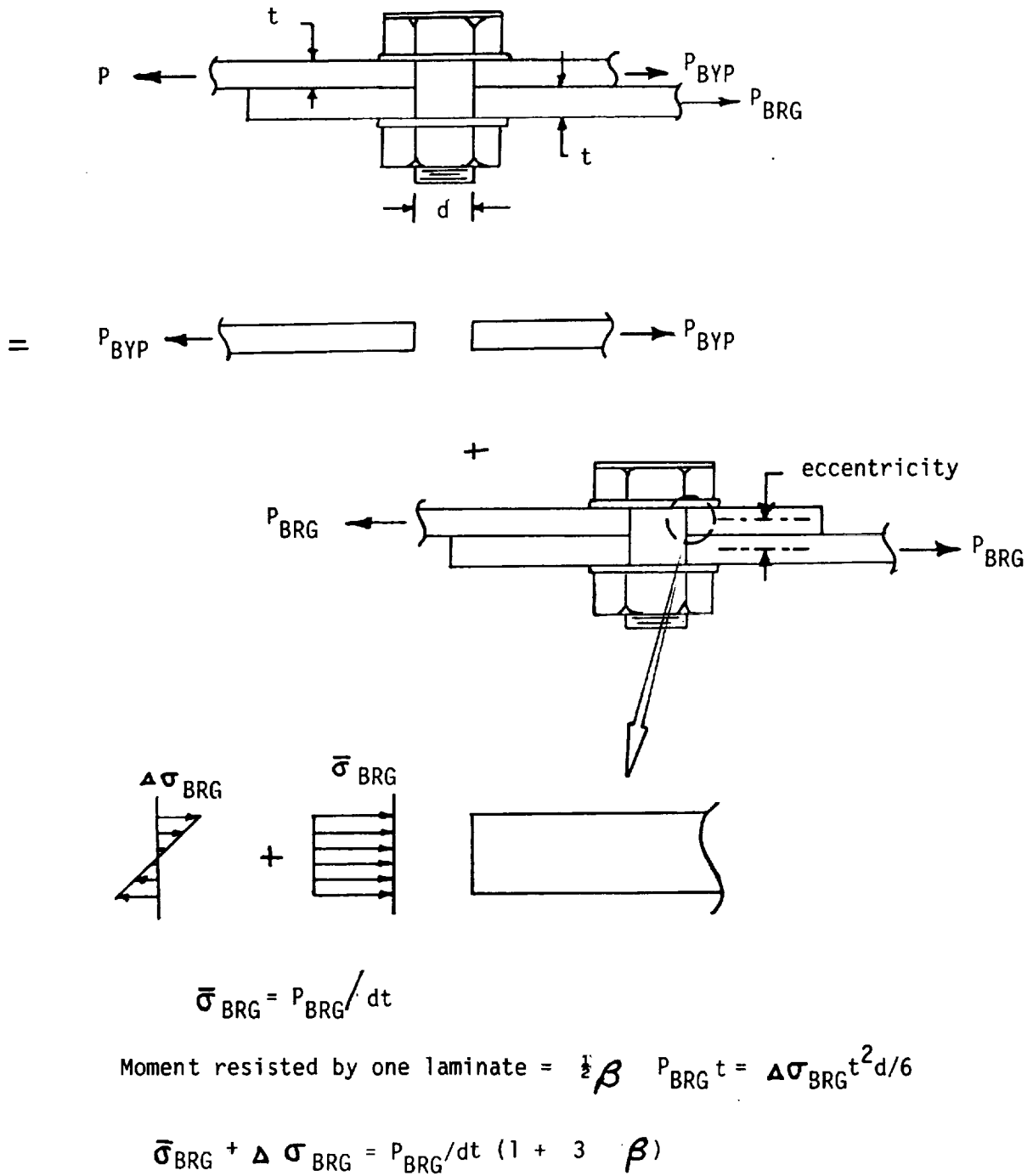


FIGURE 31. SINGLE SHEAR BEARING DISTRIBUTION

reacted by the nonuniform bearing stresses is defined as  $\beta$ . It can be shown (assuming the variation of bearing stress is linear), that the peak bearing stress is a factor of  $1 + 3\beta$  times the average bearing stress. Extending this logic allows that the peak tangential tensile stress (occurring at the "side" of the hole) for the single shear, loaded hole case is magnified by this same factor. Therefore the effective elastic stress concentration factor must be given by

$$K'_{te} = K_{te} (1 + 3\beta)$$

The unloaded hole concentration factor (for bypass loads) is assumed to be unchanged. Application of these equations to the results of the single shear test of laminate #2 with protruding head fasteners (SLT-505) suggests good agreement at  $\beta = .15$  (see Figure 32). This result is consistent with the findings of Bunin (Reference 1) which suggested a  $\beta$  of .15 for specimens with relatively small washers and a diameter to thickness ratio of 2.

A general comparison of the four curves reveals that all are bearing critical for the single fastener joint. For a two fastener joint with equal load sharing, only laminate #3 would remain bearing critical, although both laminate #4 and the single shear configuration of laminate #2 would reach bearing yield before failing in net section tension. Of the four, laminate #3 obviously is the strongest, although tailoring of the joint (to achieve a high bypass/low bearing condition at the critical fastener) would be necessary to realize really large benefits.

The same information is presented in generalized form in Figures 33 through 35. Figure 33 illustrates how the information from a bearing bypass curve for a given width to diameter (or "pitch" to diameter) ratio is plotted on the generalized curves. Point A is the bearing cutoff and the strength of a single row joint. Point B is at the "heel" of the bearing bypass curve where theoretically, the critical fastener in a multi-row joint would fail simultaneously in bearing and net section tension. Points C, D, and E are points on the failure envelope with



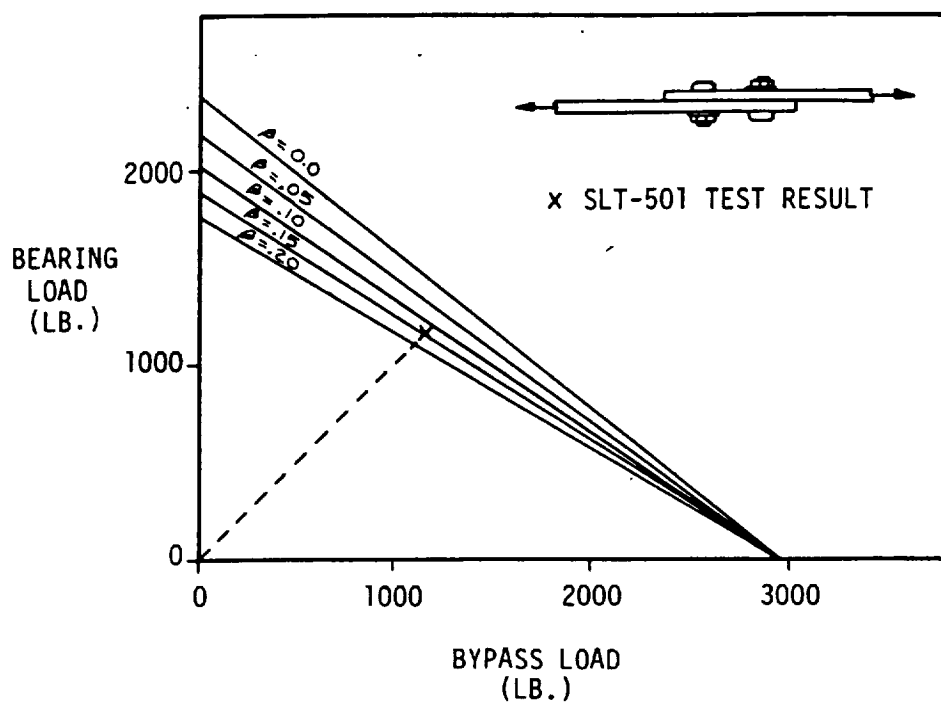
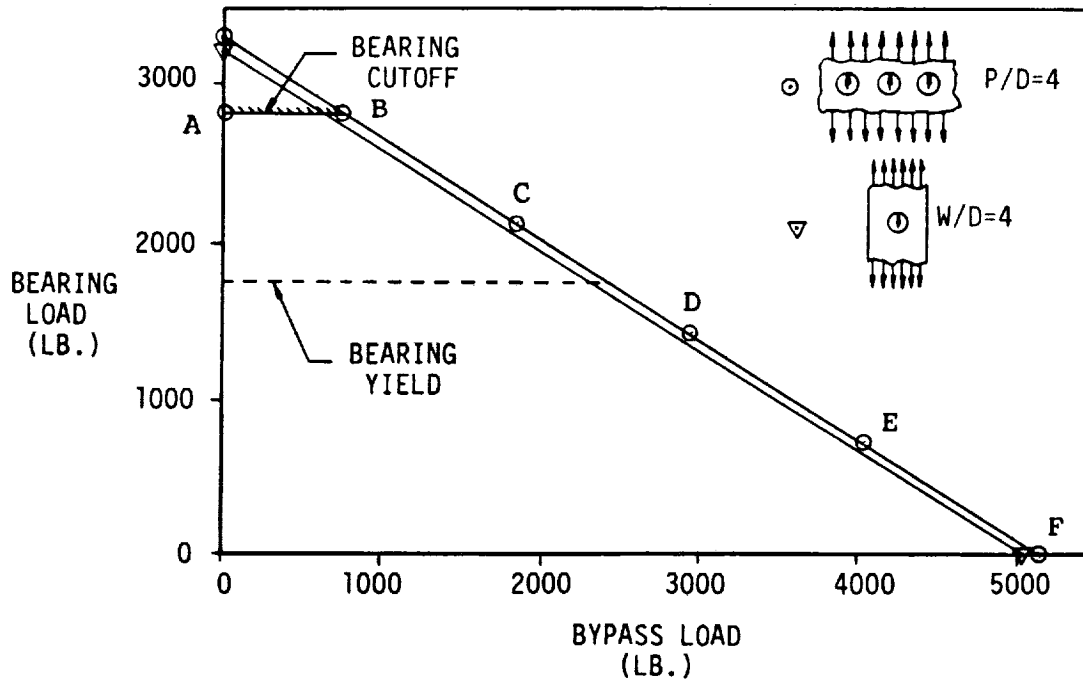
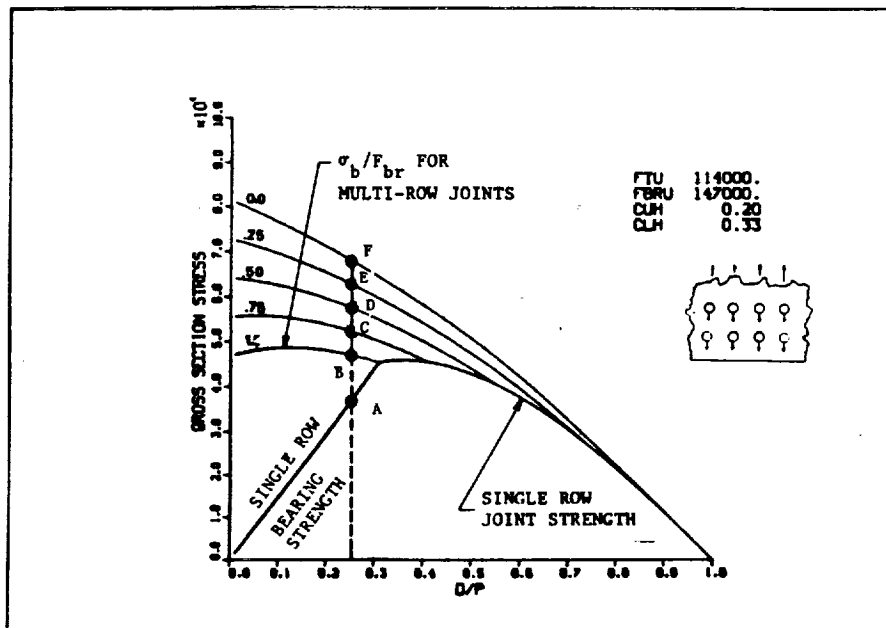


FIGURE 32. CORRELATION OF SINGLE SHEAR BEARING BYPASS  
CURVE WITH TEST RESULTS



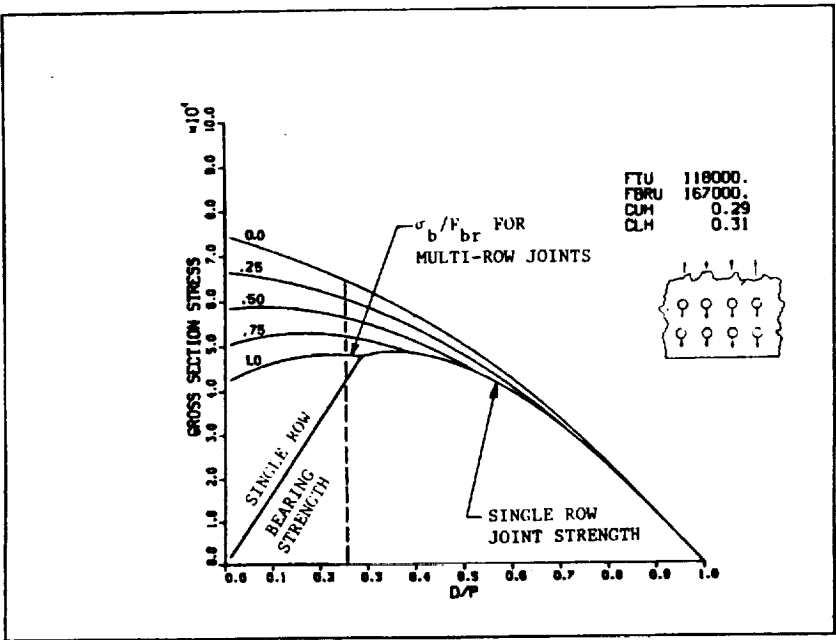
a) BEARING/BYPASS CURVE,  $P/D=4$



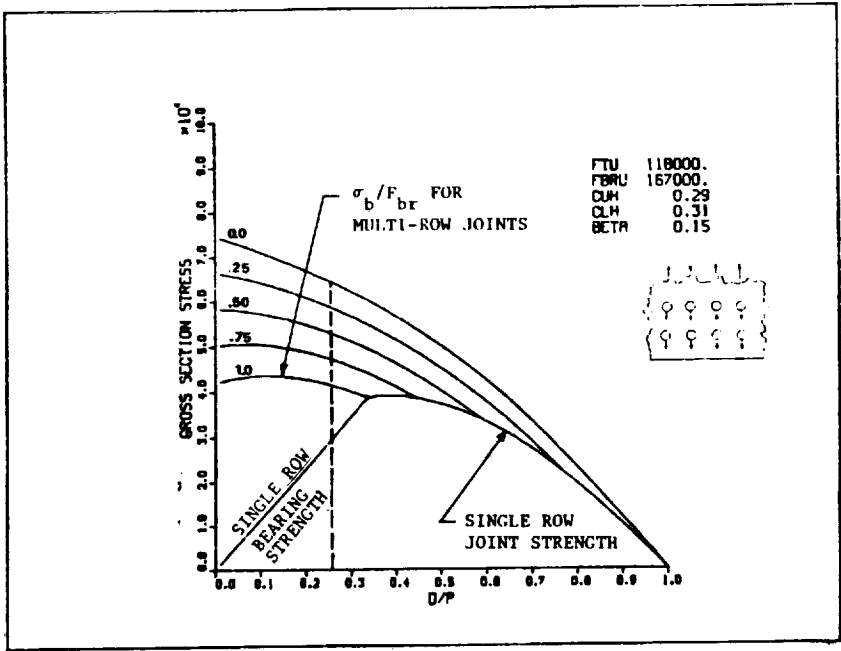
b) JOINT STRENGTH CURVE

FIGURE 33.

JOINT STRENGTH VERSUS BOLT SPACING  
FOR LAMINATE #4



a) LAYUP #2, DOUBLE SHEAR



b) LAYUP #2, SINGLE SHEAR

FIGURE 34. JOINT STRENGTH VERSUS BOLT SPACING FOR LAMINATE #2

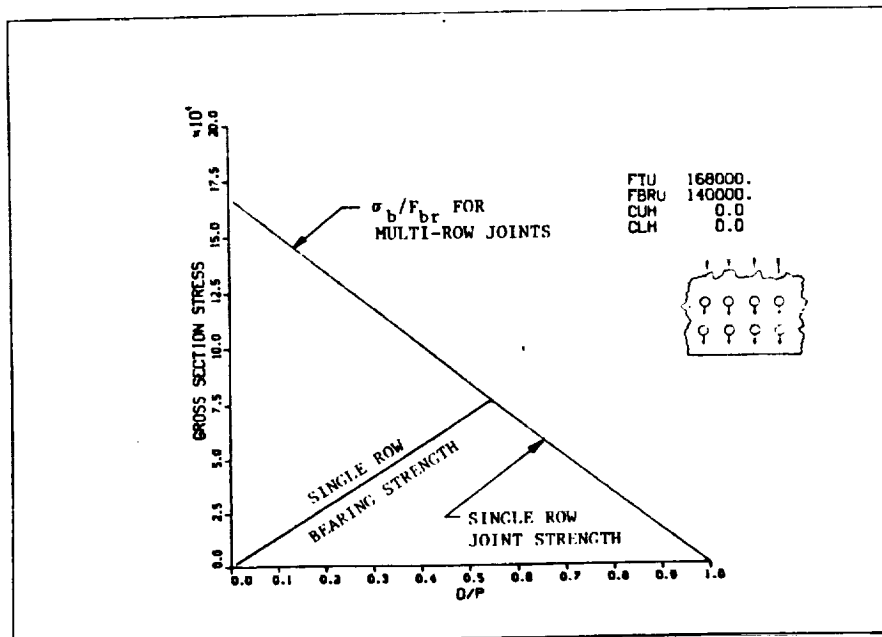
increasing levels of bypass load (or decreasing levels of bearing load), at the critical fastener. Point F is the theoretical upper limit for a joint with a  $P/D$  of 4. Physically it represents the case where the "critical fastener" is simply an open hole, and the joint strength is the unloaded hole tension strength.

The curves of Figures 33 through 35 are plotted using the  $C$  factors determined from testing at width to diameter ratios of 3 (loaded hole) and 4 (unloaded hole). As has been previously noted, these factors often vary with  $W/D$ , thus these curves should only be considered accurate for  $D/P$  ratios close to .3. Also, practical considerations would limit possible choices of bolt pitch to something between  $3D$  and  $10D$ . Consequently, the only real region of interest on these curves is a vertical "band" bounded roughly by  $D/P = .10$  and  $D/P = .30$ .

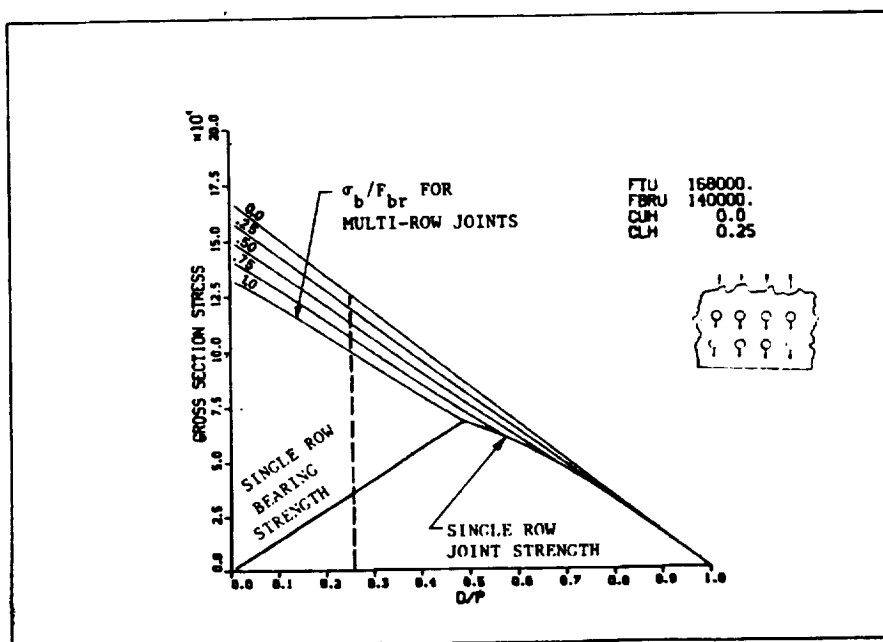
Curves are given for laminate #4 (Figure 33), laminate #2 for double and single shear (Figure 34), and laminate #3 for  $C_{1h} = 0.0$  and  $C_{1h} = .25$  (Figure 35).

Figure 35a appears to have a different form and is in fact, the same failure envelope as would be drawn for an equivalent (same ultimate tensile and bearing strengths) metal material. The lack of any stress concentrations (at failure) requires the strength of any joint not limited by the bearing cutoff, to be very simply, the net section strength of the critical member.

A general comparison of Figures 33 through 35 reveals that the "optimum"  $D/P$  ratio for single row joints varies from .35 (bolt pitch approximately  $3D$ ) for laminate #2 in double shear, to .55 (bolt pitch approximately  $1.8D$ ) for laminate #3 with  $C_{1h}$  equal to zero. The high bearing strength to tensile strength ratio of laminate #2 allows that the bearing strength has no effect on the optimum bolt pitch. The optimum is therefore a true optimum, where the benefits of additional bolts (increased capacity for load transfer) are balanced against the penalties of reduced net section and higher stress concentrations. The same behavior is evidenced by



a) LAYUP #3,  $C_{1h} = 0.0$



b) LAYUP #3,  $C_{1h} = 0.25$

FIGURE 35. JOINT STRENGTH VERSUS BOLT SPACING FOR LAMINATE #3

laminate #4 in Figure 33, this laminate also having a favorable ratio of ultimate bearing to tensile strength. Contrast this with Figures 35a and 35b where the "optimum" bolt pitch is that which, in essence, is finally narrow enough to overcome the tendency of these laminates to fail in bearing. (Note how the bearing critical line "cuts off" the net section critical curve before it reaches a peak). Again, however, practical designs would likely limit the bolt pitch to 4D. Consequently all of these laminates would be bearing critical and laminate #2, having the best balance of  $0^\circ$ ,  $90^\circ$  and  $\pm 45^\circ$  layers, would achieve the highest gross section stress. One must remember however, that these laminates are only available in discrete thicknesses (whole number multiples of the basic stacking sequence), and therefore the true optimum will actually be a function of the absolute design load.

Comparison of Figures 34a and 34b reveal the expected decrease in single fastener joint strength for all ratios of D/P. Note however, that multi-row joints, if designed such that the critical fastener is lightly loaded in bearing, can be made almost as strong in single shear as in double shear. This of course follows from the assumption used in the analysis, that stress concentrations for bypass loads are the same for both single and double shear configurations.

One further point to be made regarding these figures concerns the potential strength of multi-row joints. Laminate #3, being the most severely limited by bearing strength for the single row case, clearly shows the largest potential for increase. At a bolt pitch of 4D, the theoretical maximum for this laminate is roughly 125 ksi or 350% of its single fastener strength. Compare this to the same case of laminate #2 (double shear) where the theoretical maximum is about 150% of its single row strength.

Load deflection devices, developed under an independent Douglas program, are designed to measure the relative edge displacement of the joint members at points which are initially aligned with the fastener (see Figure 36). Photographs of test setups with the devices for single lap and double lap tension specimens are shown in Figures 37 through 39. Test results of specimens using the load/deflection devices are shown in Figures 40 through 44.

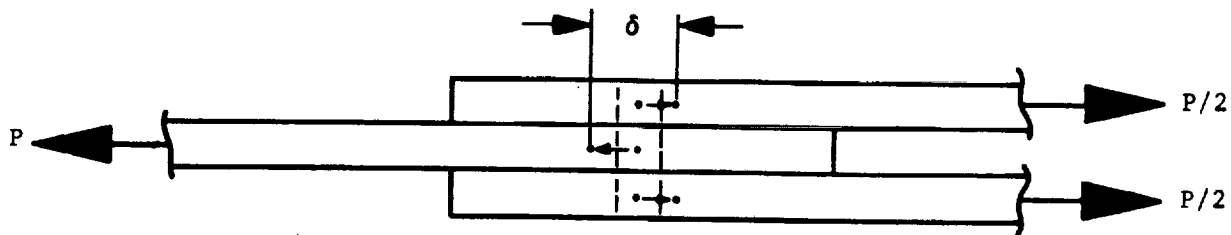


FIGURE 36. FASTENER FLEXIBILITY MEASUREMENT

The formula for predicting the linear portion of these load deflection curves, developed as part of the Critical Joints program (NASA Contract NAS1-16857) are given as:

$$\text{for single shear } \delta = P[C_{b_s} + (C_{b_{br}} + C_{p_{br}} + C_{s_{br}}) (1 + 3\beta)]$$

$$\text{for double shear } \delta = (P/2) (C_{b_s} + C_{bb} + C_{b_{br}} + 2C_{p_{br}} + C_{s_{br}})$$

The single shear equation includes terms for shear deformation of the bolt ( $C_{bs}$ ) bearing deformation of the bolt ( $C_{b_{br}}$ ) and bearing deformation of the "plate" and "splice" ( $C_{p_{br}}$  and  $C_{s_{br}}$ ). It also includes the factor  $1 + 3\beta$  to account for the incremental bearing stresses required to balance the eccentric moment of a single shear joint (see Figure 31). The double shear equation drops the eccentricity factor and adds a term to account for bolt bending ( $C_{bb}$ ). The expansion of these terms is given in Reference 1; it should be noted that the bearing terms will differ slightly for the single and double shear cases.

The equations in this form do not account for any width effects, and thus predict the same load/deflection slope for any width to diameter ratio. The measurements however, are taken at the edge of the specimens and therefore, include any additional displacement accumulated across the width. To account for this effect, the "plate" and "splice" bearing terms in these equations were replaced with  $C_{p_{fem}}$  and  $C_{s_{fem}}$ . These coefficients are then determined from simple finite element models and include the bearing deformation while also accounting for the width effects. An example of one of these models is shown in Figure 45.

Table III presents a detailed breakdown of the load/deflection calculations for the three laminates tested. Calculations are included for both the old and new methods for comparison. The difference between the values for  $W/D = 3$  and  $W/D = 6$  range from only 6% for laminate #2, single shear, to 16% for laminate #3. The values for laminate #2, both single and double shear, also agree quite well with those predicted by the old formulae. A large discrepancy however, exists for laminates #3 and #4. It is suggested that the old formulae cannot adequately account for the relatively low shear moduli of these laminates.

Predicted load/deflection slopes (using the modified technique) are plotted with the test data in Figures 40 through 43. No prediction is plotted for the single shear/countersunk results (Figure 44) because, as yet no satisfactory method of predicting these slopes has been developed.



TABLE III FASTENER FLEXIBILITY CALCULATIONS FOR TESTED LAMINATES

Laminate	$C_{bs}$ $\mu\text{in/lb}$	$C_{bb}$ $\mu\text{in/lb}$	$C_{bbr}$ $\mu\text{in/lb}$	$C_{pbr}$ $C_{sbr}$ $\mu\text{in/lb}$	$\delta/p^1$ $\mu\text{in/lb}$	W/D = 3		W/D = 6		$G_{xy}$ MSI
						$C_{p\text{fem}}$ $C_{s\text{fem}}$ $\mu\text{in/lb}$	$\delta/p^2$ $\mu\text{in/lb}$	$C_{p\text{fem}}$ $C_{s\text{fem}}$ $\mu\text{in/lb}$	$\delta/p^2$ $\mu\text{in/lb}$	
#2	.533	.134	2.056	1.266	3.261	1.372	3.420 (+5%)	1.540	3.672 (+13%)	3.30
#3	.862	.569	1.270	.757	2.486	1.620	3.728 (+50%)	1.979	4.319 (+74%)	1.55
#4	.596	.188	1.838	1.187	3.092	1.732	3.909 (+26%)	2.008	4.323 (+40%)	1.94
#2 Single Shear	.710	-	2.741	1.266	8.3563	1.372	81663 (+4%)	1.540	9.150 (+10%)	3.30

- 1 Calculated using  $C_{pbr}$  and  $C_{sbr}$
- 2 Calculated using modified formula with  $C_{p\text{fem}}$  and  $C_{s\text{fem}}$
- 3  $\beta = .15$

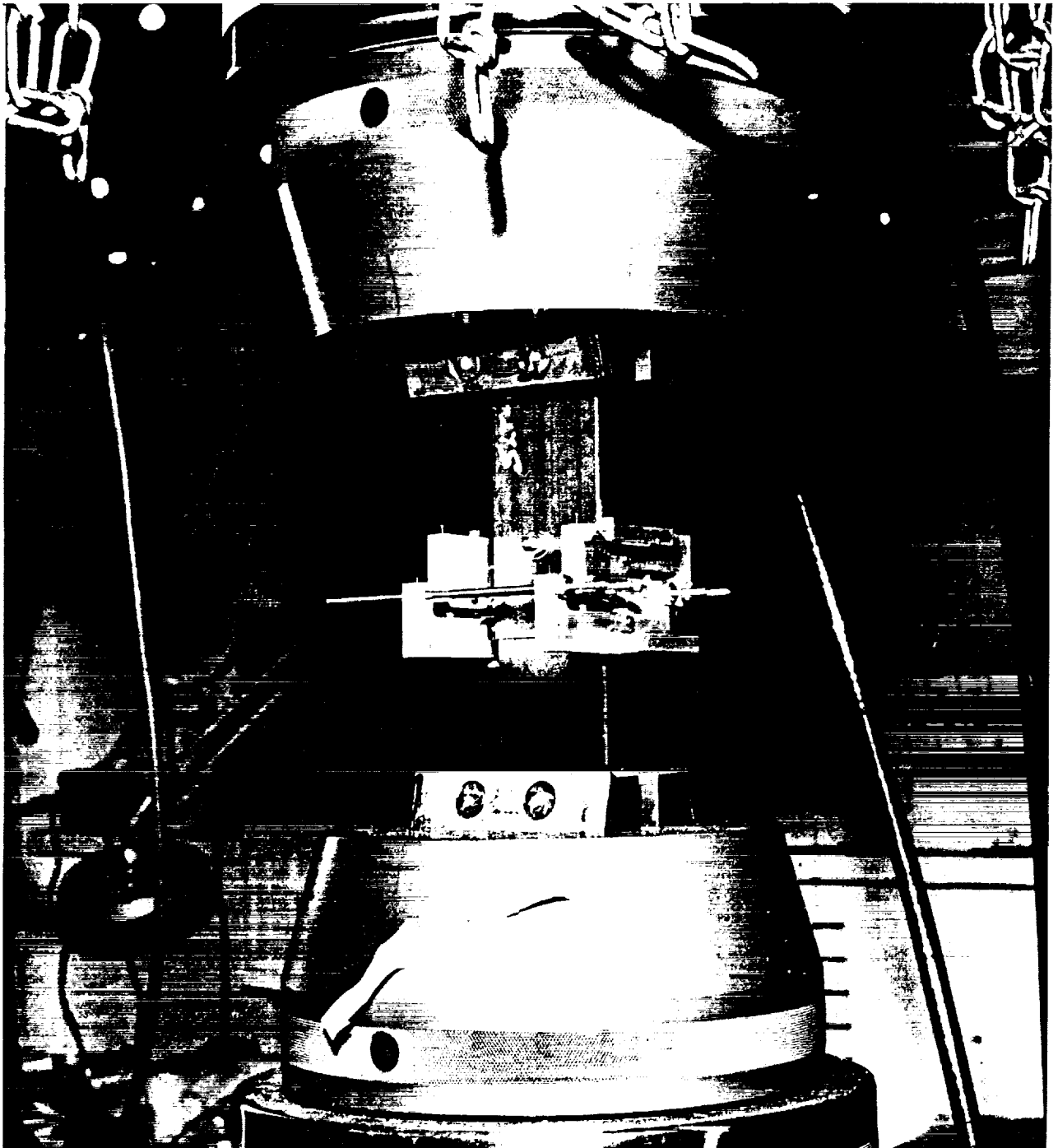


FIGURE 37. SINGLE LOAD/DEFLECTION DEVICE (EXTENSOMETER REMOVED)

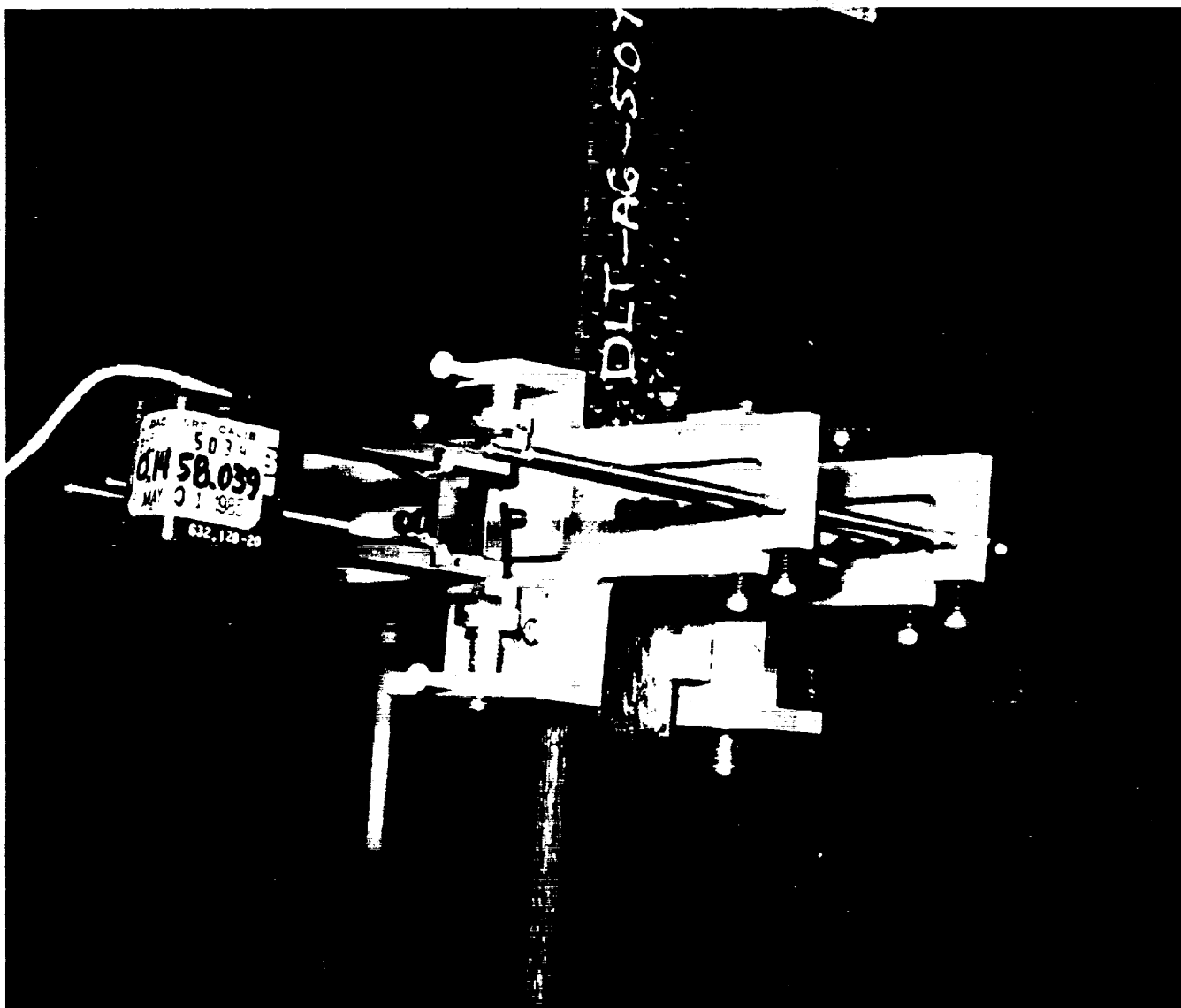


FIGURE 38. DOUBLE SHEAR DEVICE

ORIGINAL PAGE  
BLACK AND WHITE PHOTOGRAPH

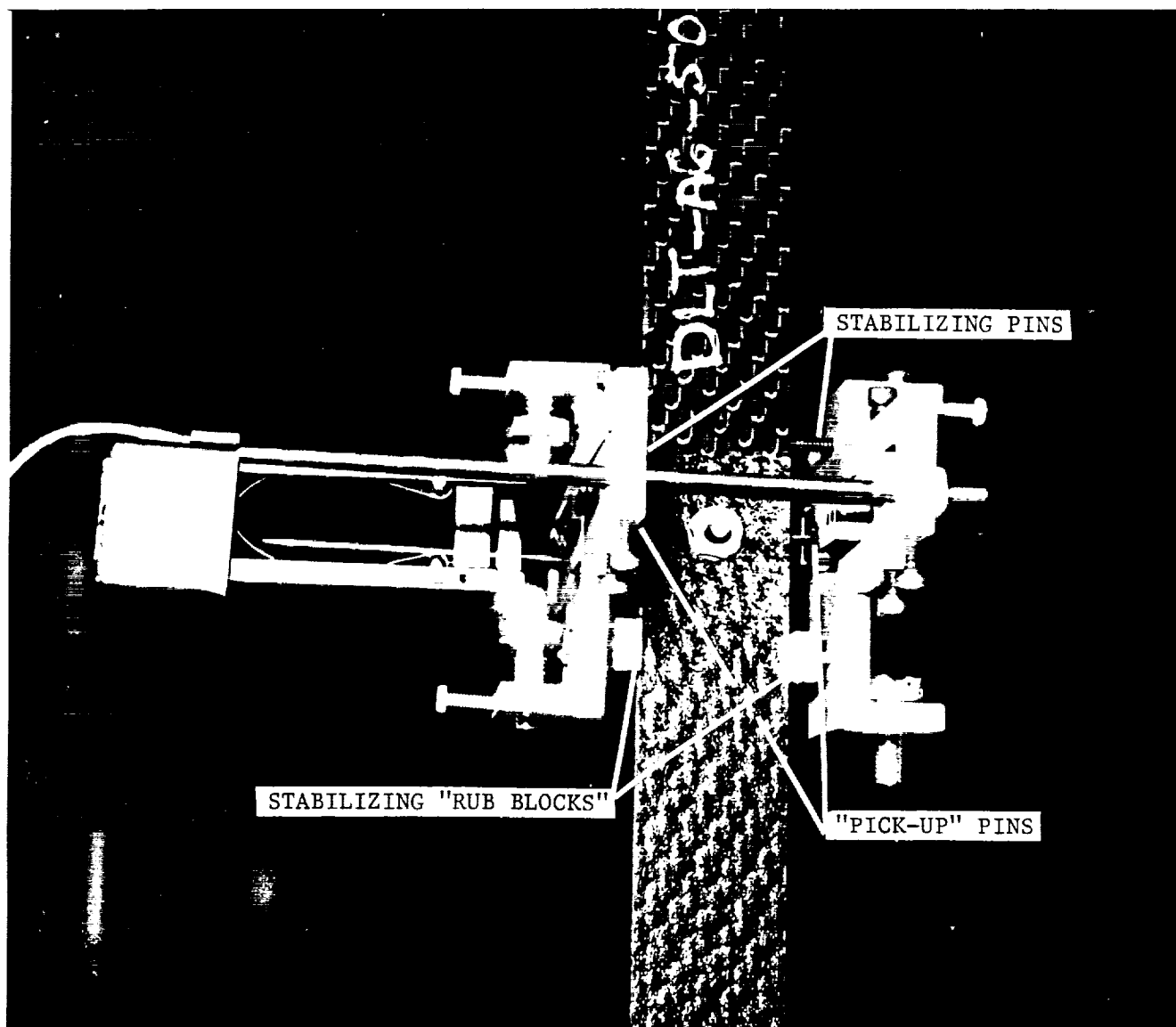


FIGURE 39. DOUBLE SHEAR DEVICE

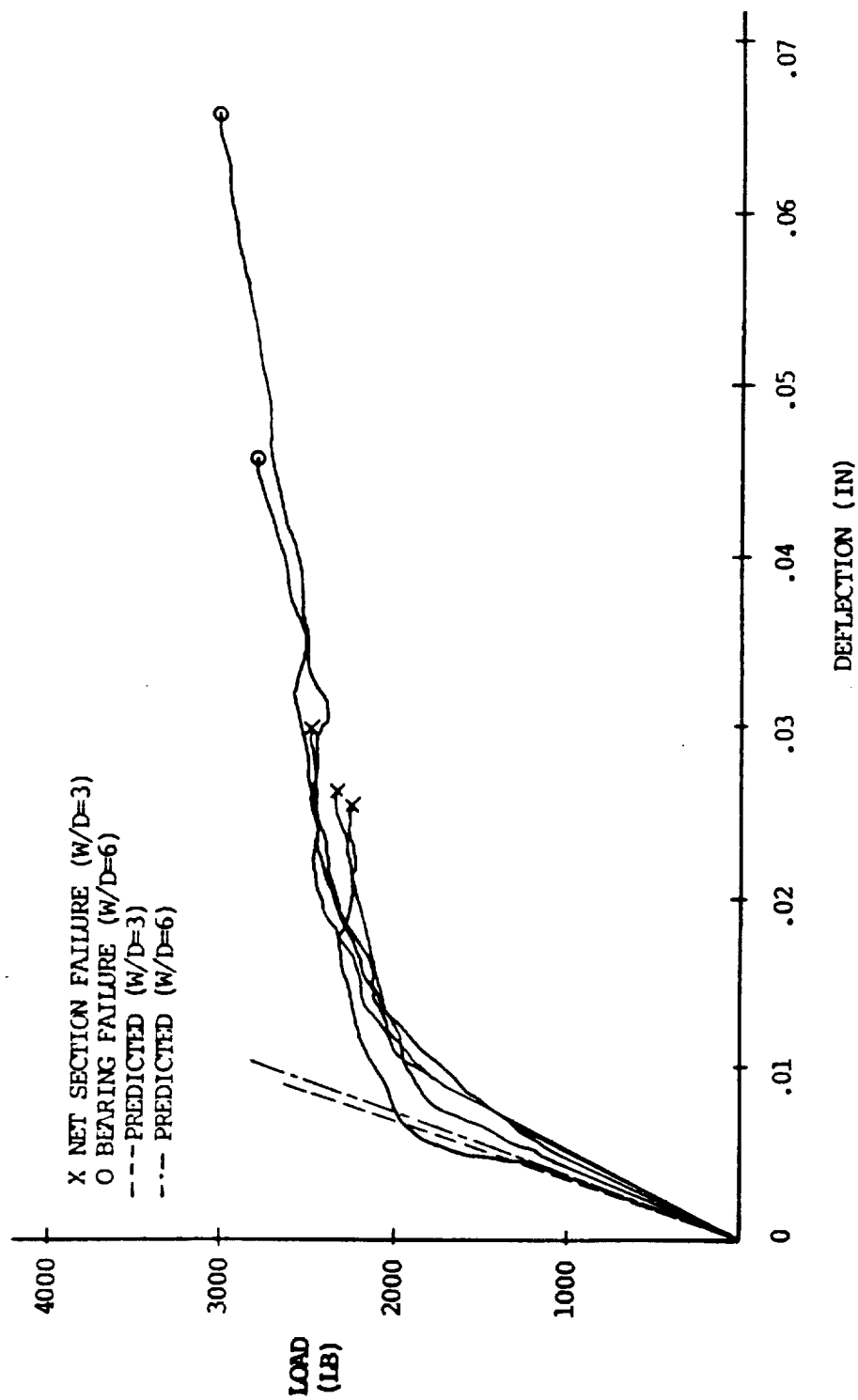


FIGURE 40 LOAD/DEFLECTION CURVE, DOUBLE SHEAR TENSION, LAMINATE #2 (25, 50, 25)

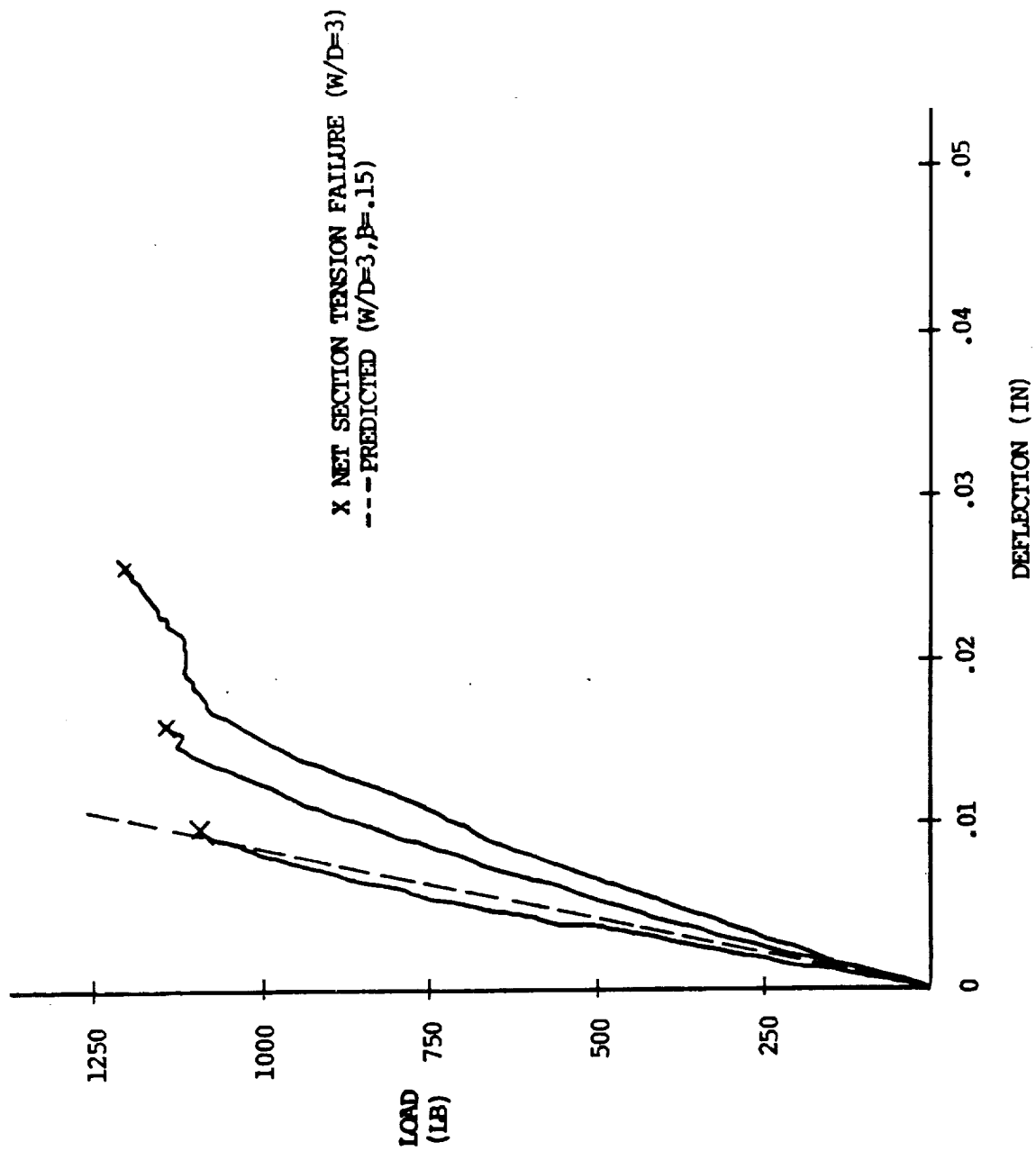


FIGURE 41 LOAD/DEFLECTION CURVE, SINGLE SHEAR TENSION, LAMINATE #2 (25,50,25)

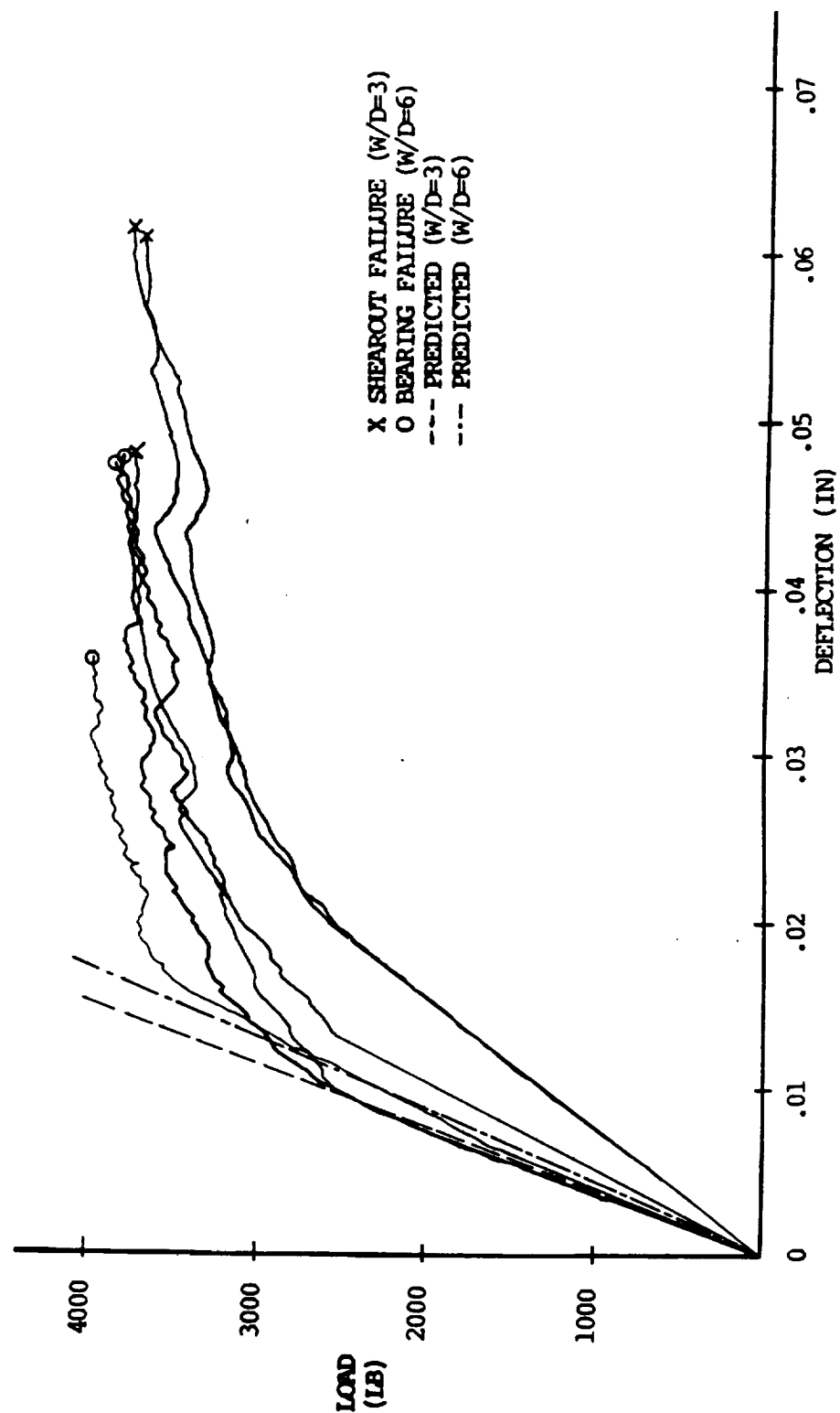


FIGURE 42 LOAD/DEFLECTION CURVE, DOUBLE SHEAR TENSION, LAMINATE #3 (60,20,20)

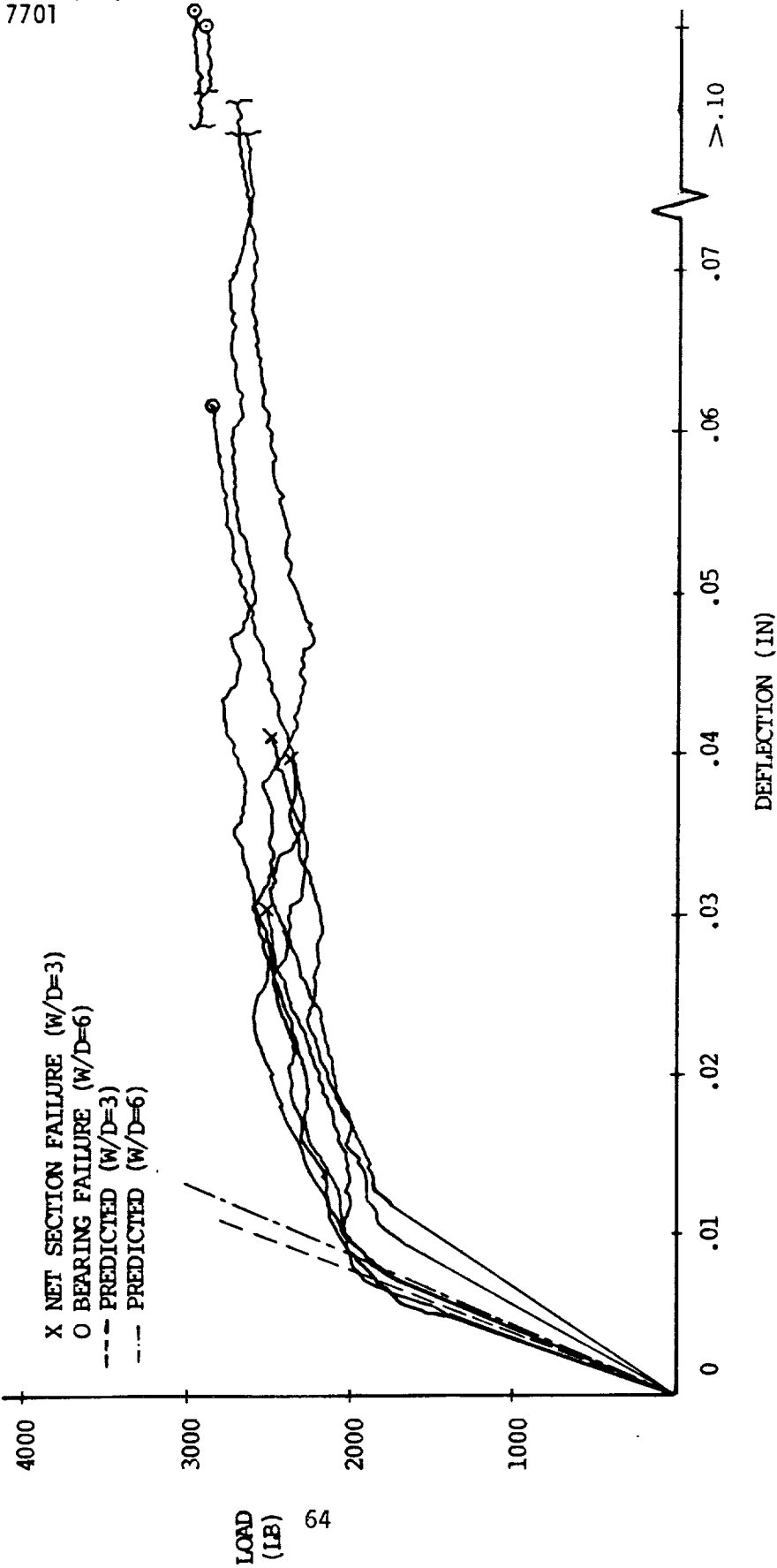


FIGURE 43 LOAD/DEFLECTION CURVE, DOUBLE SHEAR TENSION, LAMINATE #4 (33,33,33)



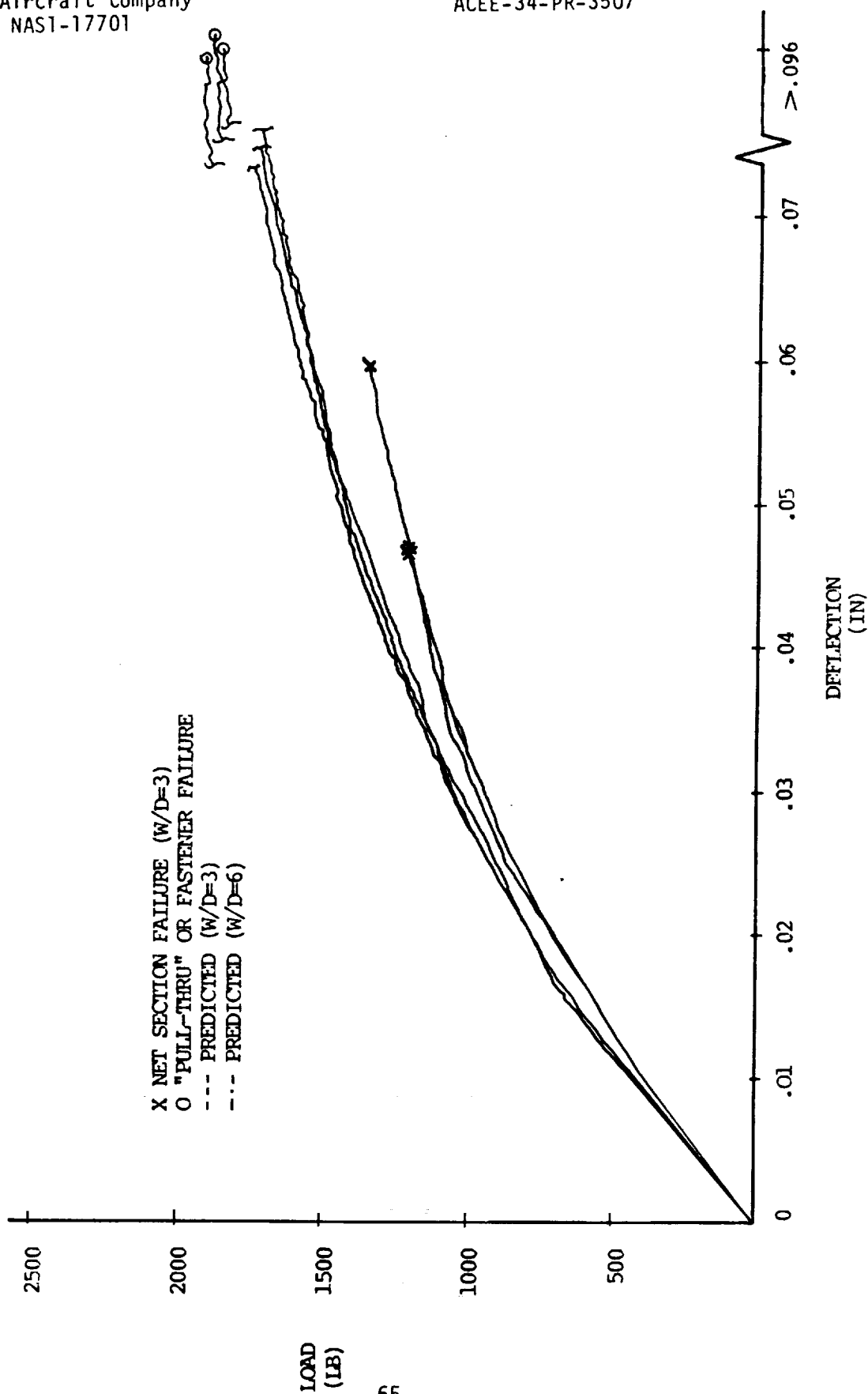
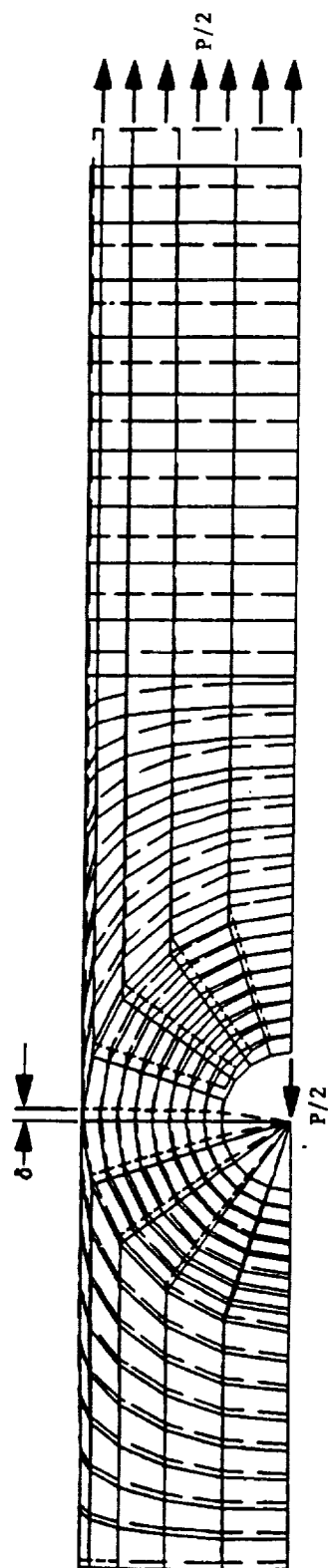


FIGURE 44 LOAD/DEFLECTION CURVE, SINGLE SHEAR TENSION, LAMINATE #2 (25, 50, 25), COUNTERSUNK



$$C_{p_{fem}} \text{ and } C_{s_{fem}} = \frac{\delta}{P}$$

FIGURE 45. FINITE ELEMENT MODEL FOR DETERMINING  $C_p$  and  $C_{s_{fem}}$

Cursory examination of these results reveal an appreciable amount of scatter, especially for laminates #3 and #4 (Figures 42 and 43). Possible sources of this scatter include variations in hole quality and fastener fit, and perhaps more significant, inaccuracies in the load/deflection measurements themselves. It is observed that the "stiffest" of the curves recorded for each laminate correlate quite well with the predictions, with the scatter spread out below. It seems reasonable to assume that the "better fit" fasteners would indeed exhibit stiffer load/deflection characteristics with any irregularities serving to soften the connection. Likewise, if the "stabilizing blocks" and "stabilizing pins" shown in Figure 39 were over-tightened, the measured stiffness would tend to be less, as the device would effectively be measuring the accumulated relative displacement between the "blocks" and "pins" rather than the fastener.

There seemed to be no real pattern to the relative stiffnesses of the load/deflection measurements for the narrow ( $W/D = 3$ ) and the wide ( $W/D = 6$ ) specimens. The wide scatter of the results for both types of tests effectively rendered the small difference in their predictions inconsequential. Interestingly enough, the countersunk specimens (Figure 44) exhibited the most consistent results. Work is continuing in an effort to develop a relation for the load/deflection characteristics of these joints. It should be noted that the linear portion of the curves for these specimens is much shorter than for the equivalent joints with protruding head fasteners. This is consistent with the notion that the high bearing stresses present at the "flat" of a countersunk joint member result in permanent bearing damage at relatively low load levels.

Concurrent with the efforts to characterize the load/deflection characteristics of single shear/countersunk joints, work is underway to attempt to develop bearing bypass interactions for the same. Unlike the single shear joint with protruding head fasteners, the two members (one countersunk, one not) must be treated separately. In an attempt to gain some insight into the complex bearing distribution of these joints, a simple 2D representation of such a connection was generated using NASTRAN.

The deflected shape of this model is shown in Figure 46. Notice how the rotation of the fastener forces the countersunk head to bear on the "right" face. This phenomenon has the effect of adding to the (already) highly concentrated bearing stresses along the "left" face, especially in the area of the "flat". Similar work is underway to attempt to characterize the bypass distribution around a countersunk hole.

Another area of investigation concerns the strength of joints loaded in compression. Figure 47 illustrates a few of the important differences between tension and compression joints. First, the bearing distribution for a compression joint concentrates at the "front" of the hole, whereas the corresponding distribution for tension yields a peak tangential tension stress at the "side" of the hold. Second, the stress distribution for a compression bypass load is a function of the "fit" of the fastener. For the case where the fastener is loose, the stress distribution (concentration) is very likely similar to that for a tension bypass condition; for the ideal case where the fastener is "net fit", the load can be transferred through the fastener, reducing the stress concentration at the side of the hole, but introducing the possibility of a "bearing type" concentration at the front of the hole. Third, since compression failures are by their nature stability failures, the failure load for compression joints are strongly influenced by the degree of "clamp-up". Finally, while the failure modes for tension are relatively simple, (either bearing or net section tension) the failure modes for a laminated composite compression joint are more numerous and less clearly defined.

Figures 48, 49, and 50 present the results of the Group A unloaded hole compression (ULC) and double lap compression (DLC) tests. These are plotted with the corresponding tension bearing bypass curves to allow a comparison of the relative tensile and compressive strengths. The bearing "yield" and "ultimate" values for compression were obtained from double lap specimens with a width to hole diameter ratio of 6 and "splice plates" of the same layup and thickness as the center member. All of these specimens failed in the center member with little or no observable damage to the splice plates. (It has been observed that, when using composite

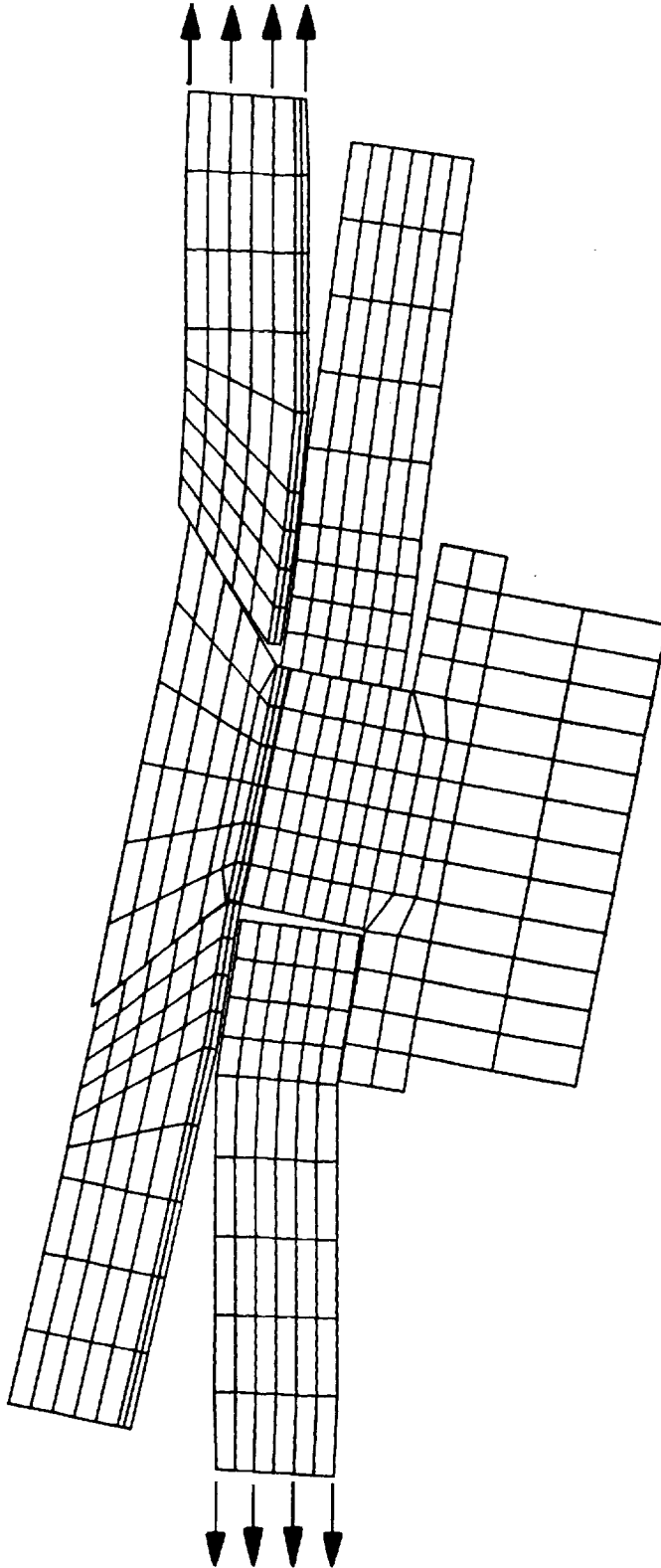
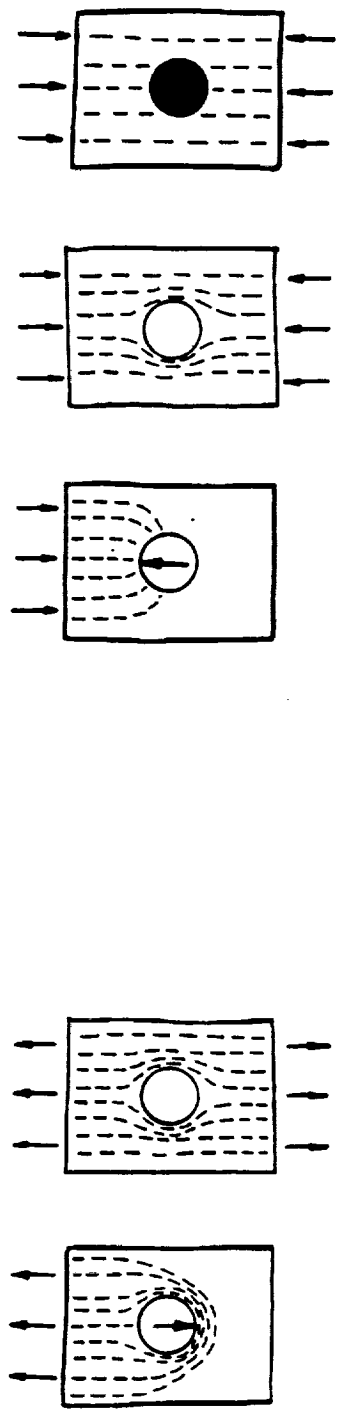


FIGURE 46. FINITE ELEMENT MODEL FOR A COUNTERSUNK, SINGLE SHEAR CONNECTION



TENSION

SIMPLE STRESS DISTRIBUTION

2 FAILURE MODES

COMPRESSION

STRESS DISTRIBUTION IS A  
FUNCTION OF FASTENER FIT

MULTIPLE FAILURE MODES

FAILURE INFLUENCED BY CLAMP UP

FIGURE 47. COMPARISON OF TENSION AND COMPRESSION JOINTS

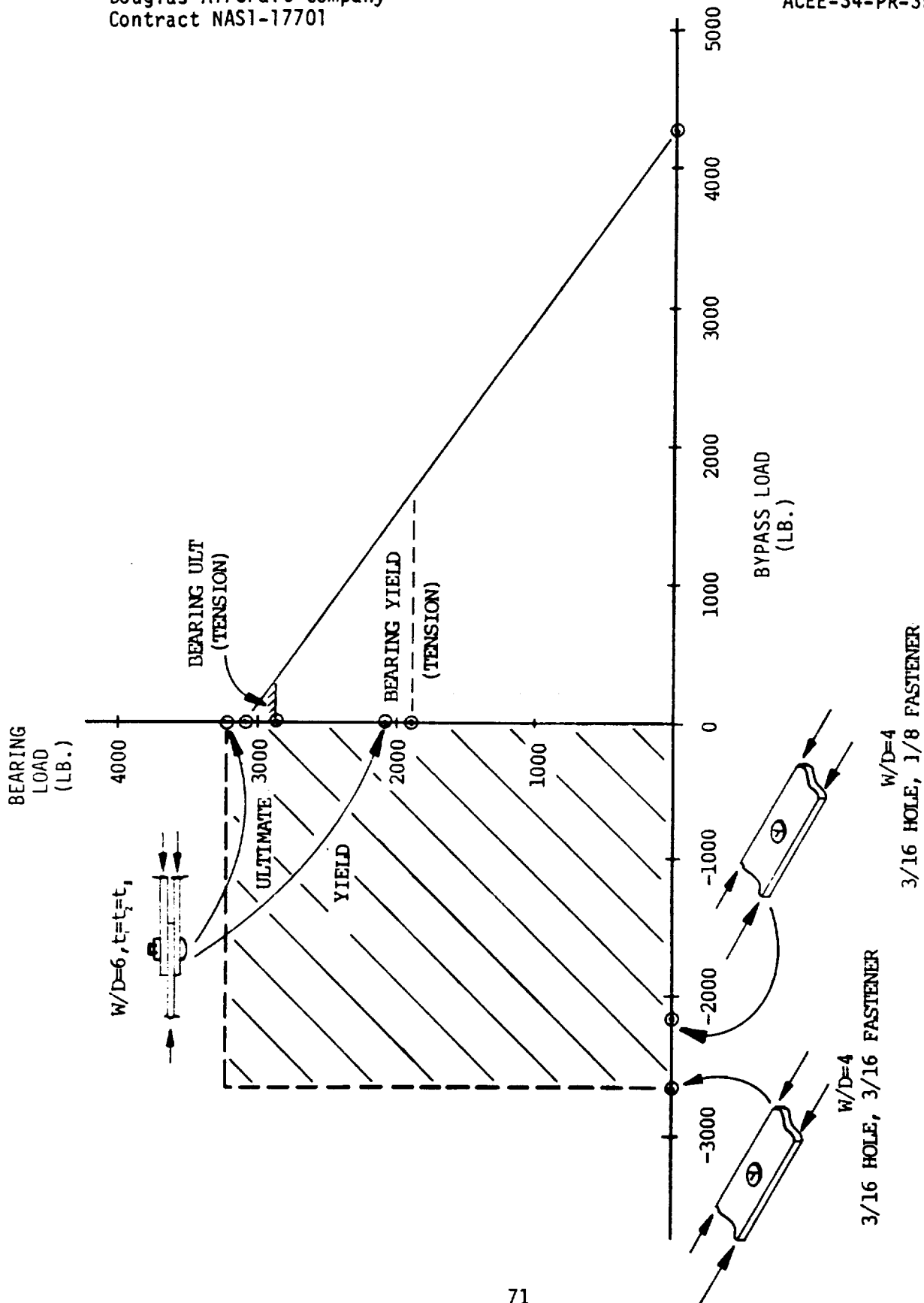


FIGURE 48. COMPRESSION JOINT TEST RESULTS - LAMINATE #2

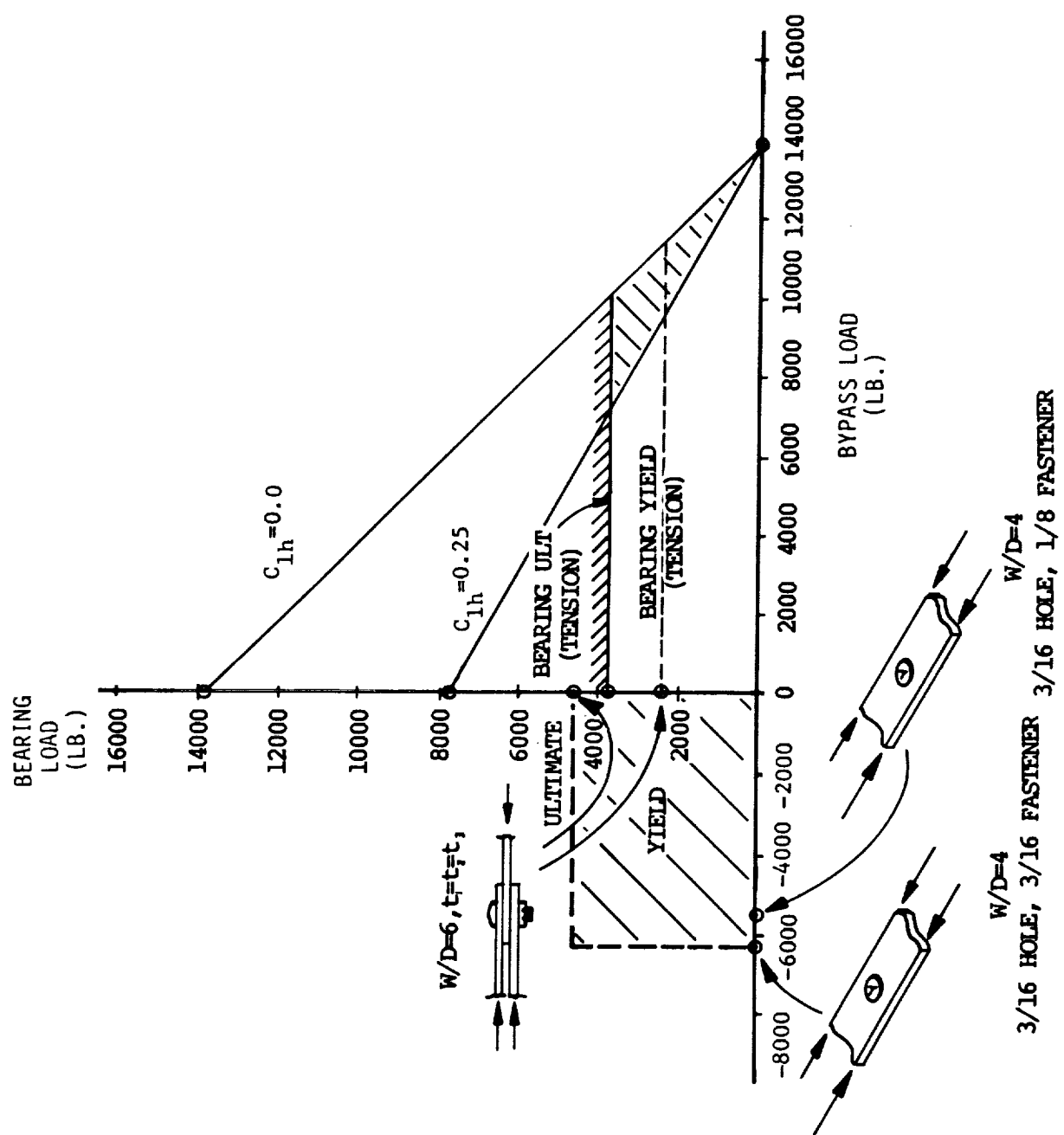


FIGURE 49. COMPRESSION JOINT TEST RESULTS-LAMINATE #3



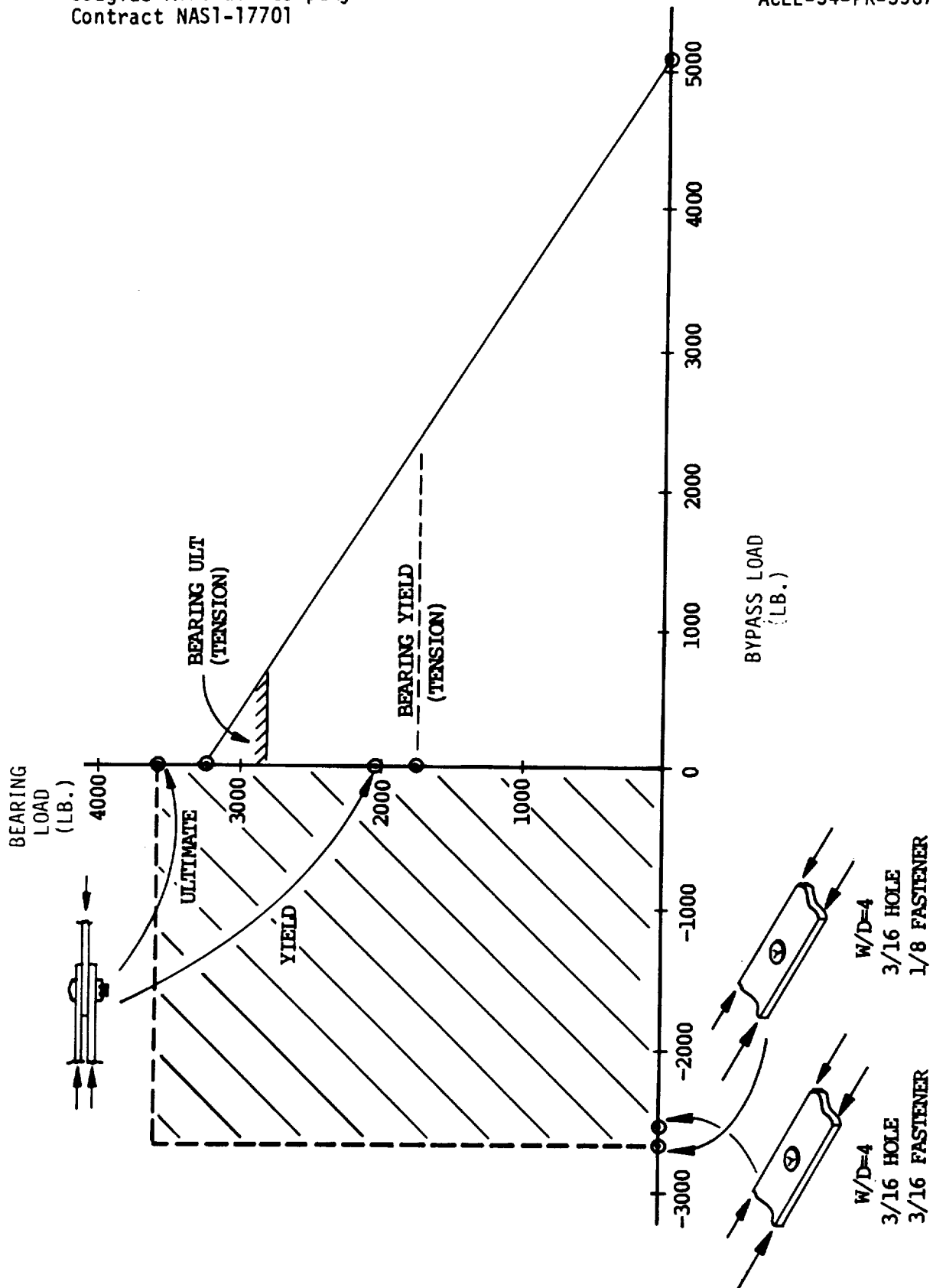


FIGURE 50. COMPRESSION JOINT TEST RESULTS-LAMINATE #4

splice plate of thicknesses in the range of half to two thirds of the center plate thickness, failures often occur in the splices due to the lack of clamp-up outside of the bolt head and washer). Generally, both bearing yield and bearing ultimate are higher for compression loading than for tension.

Unloaded hole strengths were obtained for two configurations for each of the laminates. Both types contained a 3/16" diameter hole with a width to diameter ratio of 4. One configuration utilized a 1/8" fastener to provide local clamp-up without "filling" the hole, while the other used the standard 3/16" fastener. Generally, the "filled-hole" specimens failed at higher loads. The average values plotted for laminate #4 (Figure 50) would appear to reverse this trend; it should be noted however, that the "filled hole" specimens for this laminate exhibited more scatter than any of the other ULC specimens, and there was in fact one specimen which failed at 2890 lbs. (compared to 2710, 2700, and 2710 for the comparable "loose fit" specimens).

It should be noted that no interaction curves were plotted for compression-compression bearing bypass combinations. Some additional tests are planned to assist with the formulation of the needed interaction. Again, however, given the sensitivity of these failures to variations in hole fit and clamping support, it may prove impossible to accurately characterize these joints with any simple relation.

Regardless of the interaction, strengths of compression joints with these laminates, should be roughly limited by the boundaries of the shaded regions of Figures 48 through 50. (The bypass strength of the center member of a double lap splice could actually be slightly better, since the splice members would provide improved clamp-up over the bolt head and washer from the "filled hole" tests. The single row joint strength for a W/D of 4 would most likely be less however, since a bearing failure would probably be preceded by some form of a section failure). Most noticeable are the low unloaded hole strengths when compared to the tension values. This would suggest the need for caution if sizing a joint for tension, when the design loads for compression are nearly as high or higher.

A seemingly conservative interaction which might serve well for design purposes is depicted in Figure 51. The particular case shown would be appropriate for the center member of a double shear joint, although adjustments could be made to account for other cases. The values  $P_{1h}$  and  $P_{uh}$  would best be determined from simple tests,  $P_{1h}$  from a double lap specimen with the design  $W/D$  (and preferably the design thickness splice plates), and  $P_{uh}$  from a "loose bolt" unloaded hole test with the appropriate degree of clamp-up. Given these two values, the worst case for the bypass load is assumed to be when the bolt is loose, with all the load being diverted "around" the hole. For this condition, no interaction is assumed between the peak tangential stresses at the side of the hole (for bypass loads), and the peak normal stresses at the front of the hold (for bearing loads); thus the vertical cutoff. The worst case for the interaction of bearing and bypass is assumed to be when the bolt exactly fills the hold and the load is transferred through the bolt. The gross section bypass stress ( $P_{byp}/tW$ ) is assumed to add to the peak bearing stress at the front of the hold ( $2P_{byp}/Dt$ ) to yield the equivalent failure stress from test ( $2P_{1h}/Dt$ ). This equation reduces to the form given in Figure 51 to define the sloped interaction line.

In the absence of any test values,  $P_{uh}$  and  $P_{1h}$  could be taken to be:

$$P_{uh} = [k F_{cu} t (W-D)] K_t$$

$$P_{1h} = F_{bry} t D$$

where  $k$  is a factor to account for the increased compression allowable at the hole due to the clamp-up,  $F_{cu}$  is the unnotched compression strength,  $F_{bry}$  is bearing yield,  $t$  the thickness of the center member,  $W$  the width, and  $D$  the hole diameter.  $K_t$  is the orthotropic net section stress concentration factor for a hole in a finite strip. Values for  $k$  from the ULC tests with "loose fit" bolts varied from roughly 1.3 for laminate #2 to 1.5 for laminates #3 and #4. The approach used for  $P_{1h}$  would yield conservative predictions for all of the narrow ( $W/D = 3$ ) double lap specimens.

As stated previously, this approach is thought to be conservative, although none of the test data from the compression-compression interaction tests are yet available to verify this. Its main drawback might in fact be that it is simply too conservative.

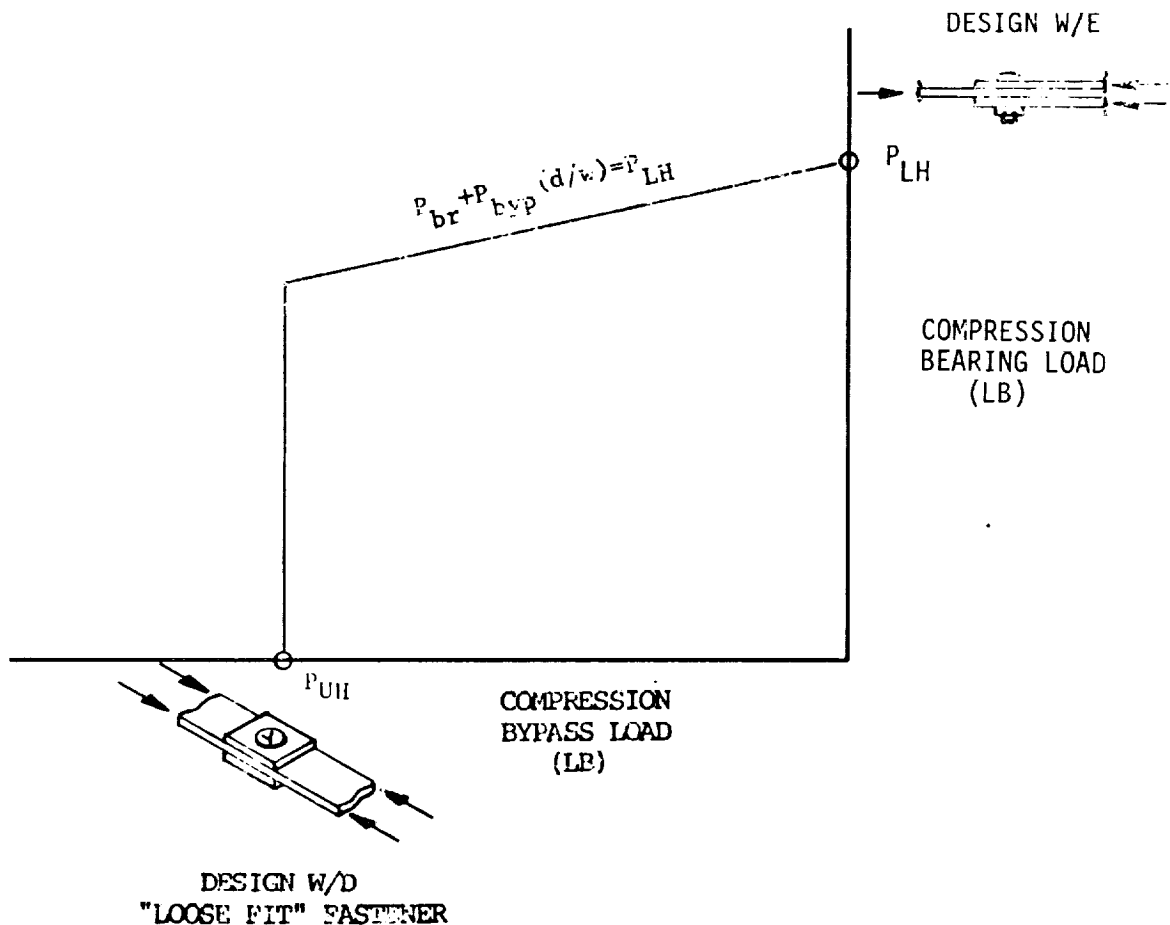


FIGURE 51. PROPOSED INTERACTION FOR DESIGN OF COMPRESSION JOINTS

### Cutouts

Work related to cutouts has focused on the analysis of the "stiffened" and "unstiffened" cutout test specimens (Group B). The stiffened cutout test panels are designed to test a reasonably large cutout in shear. These panels have a 5" x 7" rectangular cutout in a 24" x 24" panel. J-section stiffeners are bonded on the pre-cured panel to reduce the size of the center bay and eliminate shear buckling. These panels will be loaded in diagonal tension through a "picture frame" type fixture. The unstiffened cutout specimens have a 6" wide cutout in a 16" wide panel which will be loaded in tension.

Finite element models have been generated for each of the unstiffened panel configurations. A typical model is shown in Figure 52. Two of the configurations are "softened" by substituting fiberglass for carbon in the areas referred to as the "softened band". The "transition band" is the area where the carbon layers are dropped off and the fiberglass layers added. As can be seen in the figure the panel is loaded by means of a central pin. Thick aluminum doublers are bonded to the panel ends to assist in distributing the load laterally. The model is a quarter panel model and is constructed with NASTRAN membrane elements. Rod elements with very low stiffnesses ("strain bars") are used along the edges to pick up the peak strains at the cutout.

Figure 53a gives the results of three of these models. The "unsoftened" panel is pseudo-isotropic, all carbon tape laminate with no buildup at the cutout. This panel serves as the baseline. The "softened (0/90's)" panel is the same layup except that in the softened band the 0° and 90° layers of carbon are replaced by 0°/90° layers of 120 weave E glass cloth. The "fully softened" panel is similar except all of the carbon layers are replaced with fiberglass in the softened band. One can see from this figure that the stress levels at the critical location ( $\theta = 0^\circ$ ) decrease significantly for the two softened configurations. Figure 53b however, reveals the other half of the story. The E glass, in addition to being much less stiff, also has a significantly lower strength. Thus the allowable stresses have also dropped off dramatically. Indeed Figure 54

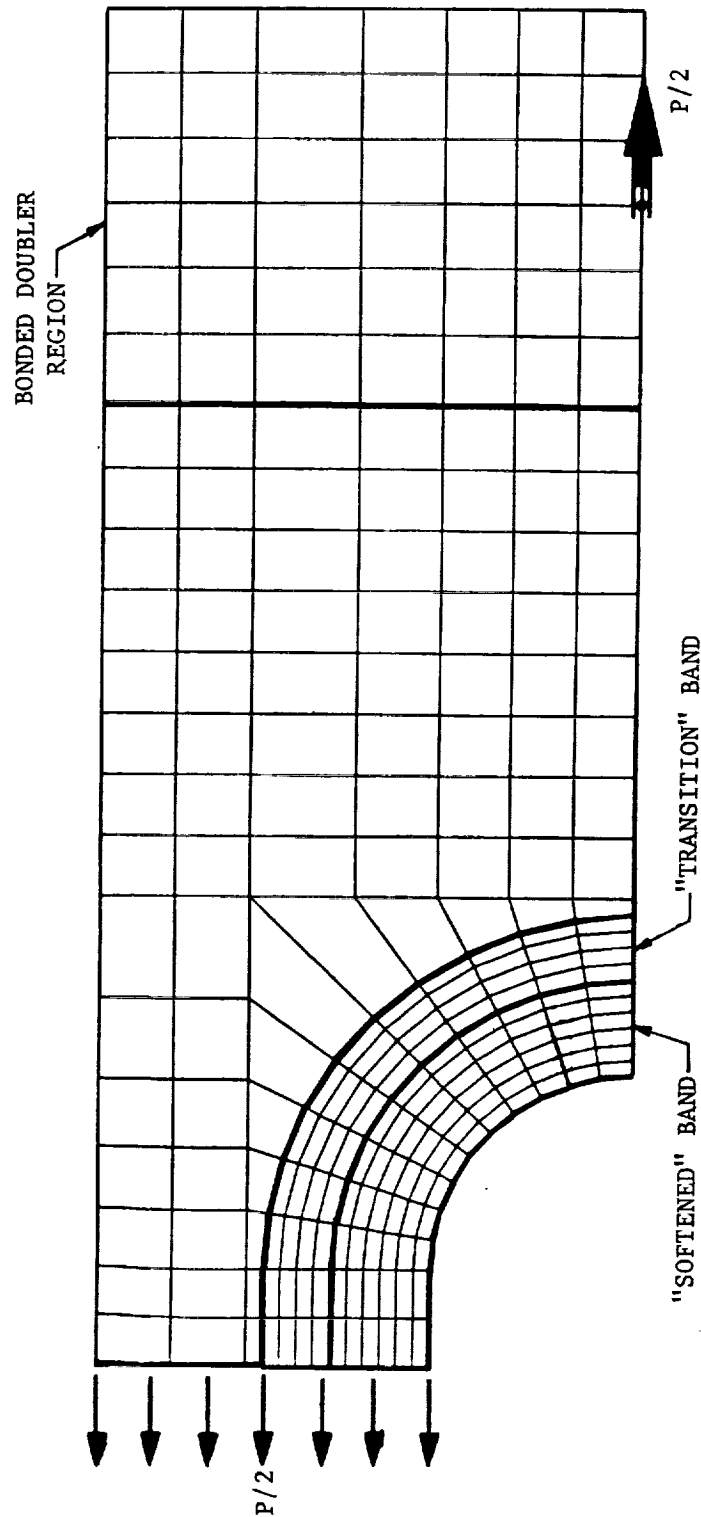


FIGURE 52. UNSTIFFENED CUTOUT FINITE ELEMENT MODEL

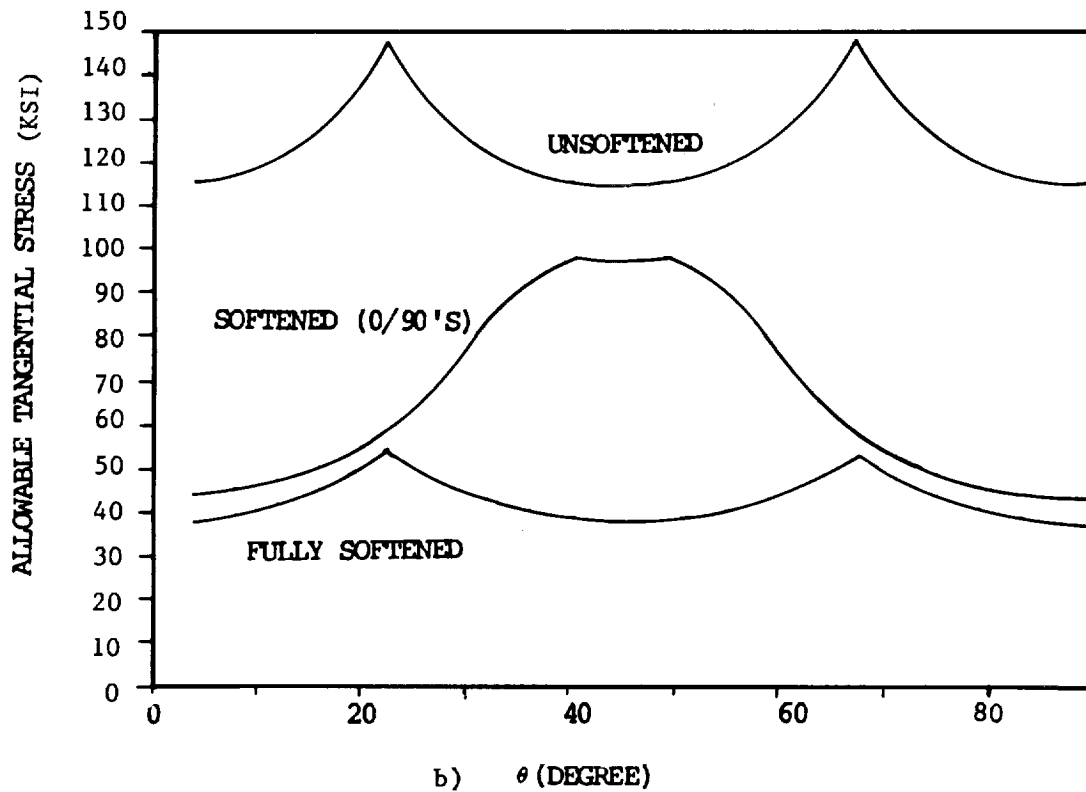
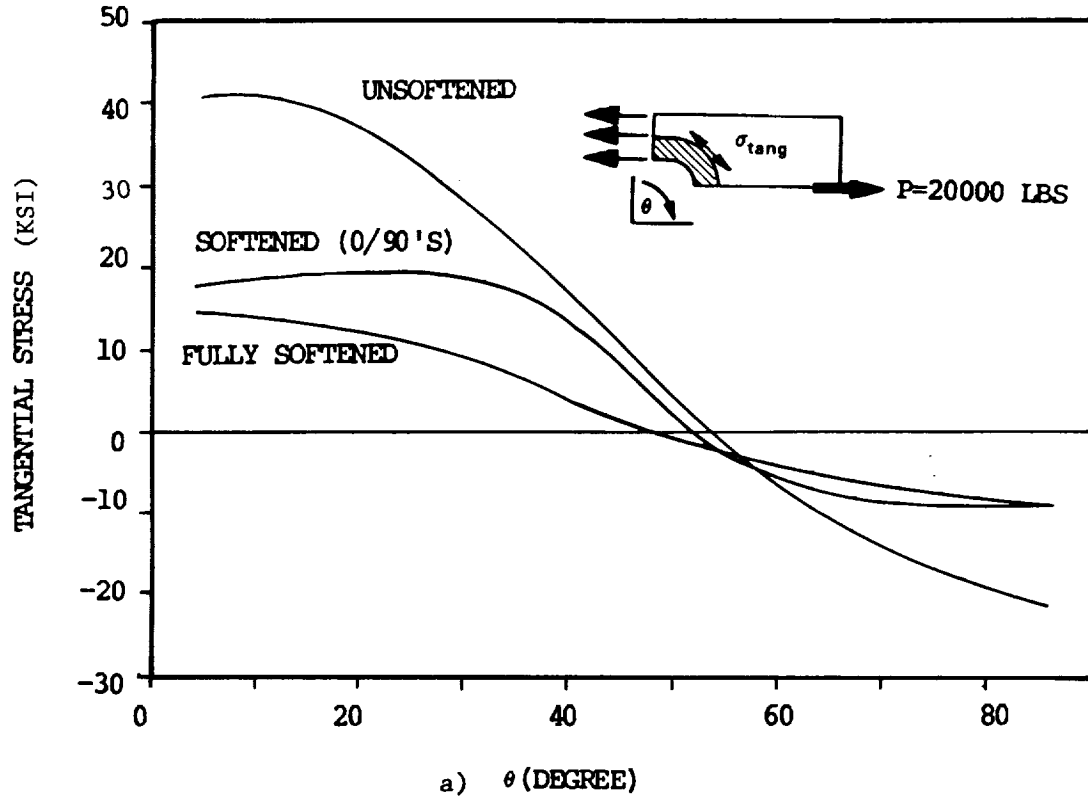


FIGURE 53. TANGENTIAL STRESS AND ALLOWABLES FOR UNSTIFFENED CUTOUT PANELS SOFTENED WITH E GLASS

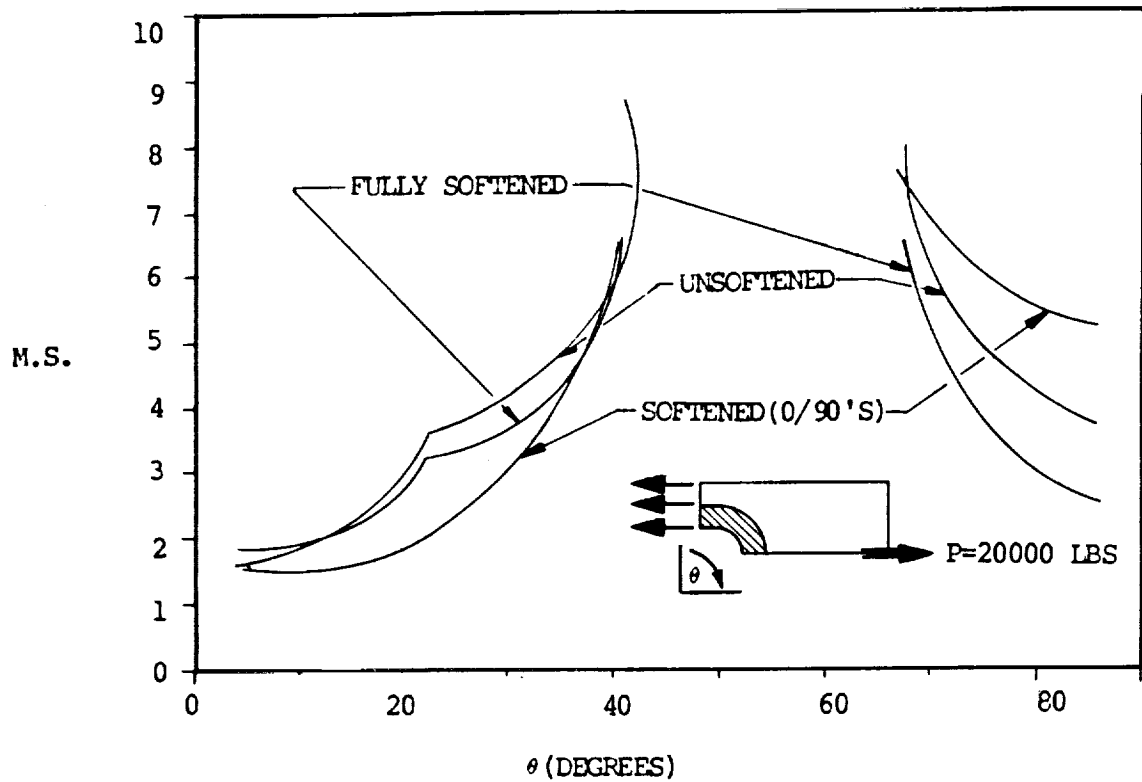


FIGURE 54. MARGINS OF SAFETY AT CUTOUT FOR UNSTIFFENED CUTOUT PANELS SOFTENED WITH E GLASS



indicates that, despite the large reductions in stress at the edge of the cutout, the two softened panels have lower margins of safety.

Figure 55 illustrates the same analysis for panels softened with S2 glass instead of E glass. The S2 glass being slightly stiffer produces less of a stress reduction, however the allowable stresses have improved substantially. Figure 56 confirms that the margin of safety at the edge of the cutout has in fact, shifted in favor of the softened laminates. These figures, however, ignore the possibility that the critical location may have moved away from the edge of the cutout. Other points of concern with the softened laminates are the edges of the "softened band" and the "transition band" where there are discontinuities in both stiffness and strength.

Figure 57a gives the stress distribution across the panel width for the three configurations. (Note that the stresses at  $X = 0$  do not coincide with those at  $\theta = 0$  in Figure 55a. This is because the stresses plotted in Figure 57a are from elements along the panel centerline, whereas  $\theta = 0$  in Figure 55a corresponds to the point where the end radius becomes tangent to the straight sides). For the unsoftened panel the stress steadily drops off from the edge of the cutout to the outer edge of the panel. The two softened panels exhibit sharp discontinuities at the edges of the "softened" and "transition" bands. Examination of the Margin of Safety plots (Figure 57b) reveals that the minimum margins of safety for the softened panels have moved 1.5 inches away from the edge of the cutout and show little or no improvement over the unsoftened panel.

These plots illustrate the difficulty of improving the performance of a single load path system with a relatively gentle stress gradient. For a given load, the area under each of the curves in Figures 57a must be equal. Thus any stress "subtracted" from the baseline curve in the softened region must be "added" to the curve elsewhere. Given the absence of a sharp stress peak it becomes very difficult to even match the strength of the baseline, let alone improve it. This does not rule out, however, the potential for beneficial use of this technique in situations

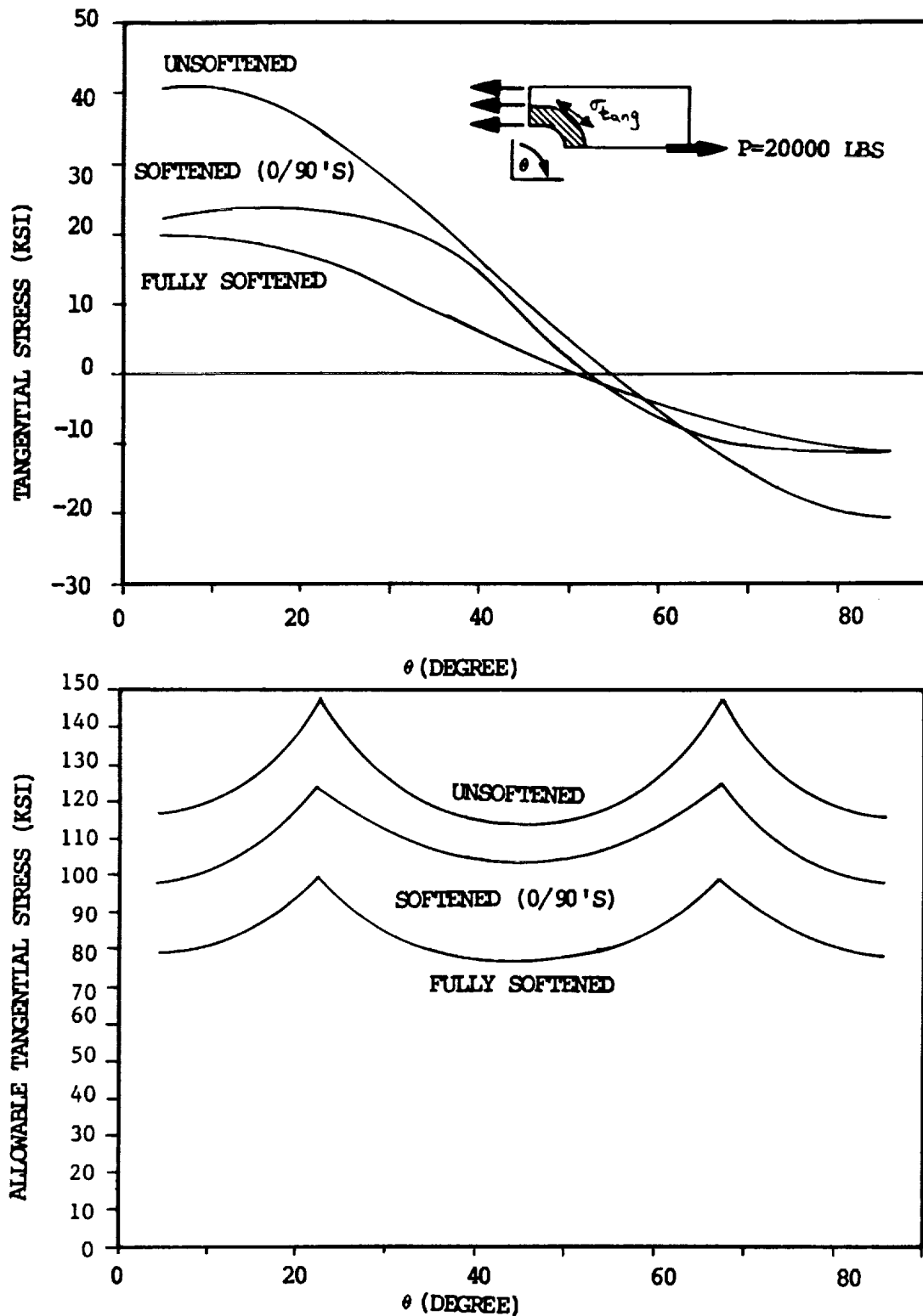


FIGURE 55. TANGENTIAL STRESS AND ALLOWABLES FOR UNSTIFFENED CUTOUT PANELS SOFTENED WITH S2 GLASS

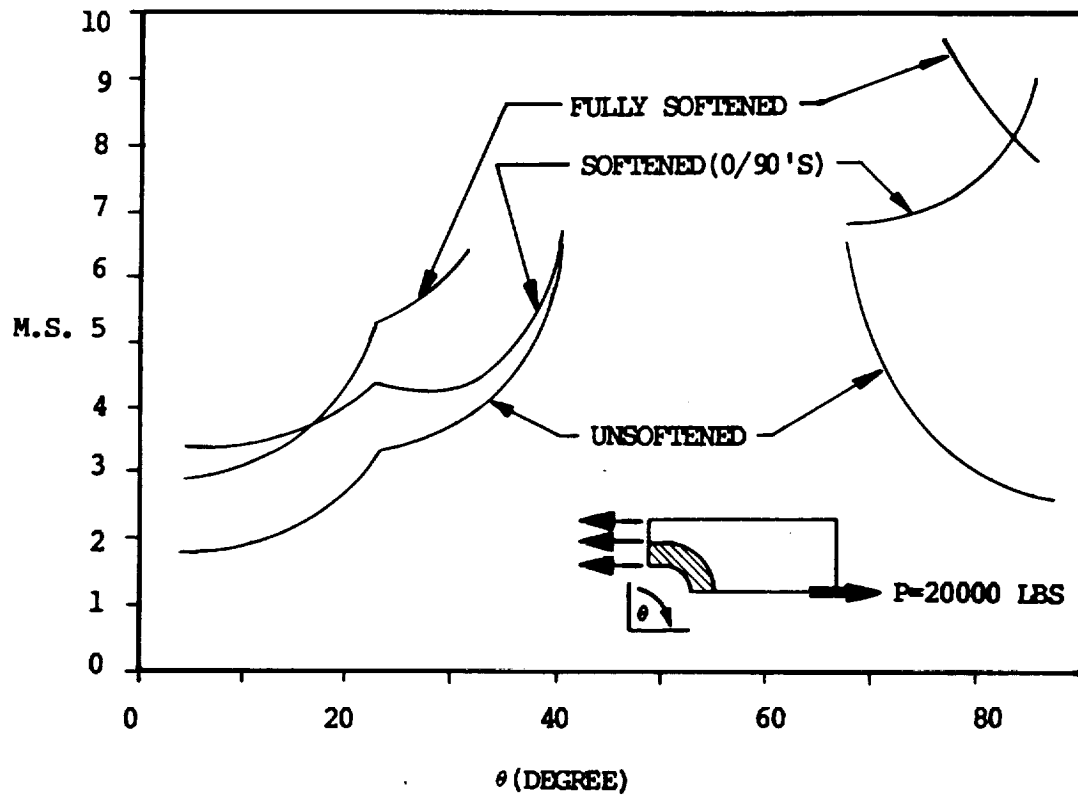


FIGURE 56. MARGINS OF SAFETY AT CUTOUT FOR UNSTIFFENED CUTOUT PANELS SOFTENED WITH S2 GLASS

where the presence of highly localized stress concentrations, or the existence of multiple load paths might make it advantageous to redirect the load to other less highly loaded areas.

An example of one of the stiffened cutout models is shown in Figure 58. This model is similar to those for the unstiffened cutout except that it uses plate elements instead of membrane elements. This was done so that a buckling solution could be performed to insure that failure of the cutout would precede shear buckling of the center bay. The J-section stiffeners are modeled as bending bars making use of the offset capability of the NASTRAN CBAR to correctly locate the neutral axis. The "picture frame" fixture is represented by very stiff bars along the panel edges with the rotational degrees of freedom released at the four corners (to simulate pinned ends). Loading is accomplished with enforced displacements on the four corners, "out" on the lower left and upper right, "in" on the upper left and lower right.

Tangential stresses along the radiused corners of the cutout are given for unsoftened and softened configurations in Figure 59a. Again significant reductions in the peak stress are effected. Figure 59b presents the applicable allowables for an all carbon (pseudo-isotropic) laminate and one softened with S2 glass  $\pm 45^\circ$ 's. Note that the stresses shown as positive in Figure 59a could also be taken as negative since the doubly symmetric panel subjected to pure shear has equal and opposite loading on the tension and compression diagonals. Thus both the tension and compression allowables are shown in Figure 59b. It is observed that, while the all carbon laminate is critical in compression for any angle  $\theta$ , the softened laminate changes from compression critical to tension critical at angles close to  $45^\circ$ . This situation arises because of the low (when compared to the tension allowable) compression allowable for the carbon  $0^\circ$ 's and  $90^\circ$ 's, and the relatively high compression allowable for the fiberglass  $\pm 45^\circ$ 's. The margins of safety, using the lesser of the tension and compression allowables for a given  $\theta$ , are given for the two configurations in Figure 60. This figure indicates over a 40% increase in load carrying capacity for the softened configuration.

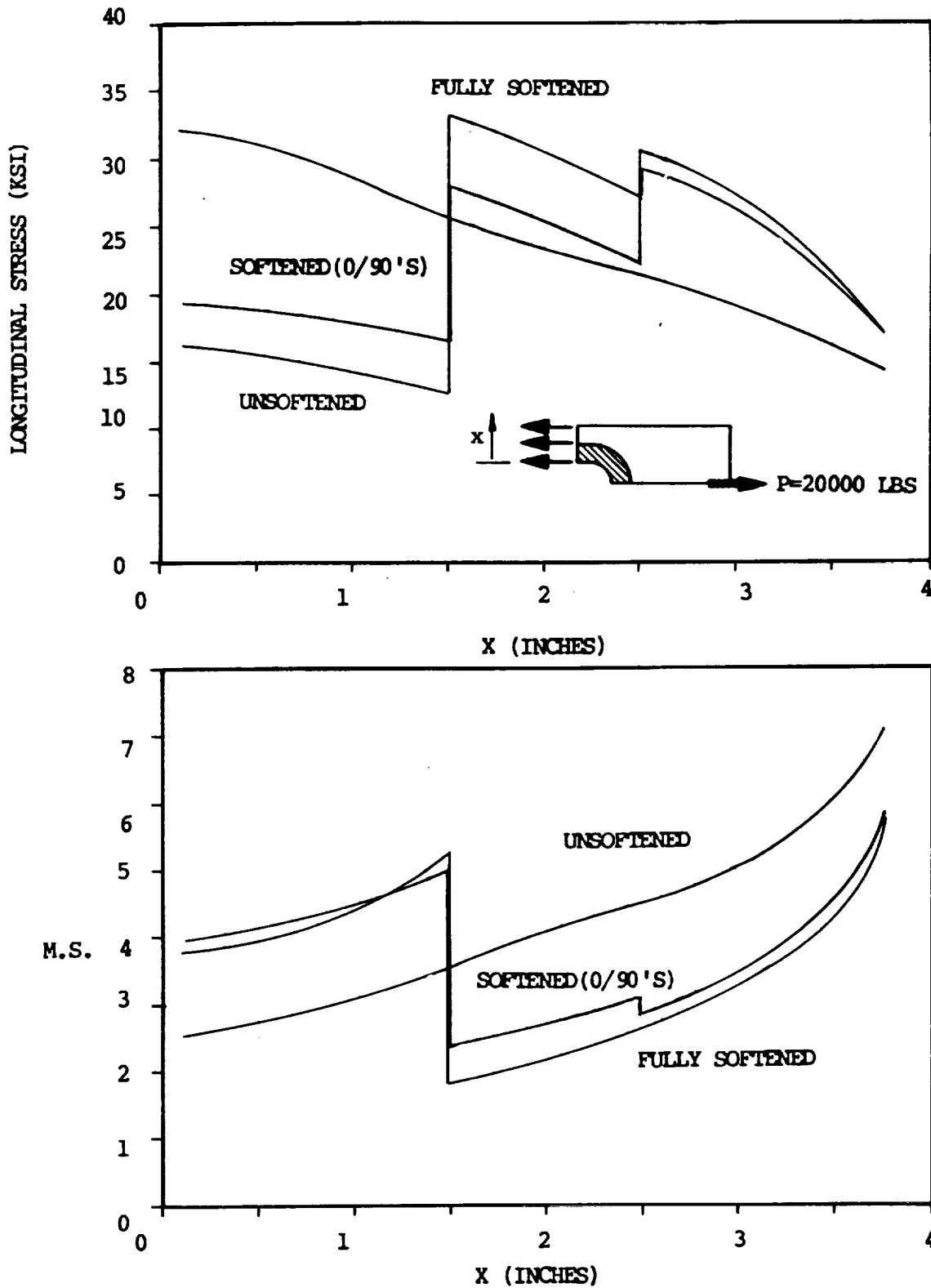


FIGURE 57. VARIATIONS OF STRESS AND MARGIN OF SAFETY ACROSS THE WIDTH OF UNSTIFFENED CUTOUTS SOFTENED WITH S2 GLASS

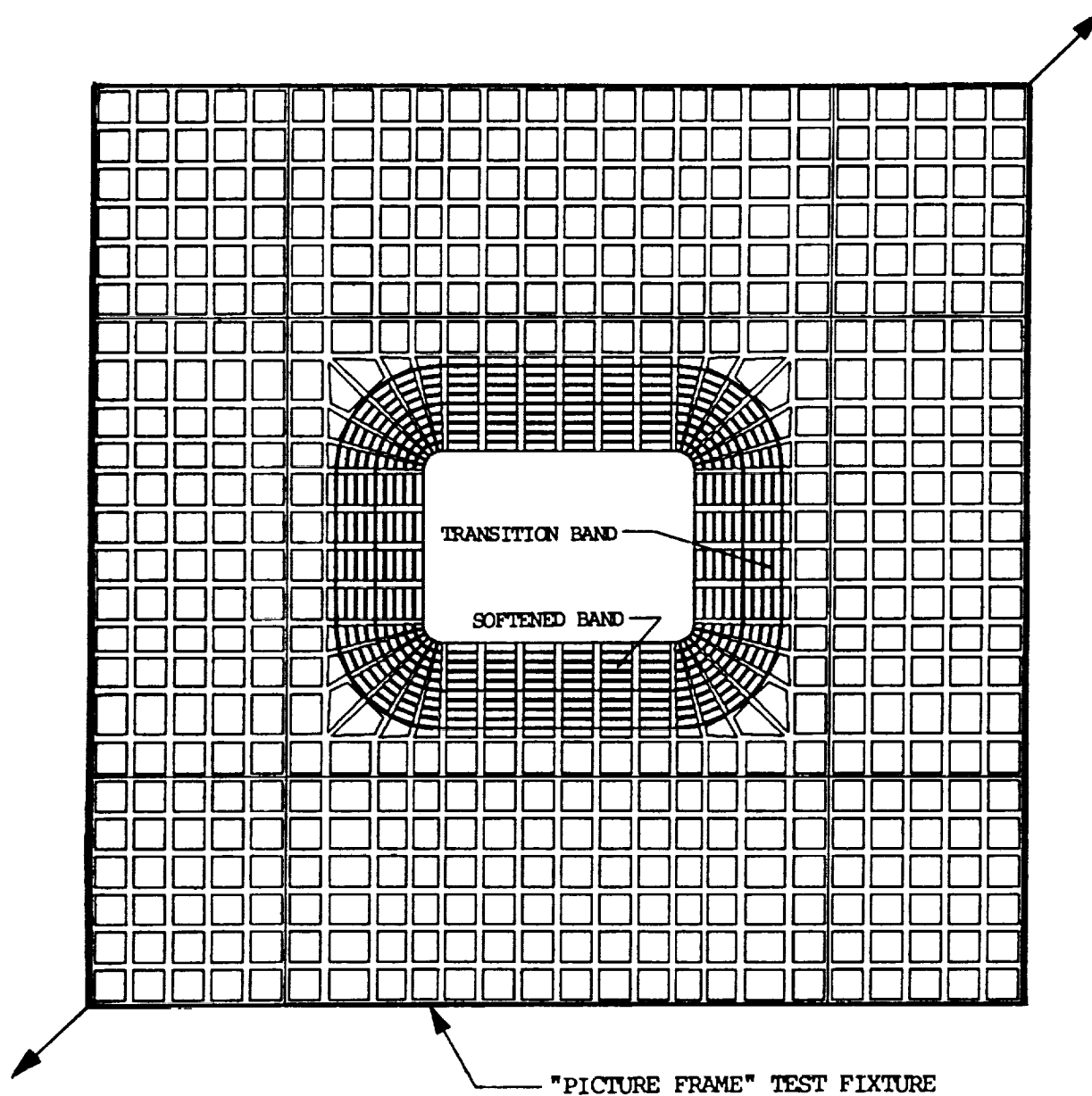


FIGURE 58. STIFFENED CUTOUT FINITE ELEMENT MODEL

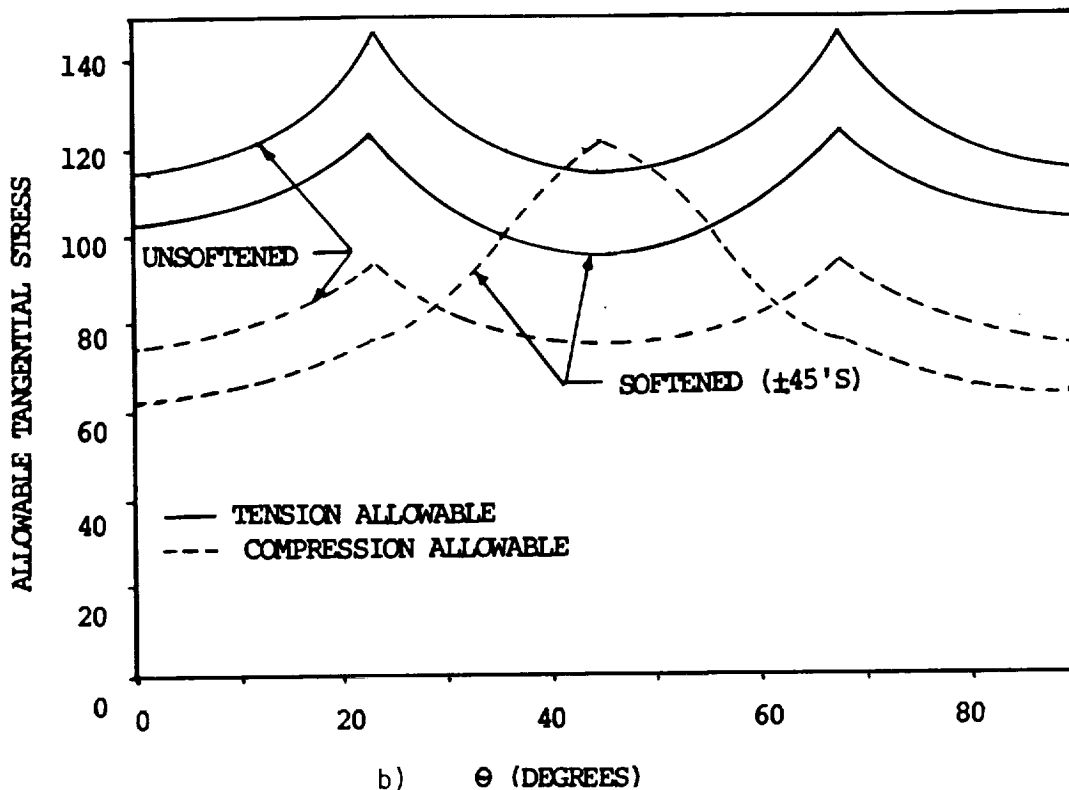
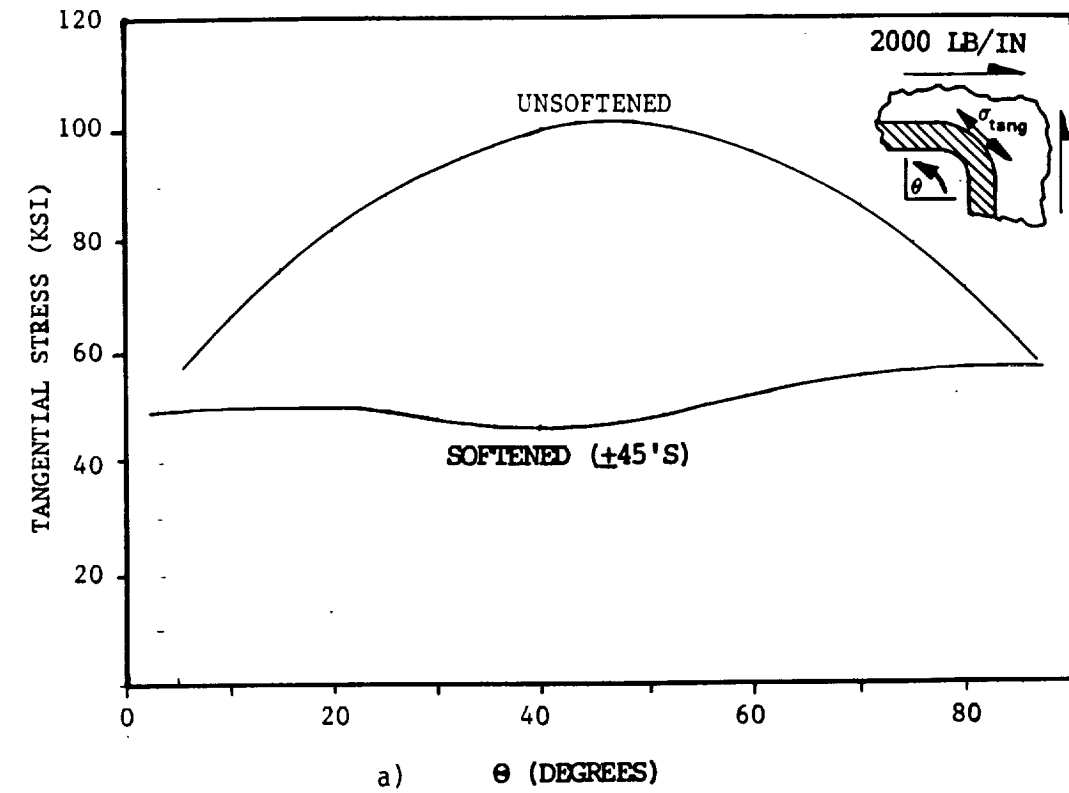


FIGURE 59. TANGENTIAL STRESS AND ALLOWABLES FOR STIFFENED CUTOUT PANELS SOFTENED WITH S2 GLASS

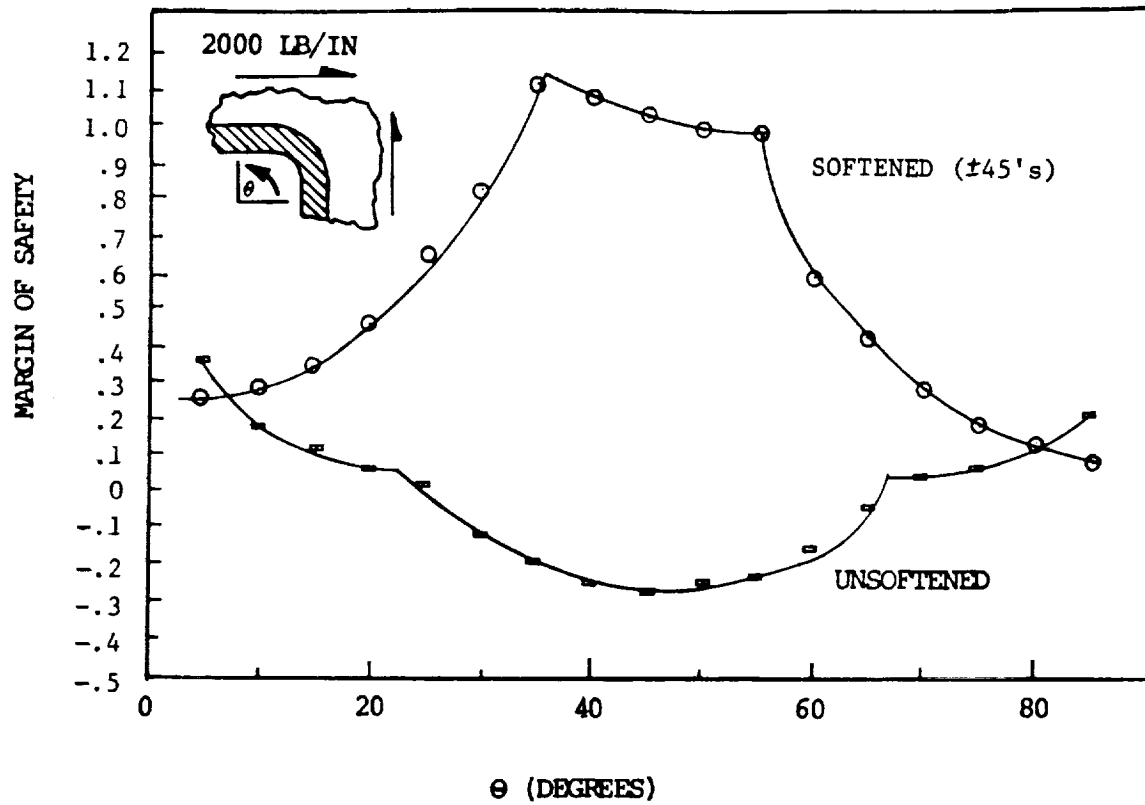


FIGURE 60. MARGIN OF SAFETY AT CUTOUT FOR STIFFENED CUTOUT PANELS SOFTENED WITH S2 GLASS



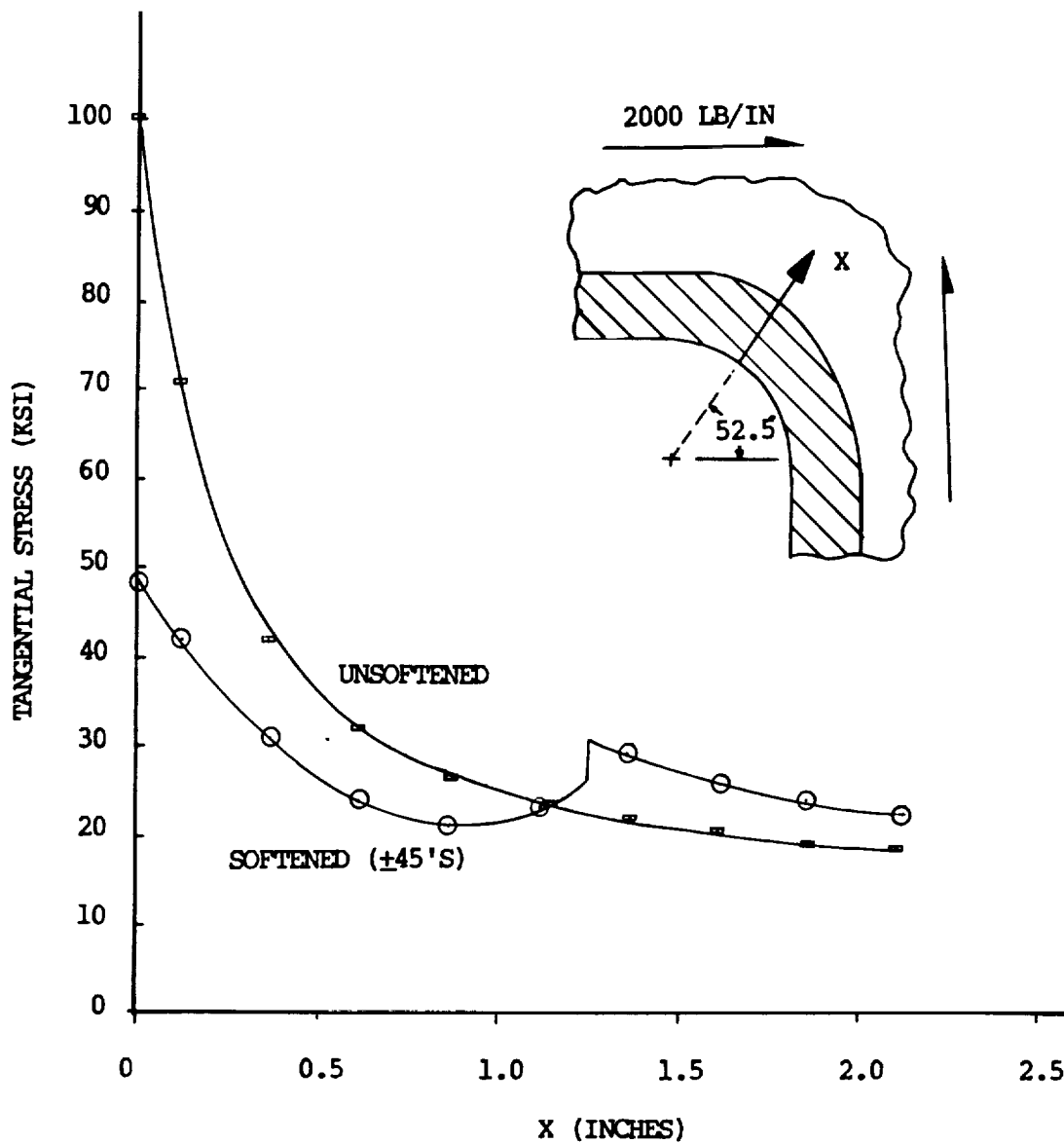


FIGURE 61. RADIAL VARIATION OF STRESS FOR STIFFENED  
CUTOUT PANELS SOFTENED WITH S2 GLASS

The stress variation along a "cut" through the panel at  $\theta = 52.5$  is given as Figure 61. Notice again the discontinuity at  $x = 1.25$ ". Figure 62 reveals that again the margin of safety for the softened configuration drops sharply at the edge of the softened band ( $x = 1.25$ "). In contrast to the unstiffened cutout distribution, this margin remains higher than that which occurs at the cutout. In this case, the stress gradient for the baseline case was sharp enough to allow the softening to have some beneficial effect.

It is interesting to observe that the strengths of all of these configurations (stiffened and unstiffened, softened and unsoftened) have been limited by the strain to failure of the carbon fibers. The fiberglass fibers being softer and having over twice the allowable strain to failure effectively "stretch" out of the way, soaking up roughly half the load and shedding the remaining half into the adjacent carbon fibers. These carbon fibers then, eventually reach their strain limit and determine the failure load.

Testing of the Group B cutout specimens is scheduled to begin early in May. Although the softened configurations for the unstiffened panels (those manufactured with E glass) may actually fail at lower loads than the baseline, their only real purpose was for manufacturing and process development, and analysis correlation. Data from these tests will provide the confidence that this technique can be used in other, more practical applications.

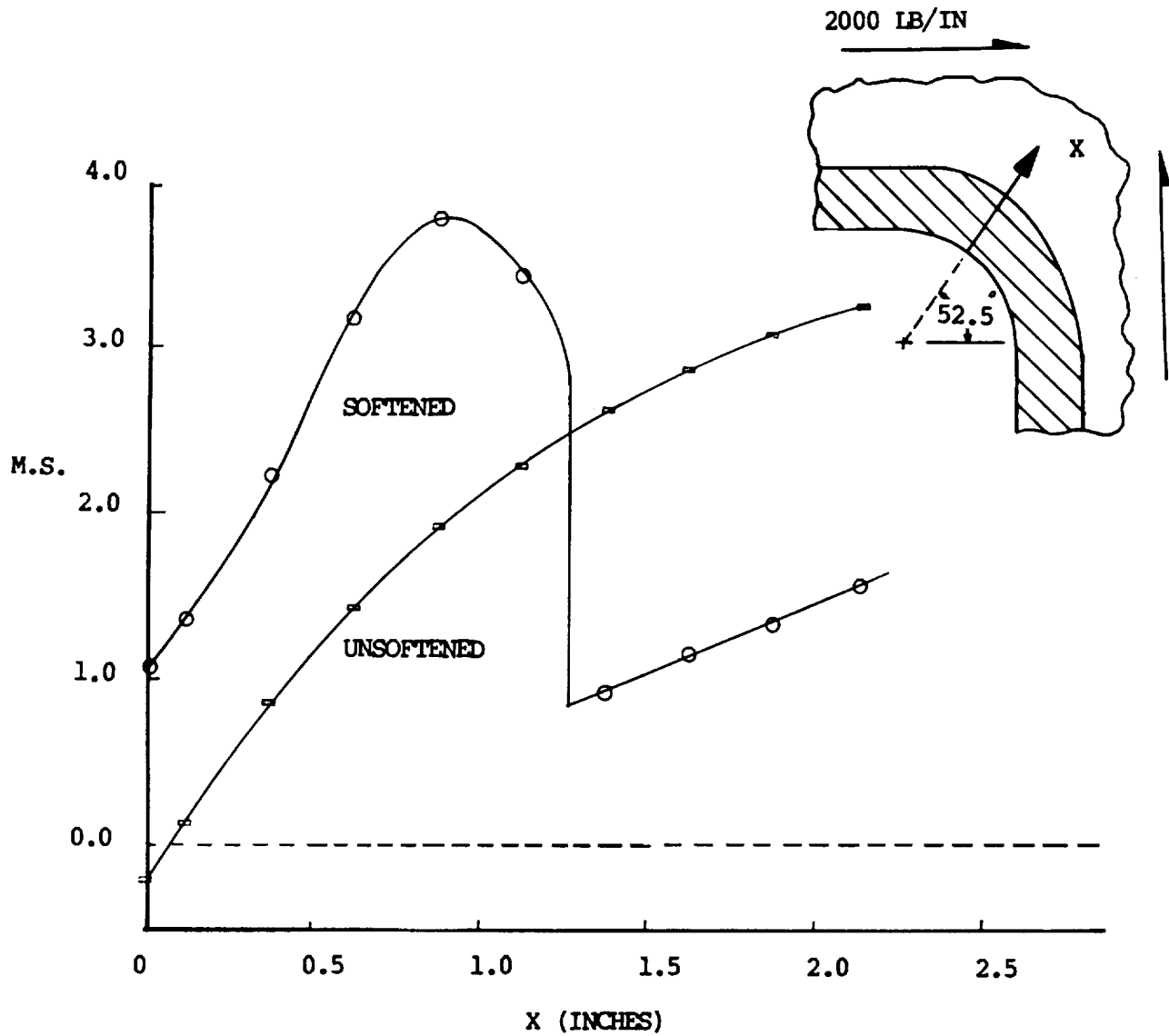


FIGURE 62. RADIAL VARIATION IN MARGIN OF SAFETY FOR STIFFENED CUTOUT PANELS SOFTENED WITH S2 GLASS



## SECTION 4

### PROCESS DEVELOPMENT AND FABRICATION

#### 4.1 PROCESS DEVELOPMENT

##### Materials

All of the F584/IM6 tape (600 lbs) and 5 harness satin (5HS) cloth (250 lbs) needed for the program were received during October 1984 to January 1985. In addition, Ciba-Geigy woven Hercules carbon fiber with 8 mil. aluminum wire and the American Cyanamid nickel coated Hercules carbon fiber impregnated with F584 resin by Hexcel were received in January 1985. The latter material systems were used for lightning protection tests. Woven 120 grade E-glass has been received for use as a softening material around cutouts. S2 cloth has also been ordered for tests with the expectation that the higher strain-to-failure and higher modulus will be a superior softening material in cutout regions.

##### Testing

Progress on process development testing is shown in Table IV, Standard toughness tests were conducted as outlined in NASA Reference Publication 1092, "Standard Tests for Toughened Resin Composites." Results for tests ST-1, ST-3, ST-4, and ST-5 are shown in Tables V, VI, VII, and VIII.

Results from the material quality tests conducted on the F584/IM6 tape and five harness satin (5HS) cloth are shown in Tables IX and X respectively. Actual values for F584/IM6 tape and cloth received for the fuselage program were very good, exceeding required values by an average of 17%.

The short beam shear test is primarily a materials screening tool. Since a materials screening effort is not a task for this program, the 200°F test values which are below the strength requirement will be for record purposes only. It should be noted that values for the same test at room temperature are 23 percent higher than the requirement. Overall, the material received does meet the requirements set for this program.

TABLE IV  
PROCESS DEVELOPMENT SPECIMEN STATUS

SPECIMEN DESCRIPTION	FABRICATION STATUS	TESTING STATUS
TENSION STR.	COMPLETED	COMPLETED
TENSION MOD.	COMPLETED	COMPLETED
COMPRESSION R.T.	COMPLETED	COMPLETED
COMPRESSION 200 F	COMPLETED	COMPLETED
SHORT BEAM SHEAR R.T.	COMPLETED	COMPLETED
SHORT BEAM SHEAR 200 F	COMPLETED	COMPLETED
COMP. AFTER IMPACT (ST-1)	COMPLETED	COMPLETED
OPEN HOLE TENSION (ST-3)	COMPLETED	COMPLETED
OPEN HOLE COMPRESSION (ST-4)	COMPLETED	COMPLETED
DBL. CANT. BEAM (ST-5)	COMPLETED	COMPLETED
DBL. LAP SHEAR	--IN FAB	-----

TABLE V  
COMPRESSION AFTER IMPACT TEST DATA (ST-1)

Company affiliation: Douglas Aircraft  
Material: Hexcel F584/IM6 h=5.6 mils/ply  
Laminate orientation: [+45/0/-45/90]6s 48 ply  
Resin content: 33% by weight  
Test condition: 750F dry

Specimen ID	Thickness in.	Width in.	Impact Energy ft-lb	Failure Load Kips	Failure Stress ksi	Failure Strain in/in	Compression Modulus psi
ST-1-1	.268	4.999	20	39.1	29.18	3659	$7.95 \times 10^6$
ST-1-2	.270	4.998	20	38.7	28.68	3672	$7.75 \times 10^6$
ST-1-3	.282	4.999	20	37.4	26.58	3451	$7.71 \times 10^6$
AVERAGE				38.4	28.14	3594	$7.80 \times 10^6$

TABLE VI  
OPEN-HOLE TENSION (ST-3)

Material: Hexcel F584/IM6 h=5.6 mils/ply  
Laminate orientation: [+45/0/-45/90]6s 48 plies  
Resin content: 33% by weight  
Test condition: 750F dry

Specimen ID	Thickness in.	Width in.	Hole Diameter in.	Failure load kips	Failure stress ksi	Failure strain in/in	Tensile modulus psi
ST-3-1	.271	2.040	.250	37.15	67.20	7221	$9.31 \times 10^6$
ST-3-2	.269	2.001	.251	36.85	68.46	7341	$9.33 \times 10^6$
ST-3-3	.269	2.000	.252	36.95	68.68	7271	$9.45 \times 10^6$
AVERAGE				36.98	68.11	7278	$9.36 \times 10^6$

TABLE VII  
OPEN HOLE COMPRESSION (ST-4)

Material: Hexcel F584/IM6 h= .0056 mils/ply  
Laminate orientation: [+45/0/-45/90]6s 48 ply  
Resin Content: 33% by weight  
Test Condition: 75°F dry

Specimen ID	Thickness in	Width in.	Hole Diameter in.	Failure load kips	Failure stress ksi	Failure strain $\mu$ in/in	Compression modulus psi
ST-4-1	.2685	5.014	1.0	41.15	30.56	4706	$6.49 \times 10^6$
ST-4-2	.2700	5.008	1.0	41.05	30.36	4527	$6.71 \times 10^6$
ST-4-3	.2700	5.002	1.0	43.60	32.28	4240	$7.61 \times 10^6$
AVERAGE				41.93	31.06	4491	$6.94 \times 10^6$

TABLE VIII  
DOUBLE CANTILEVER BEAM (ST-5)

Material: Hexcel F584/IM6 h= .0056 mils/ply  
Laminate orientation: [0]24  
Resin Content: 33% by weight  
Test Condition: 75°F dry

Specimen ID	Thickness in.	Width in.	Gic direct in-lbs/in	Gic area integration in-lbs/in
ST-5-1	.141	1.508	1.20	1.165
ST-5-2	.138	1.504	1.33	1.435
ST-5-3	.136	1.506	1.07	.932
AVERAGE			1.20	1.177



TABLE IX  
MATERIAL QUALITY TEST DATA  
F584/IM6 TAPE

TEST PROPERTY	REQUIREMENT	SPECIMEN #1	SPECIMEN #2	SPECIMEN #3	AVERAGE
TENSION					
ULTIMATE KSI	270	274.2	327.5	304.0	301.9
75°F					
TENSILE					
MODULUS MSI	19	22.6	22.8	23.1	22.8
COMPRESSION					
ULTIMATE KSI	190	112.3***	200.0	205.5	202.7
75°F					
COMPRESSION					
ULTIMATE KSI	175	197.4	199.9	161.6	186.3
200°F					
SHORT BEAM SHEAR					
75°F KSI	14.3	17.91	17.90	17.33	17.71
SHORT BEAM SHEAR					
200°F KSI	12.8	10.36	10.77	10.66	10.60

\* No single test specimen result shall be more than 10% below the average requirement. Tension and compression values based on .0456" nominal thickness. (.0057"/ply).

\*\* A minimum of three test specimens shall be used to determine the average value for each condition listed. Values are based on "S" allowables as defined in MIL-HDBK-5.

\*\*\*Data point omitted from average.

Layup pattern: Tensile and compression, [0], 8 plies  
Short beam shear, [0], 16 plies

TABLE X  
MATERIAL QUALITY TEST DATA  
F584/IM6 5HS CLOTH

TEST PROPERTY	REQUIREMENT	SPECIMEN #1	SPECIMEN #2	SPECIMEN #3	AVERAGE
TENSION					
ULTIMATE KSI 75°F	80	122.8	122.1	118.3	121.1
TENSILE					
MODULUS MSI	9.0	10.5	10.1	10.2	10.3
COMPRESSION					
ULTIMATE KSI 75°F	80	89.1	94.4	87.6	90.3
COMPRESSION					
ULTIMATE KSI 200°F	70	96.7	75.8	85.9	86.1
SHORT BEAM SHEAR					
75°F KSI	8.5	10.40	10.25	10.47	10.37
SHORT BEAM SHEAR					
200°F KSI	7.5	8.47	8.23	8.53	8.41

\* No single test specimen result shall be more than 10% below the average requirement.

\*\* A minimum of three test specimens shall be used to determine the average value for each condition listed. Values are base on "S" allowables as defined in MIL-HDBK-5.

Layup patterns: All specimens, [0/90], 8 plies.

Fabrication of Group A, B and C Specimens

Group A Specimens:

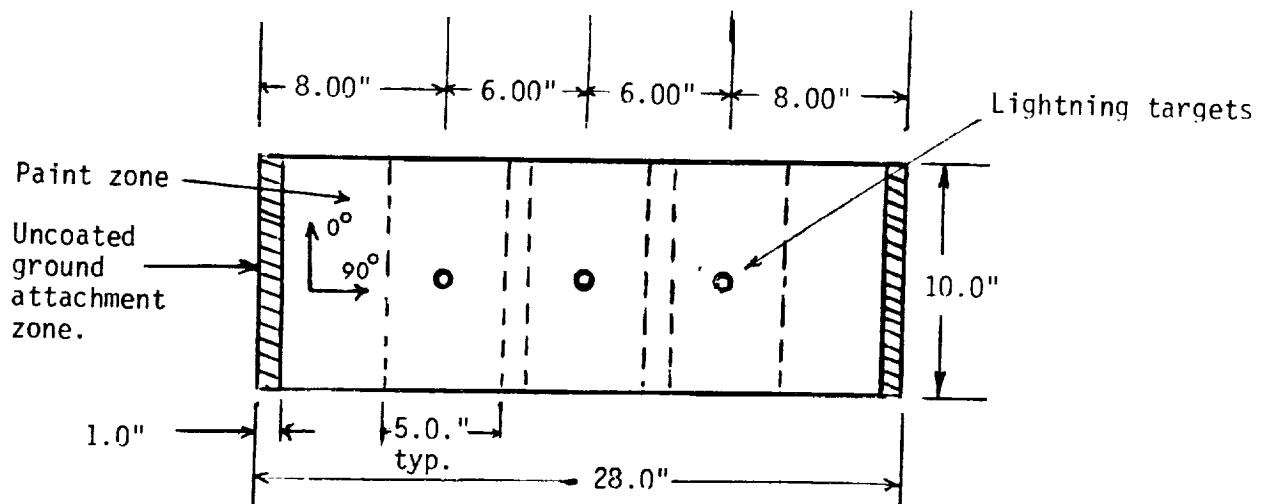
All of the initial specimens were fabricated during the reporting period.

Lightning Protection Specimens - Three basic skin panels were laid up, one with a nickel -coated protection sheet, one with a wire woven protection sheet, and one with no protection. The protection sheets were both woven graphite and replaced two plies of tape on one side of the protected panels. Each panel was cured, C-scanned, cut to 10" x 28", glazed, painted, subjected to 3 simulated lightning strikes, x-rayed, cut into 3 compression panels, 5" x 10", and then compression tested.

The lightning strike panel configuration is illustrated in Figure 63. The two protection materials are identified below:

<u>Specimen</u>	<u>CAI-505</u>	<u>CAI -507</u>
Protection System	Wire-woven, 8 mil dia. aluminum wire, 1/8" centers, warp & fill	Nickel-coated graphite fiber
Weave	5-harness satin, graphite fiber	Plain weave, graphite fiber
Weight	.0128 lb/sq-ft.	.0410 lb/sq-ft.
Resin	F584 Epoxy resin	F584 Epoxy resin
Supplier	Giba-Geigy	American Cyanamid

The three panels were painted as they would be in production using an impact resistant paint system. The composite surface was first prepared for glazing by solvent cleaning, abrading and water break testing. An epoxy fill or glazing compound was then applied. Next, the topcoat was applied using a polyurethane primer followed by a polyurethane topcoat for non-decorative surfaces. A 1.0" strip on each end was left uncoated to allow contact between the ground plate and the composite surface.



#### Layup Patterns

CAI-505,507;  
(0,90,45,0,-45,90,90  
-45,0,45,0/90 protection sheet)  
10 plies F584/IM6 tape, 1 ply prot. sheet

CAI-509:  
(0,90,45,0,-45,90)s  
12 plies F584/IM6 tape

FIGURE 63 LIGHTNING STRIKE PANEL CONFIGURATION

Group B Specimens:

Shear Tee/Skin pull off - Six configurations of shear tee/skin pull-off specimens were fabricated. Five configurations used FM-300 adhesive ( $.08 \text{ lb/ft}^2$ ) and one configuration used AF 163-2 adhesive ( $.06 \text{ lb/ft}^2$ ).

Unstiffened Cutout Panels - Major fabrication of the 4 unstiffened cutout panels have been completed. The cured panels were subjected to C-scan ultrasonic testing and found to meet test requirements. Cutouts have been created using an aluminum template and router, and aluminum doublers have been cold bonded to the ends using EA9320 adhesive with a scrim to control bondline thickness.

Test fixture holes are being drilled through the doublers on each end. Following that, photoelastic film is to be bonded to the flat side of each panel. Strain gauges will then be applied to the other side.

Two of the unstiffened cutout panels incorporate rings of F584 impregnated fiberglass cloth, in place of the F584/IM6 tape, along a 1-2" border of the cutout. These mechanical softening rings begin as uncured disks of material which are trimmed using 1/4" acrylic templates.

The panels with softened (fiberglass) rings were cured with near full size cutouts in the prepreg material, i.e., the cutouts were made 1/8-inch undersize. A temporary aluminum plug equal in thickness to the material buildup was placed in the undersize cutout area to reduce resin loss during the cure cycle. The cutout was made to final dimensions after the panel was cured. It was also believed that this approach would minimize bowing and warping in contrast to curing the panel with no cutout and removing the fiberglass in the cutout region subsequent to cure.

Monolayer tension, shear, and compression specimens have been fabricated from the fiberglass material used for mechanical softening around cutout regions. Tests have been completed and the results will be used for stress calculations.

Stiffened Cutout Shear Panels - Two of the three panels have been layed up, C-scanned, and found acceptable. Resin/void tests have been initiated. A 3/4" aluminum template for trimming edges and making center cutouts is being fabricated. A drill fixture for creating four stress-relief holes in each panel is also being fabricated. The stiffeners to be bonded to the flat side of each panel have been cured and are in non-destructive testing. A tool for fabricating the stiffeners which are to be bonded to the side of the panels with buildups, is being completed. The third panel, which is 50 percent layed up, will contain S2 glass cloth, grade 120, as a "mechanical softening" material around the cutout.

#### Group C Specimens:

Longitudinal and Transverse Splice Specimens - Approximately 20 percent of the fabrication of both specimens is now complete with the first skin panels now layed up, cured, and C-scanned.

#### Fabrication and Process Verification

The four fuselage subcomponents, namely; longeron, shear tee, frame and a 2' by 2' curved panel with integral ply build-ups were fabricated using tooling representative of full-scale components. The longerons and shear tee were secondarily bonded to the 2' by 2' panel using FM-300 adhesive (Figure 64).

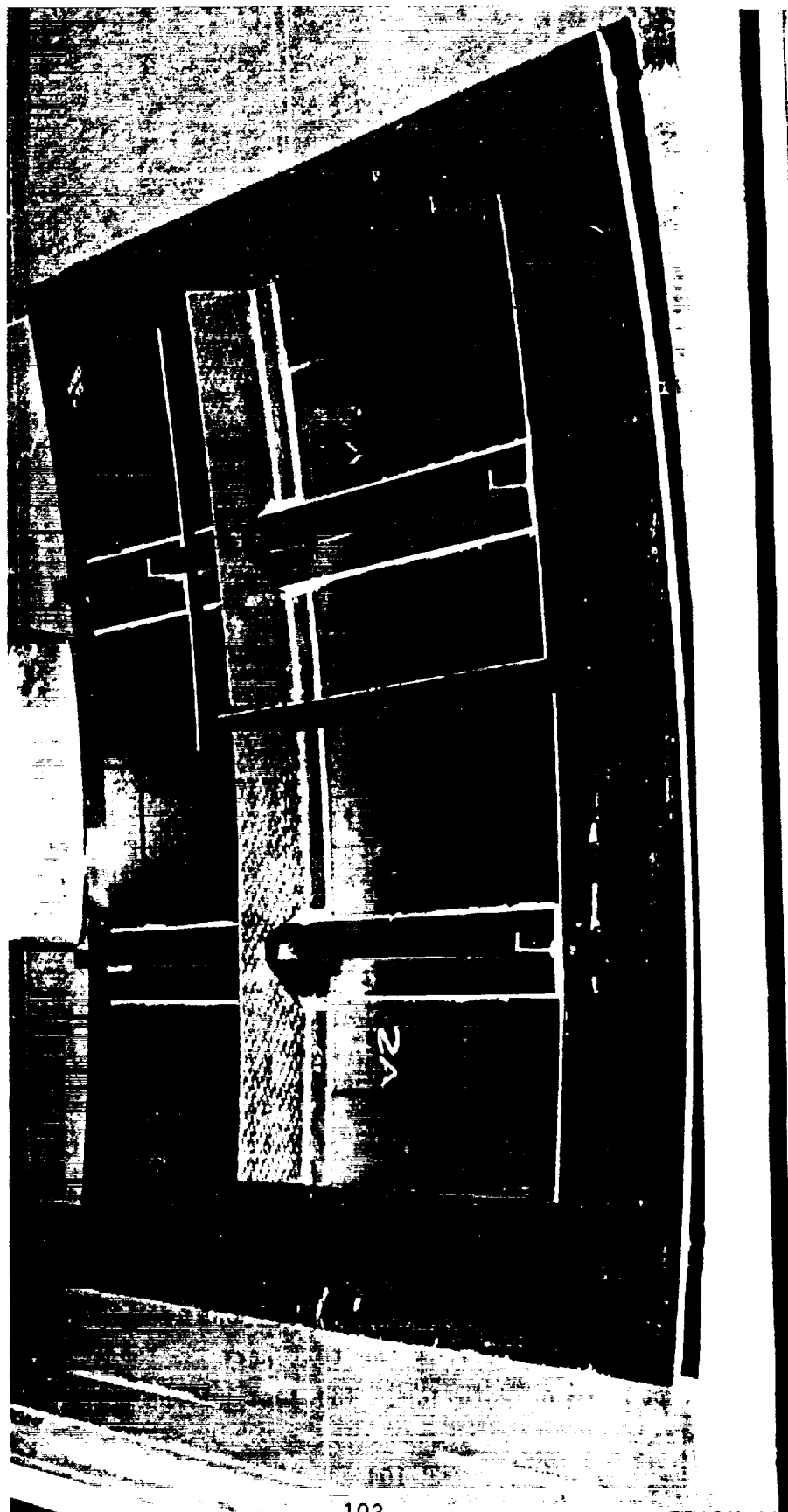


FIGURE 64 PROCESS VERIFICATION PANEL

Process verification consisted of C-scan testing, photomicrograph analysis of critical radii, cross sections and bond line thicknesses and resin/void tests of the fully cured subcomponents. Bonding thicknesses ranged from .005 to .012 inches. The results are shown in Table XI. All of the subcomponents passed these tests.

TABLE XI  
Summary of Process Verification Tests

WBS	Item	Acceptable		Resin/Void Content (%)
		C/Scan	Micrograph	
212001	Longeron	Yes	Yes	34.6/1.15
212002	Shear Tee	Yes	Yes	34.1/.98
212003	Frame	Yes	Yes	33.1/1.82
212004	Curved Panel (before bond)	Yes	Yes	32.8/1.22

The panel was nondestructively evaluated for bond-line voids, unbonds, and porosity. The adhesive bond line was evaluated by resonance testing using both a Fokker bondtester Model 70 and an NDT Instruments, Inc. Bondascope Model 2100. The bondlines were found acceptable by both instruments. The panel was subsequently sectioned for optical measurement of the adhesive layer and the bondline quality of the remainder was evaluated by thru-transmission ultrasonic C-scan. The C-scan recording showed excellent correlation with bondtesters. See Figures 65, 66 and 67. Efforts to establish correlation between the actual bondline thickness and instrument readings are still in progress. In addition, a carbon epoxy test part which was cured with the panel during the bond cycle of the shear tee and longeron to the panel was tested. Post test evaluation of the specimen showed that the test specimen was not properly cut from the test part to load the specimen in the intended pattern orientation. The test result therefore is not included.



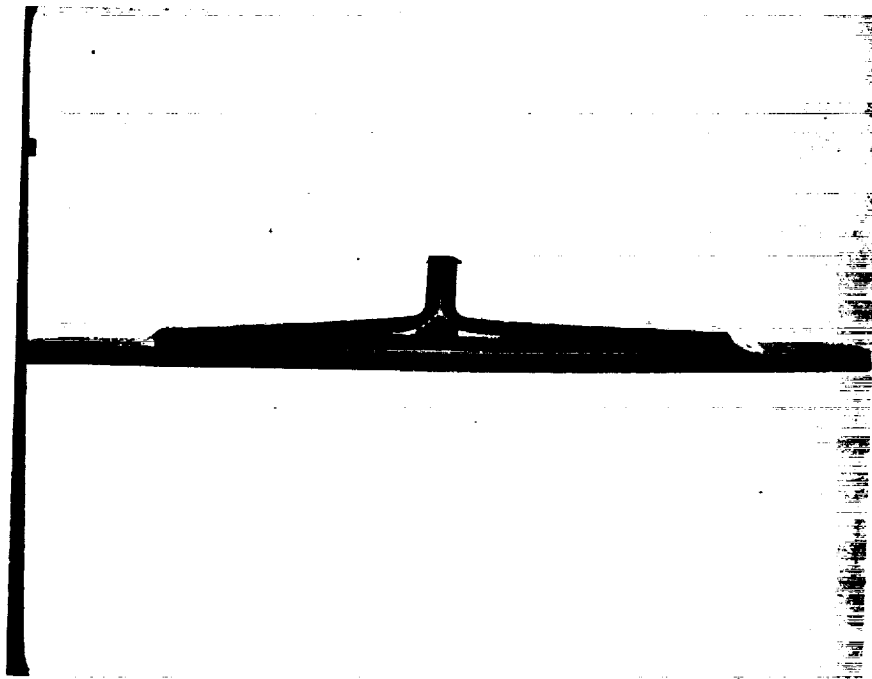


FIGURE 65 BONDED LONGERON TO SKIN CROSS-SECTION

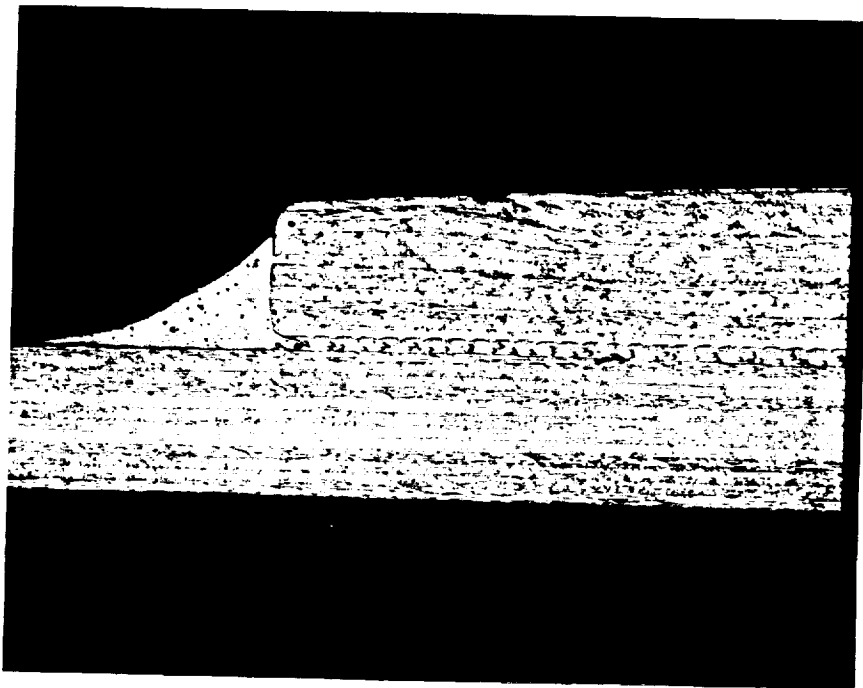


FIGURE 66 11.5 x CARBON EPOXY DETAILS BONDED WITH  
FM-300 SHOWING SCRIM CLOTH ENDS AS DOTS

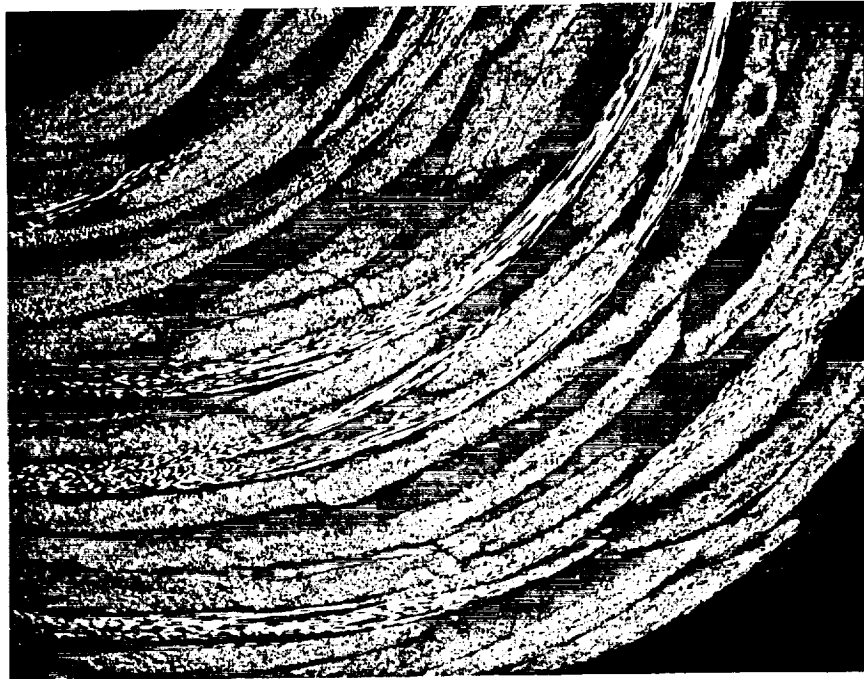


FIGURE 67 PHOTOMICROGRAPH OF LONGERON RADIUS

#### 4.2 TOOL DESIGN AND FABRICATION

##### Shear/Interaction Panels

The tooling approach for carbon/epoxy shear tees included the use of rubber mandrels (DAPCO-CAST #54 Yellow) reinforced with aluminum strips along the length. Shear tees are cured on a 135 inch radius surface using these mandrels. A nylon peel ply is used on the shear tee to fuselage skin mating surface as initial preparation for bonding of the shear tee to the skin.

Two wooden layup mandrels were fabricated for layup debulking of F584/IM6 cloth prior to final bagging. Each mandrel debulks one half of the final shear tee laminate. (Right and left half).

A wooden trough was fabricated and used to cast three sets (each set consists of a right and left side) of rubber mandrels. One 1/8-inch thick by 1/4-inch wide piece of aluminum was imbedded into each mandrel half for transverse stability. A radius of 0.10 inch and ply drop off angles were cast into each mandrel. The tooling concept is illustrated in Figure 68.

A four piece aluminum mandrel was fabricated for making the longeron design configuration. Recent longeron design changes have put the tooling into a rework phase. This completed tool will make a longeron with joggled bottom surface to fit over skin buildups at shear tee locations.

The carbon/epoxy frame will be fabricated on an aluminum mandrel with a polyacrylic rubber caul sheet over the laminate. This tooling approach has produced parts with superior finish on both sides of a part. Adequate pressure in laminate radii is assured and has been proven by photomicrograph analysis.

The aluminum mandrel was numerically control programmed for machining. Programming is complete at present and fabrication is in process. Tooling concept is shown in Figure 69.

Anticipating a possible scheduling problem with one 135 inch radius laminating tool, a 72 inch by 60 inch laminating tool was reworked to a 135 inch radius surface with Douglas funding. Rework was completed in late February and was ready for fabrication of the first 4 x 5 foot panel.

A bonding/locating tool was fabricated for the bonding of shear tees and longerons to the 4 x 5 foot carbon/epoxy skin panel. This tool will position and hold the longerons and tees in place during the FM-300 bond cycle. This locating tool can be used for panels number one through three with minor rework for use on each panel.

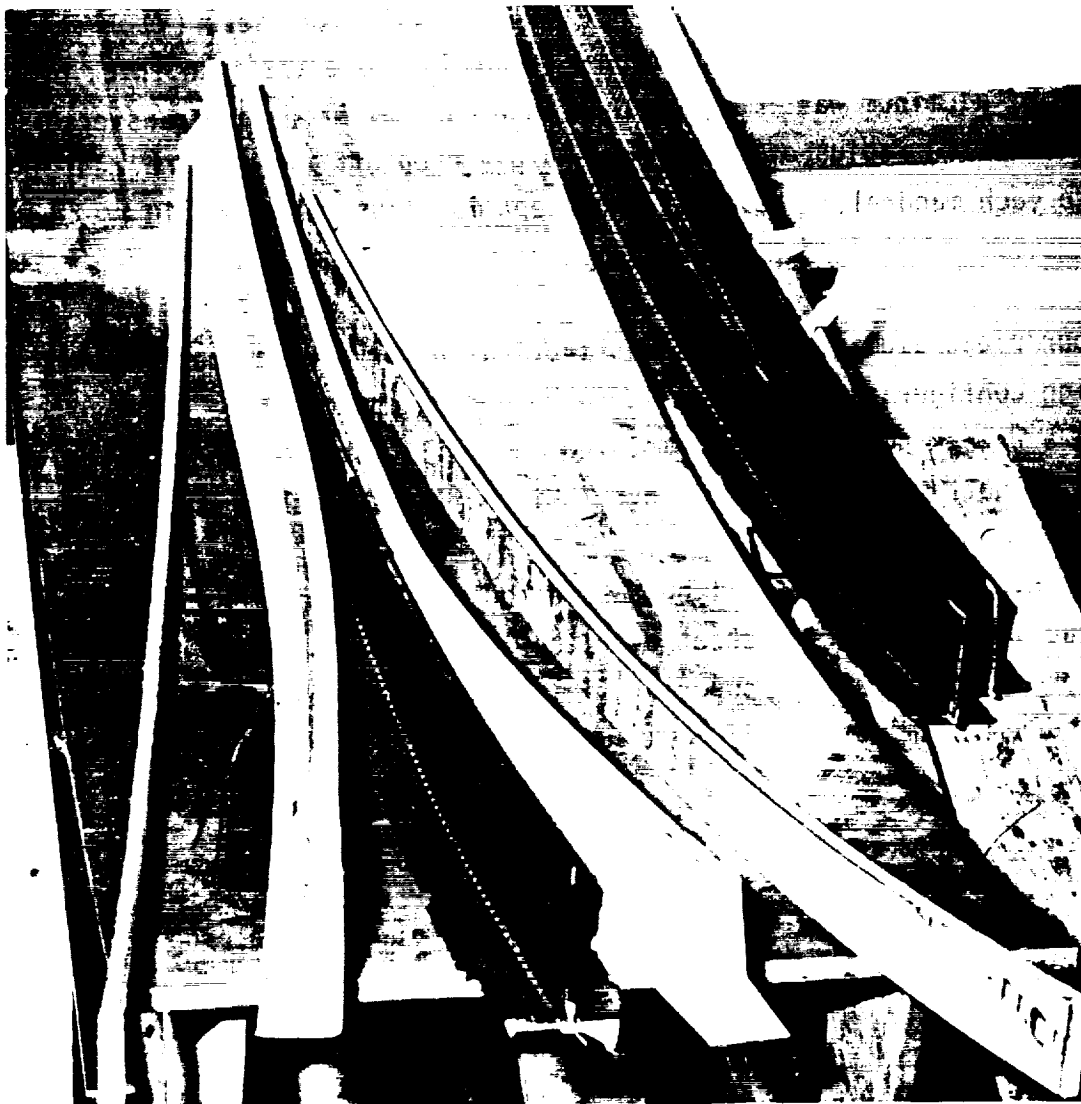


FIGURE 68 SHEAR TEE TOOLING APPROACH

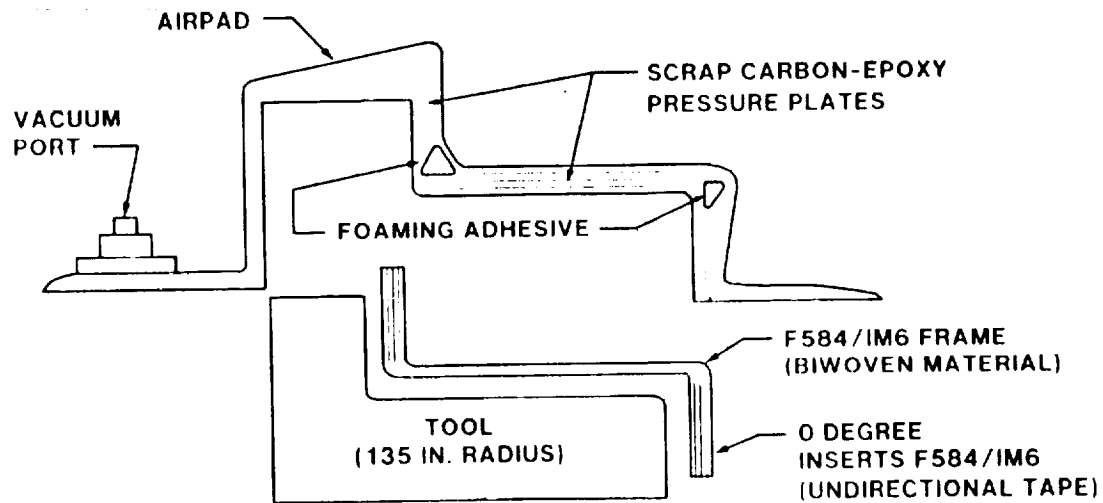


FIGURE 69 FRAME TOOLING CONCEPT

Demonstration Panel

The bonding jig for the 9' x 14' and 4' x 5' panels, as shown in Figures 70 and 71, were nearly completed at the end of the reporting period. The eggcrate backup structure details were fabricated, the assembly of the backup structure completed at DAC and stress relieved at a subcontractor's facility. In addition, studs for holding the laminating surface (bump formed steel plate) to the backup structure and to provide the necessary adjustment for altering the curvature of the surface to the required 135 inch radius were all installed. Some studs were welded to the backside of the bump formed plate while the remaining threaded fasteners were attached to the eggcrate structure.

The eggcrate structure details were completed using a numerically controlled fast-cut milling machine. Some of the steel plates in the machining process are shown in Figure 72. The details were all welded together to form the backup structure. Contour adjustment of the laminating surface is in progress and 80 percent complete. All work on the bonding jig should be completed during April.

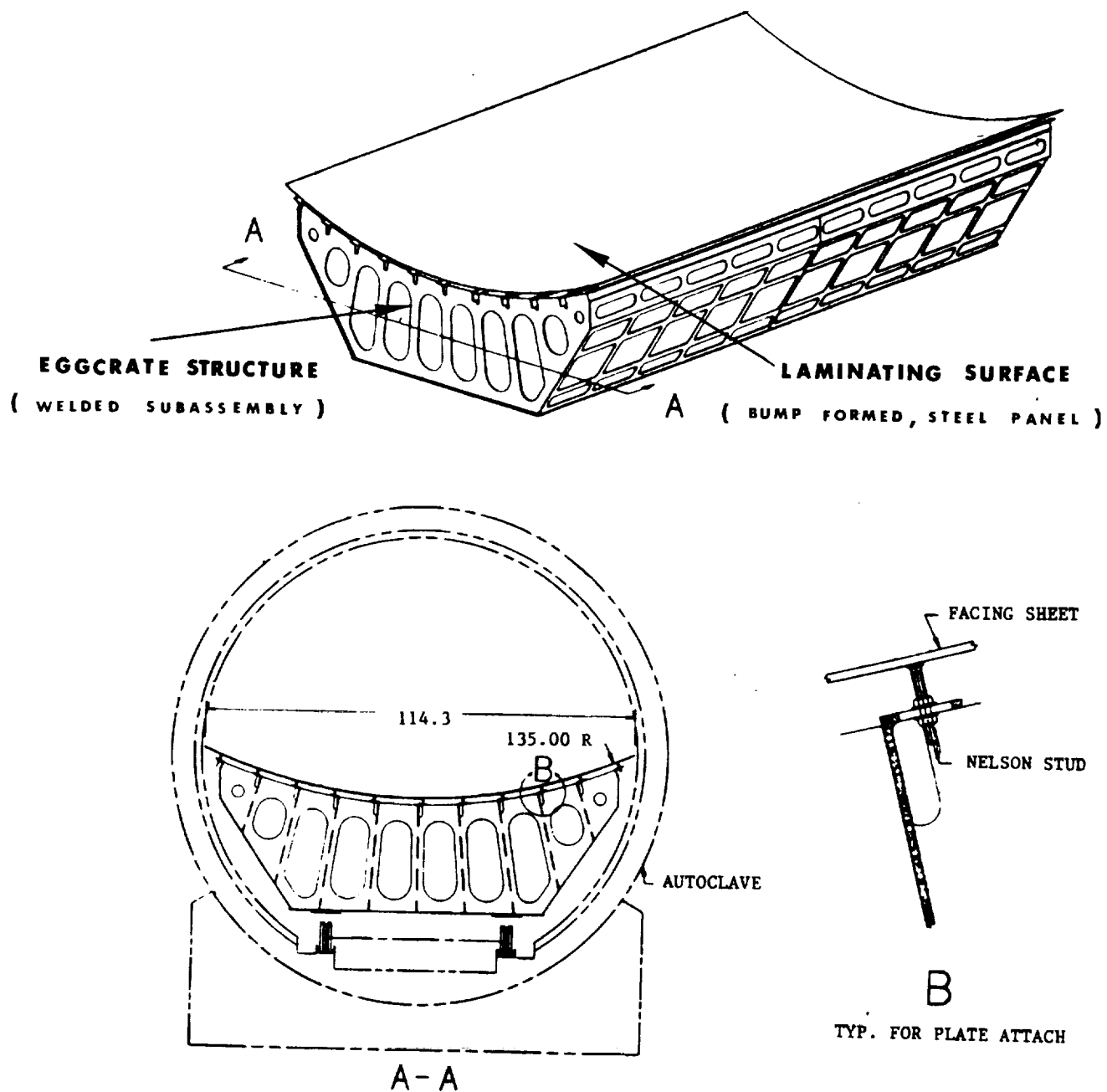


FIGURE 70 DEMONSTRATION PANEL BONDING JIG



FIGURE 71 BONDING JIG



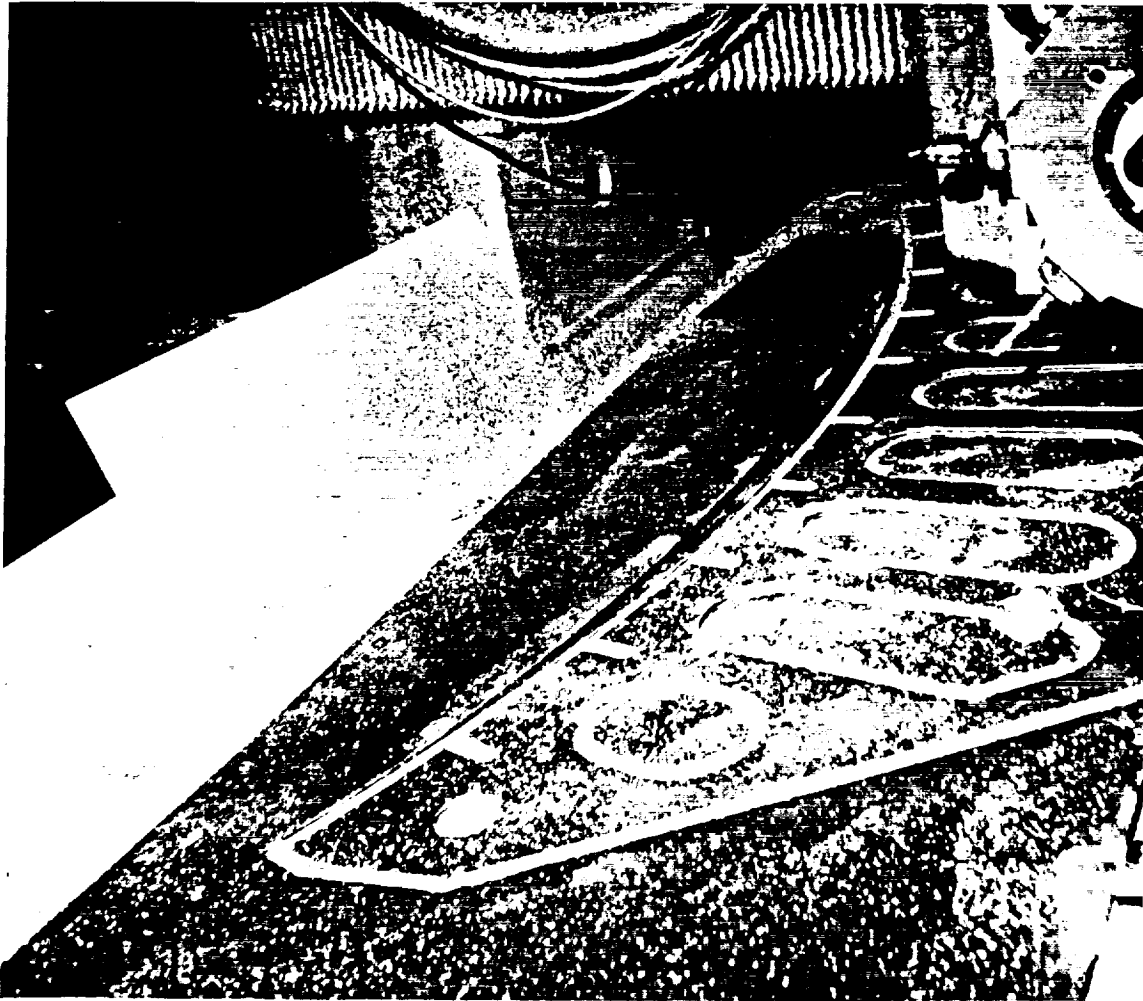


FIGURE 72 FAST-CUT, EGGCRATE STRUCTURE DETAILS

#### 4.3 TEST ARTICLE FABRICATION

Several of the peripheral doublers (aluminum) and miscellaneous metal details were fabricated and raw materials were ordered for the details that will serve as attachments to the test fixture. Carbon epoxy (F584/IM6) tape and broad-goods were cut and pre-kitted for the shear tee, longeron, frame and skin. These pre-kits were labeled and stored for use as needed.



SECTION 5  
TECHNOLOGY DEMONSTRATION

5.1 DEVELOPMENT TESTS

Group A Specimens

All specimens in this group with the exception of the biaxial stress specimens have been tested. The biaxial shear test (BAS-501) utilizes a specially designed fixture, requiring unique calibration procedures. An improved set of machined aluminum calibration coupons with strain gauges attached on both sides is being fabricated.

The nine compression-after-lightning panels have been subjected to lightning strikes and were compression tested. A review of the lightning strike tests is included in this section.

Lightning Protection Tests

The lightning strikes were conducted per Mil-Std-1757A, based on a lightning attachment zone II, which covers surfaces of the vehicle for which there is a high probability of a lightning flash being swept by the airflow from a zone I point of initial flash attachment.

The panels were subjected to a simulated two-component lightning strike. The first component represents a second high peak current return stroke which attaches to the vehicle from ground. It is of high amperage, usually 10-30,000 amperes, and is so brief, less than 50 usec, that the charge transfer is small, usually less than 3 coulombs. However, this high-peak-current phase can create large instantaneous vapor pressures which, in confined regions, can create significant explosive damage. The action integral (Reference 2) is a measure of the energy delivered during this phase

of a strike. The fuselage panels were subjected to a high peak current phase of 100,000 amperes with an action integral of  $.25 \times 10^6 A^2s$ , where A is in amperes and s is in seconds. Statistically, only .5% of the strikes sustained on aircraft today are greater in magnitude, therefore, this is considered a severe test.

The second strike component represents the continuing current phase during which the greatest charge transfer occurs. It develops a charge of approximately 400 amperes in magnitude and lasts about 1000 times longer than the high peak current phase. This results in a high charge transfer which can cause severe burning and eroding of composite material. The continuing-current phase test requirement for the fuselage panels was 400 amperes for 50 msec with a net charge transfer of 20 coulombs.

#### Panel Preparation

An unpainted panel of the same configuration and size as the test specimens was supplied to the lightning strike lab for calibration strikes. Following calibration, each panel was loaded into the test frame (Figure 73), painted side up. The lightning discharge electrode was centered over the strike target, and a steel ground plate was clamped to one end of the panel. A current probe located at the base of the test frame transmitted discharged measurements via an optical fiber cable (used to avoid electro-magnetic interference) to oscilloscopes in an RF shielded control room. The test circuit is diagrammed in Figure 74.

After charging the capacitors in the high current generator, the high peak current component and continuing current components of the simulated strike were delivered through the discharge electrode to the test specimen in rapid sequence.

Figure 75 shows the nickel-coated specimen after a strike. Waveforms for the high peak current component and continuing current components are depicted by oscilloscope photos in figures 76 and 77 respectively.

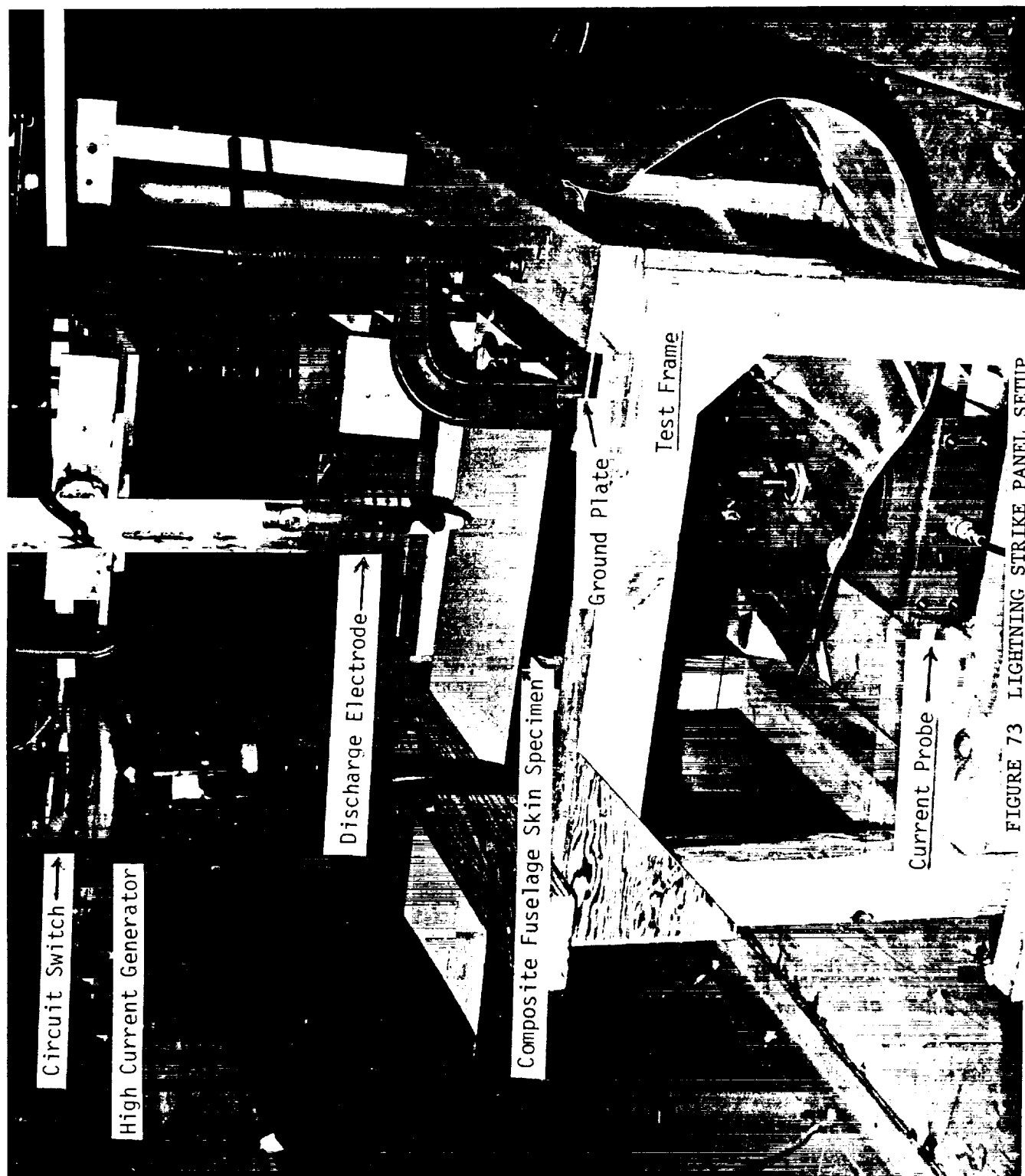


FIGURE 73 LIGHTNING STRIKE PANEL SETUP

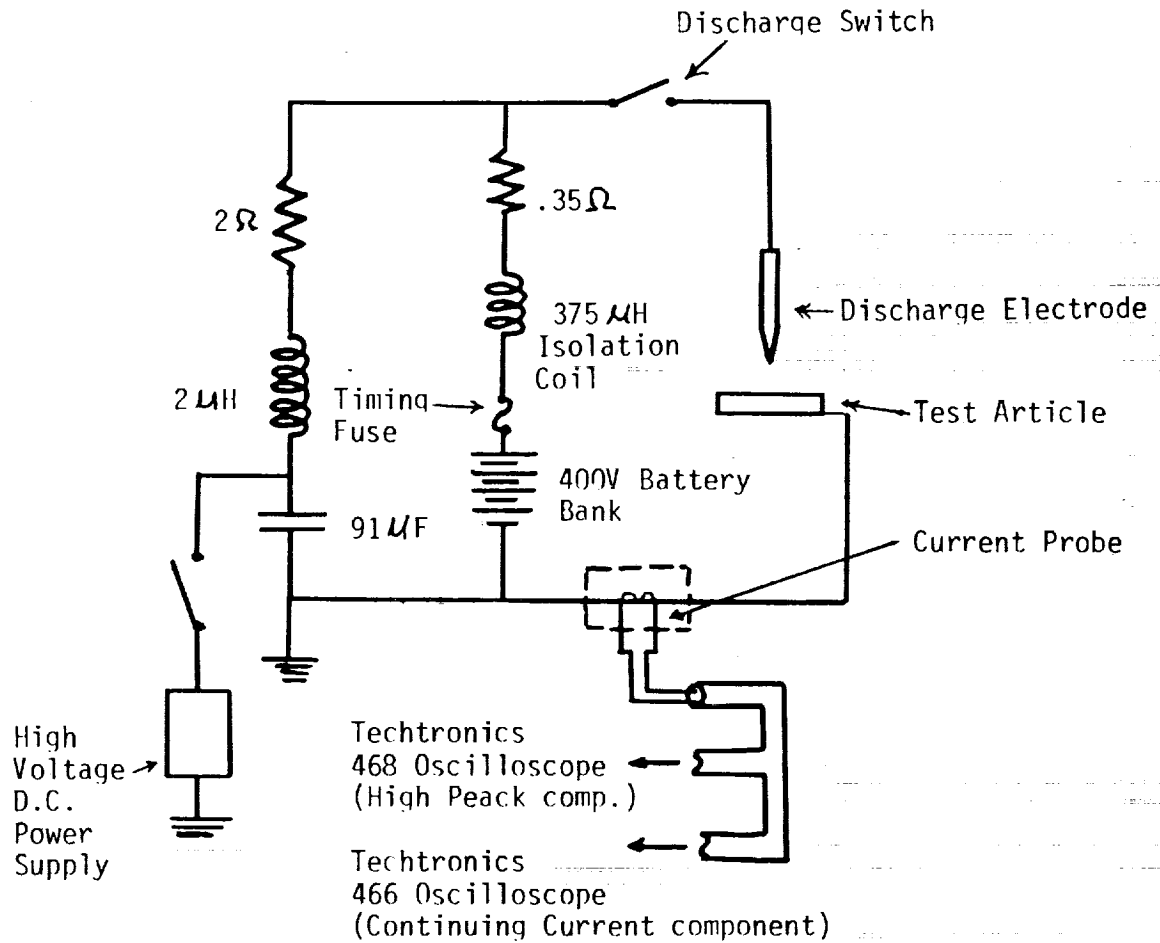
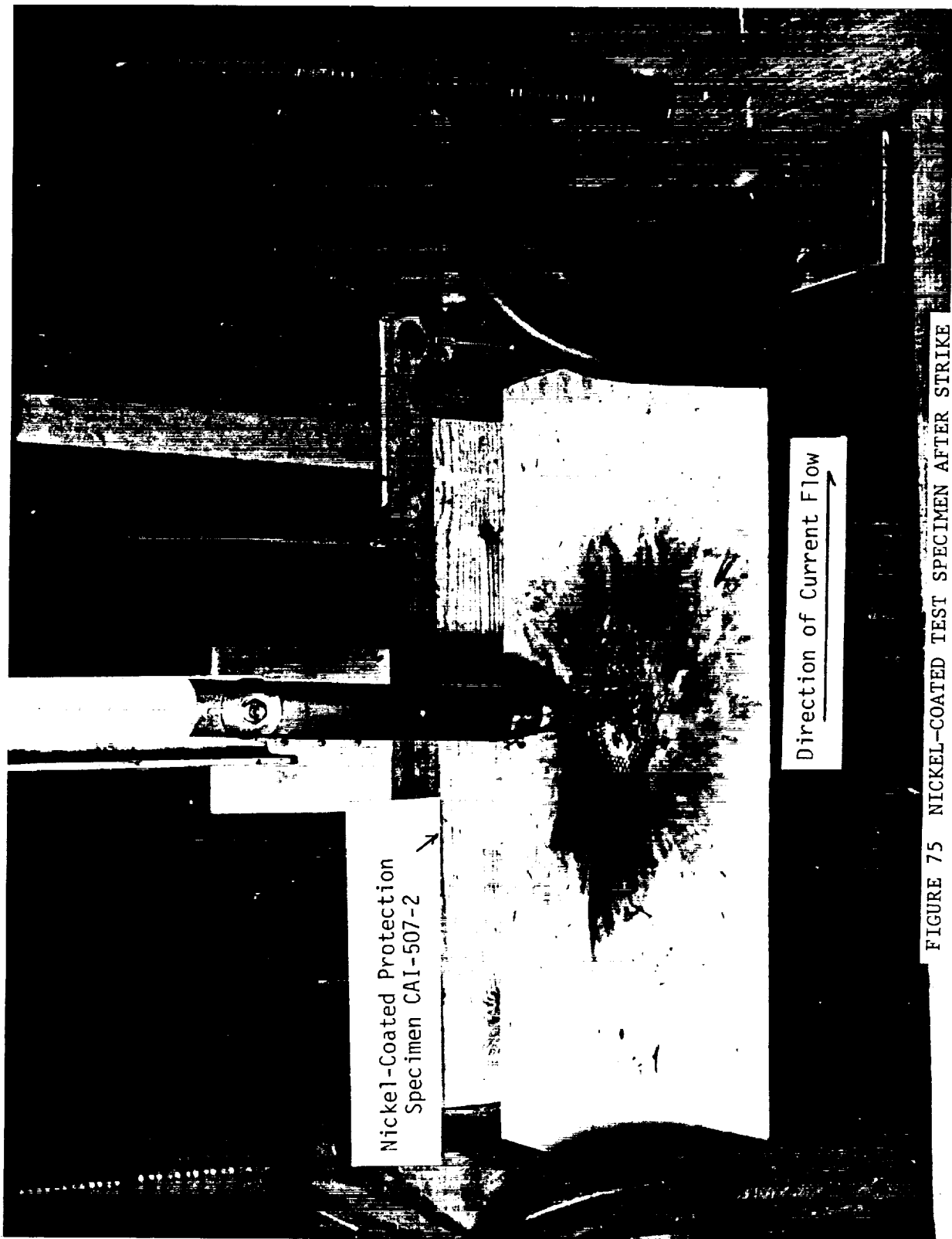


FIGURE 74 TEST CIRCUIT FOR LIGHTNING SIMULATION

Three strikes were conducted on each of the three panels. A representative photo of visual damage done to each of the three panels is shown in Figures 78, 79, and 80. Table XII details electrical measurements made from each test. Table XIII includes a description of damage.

The wire woven protection system, CAI-505, displayed the least damage, and the unprotected panel displayed the most. (CAI-509)



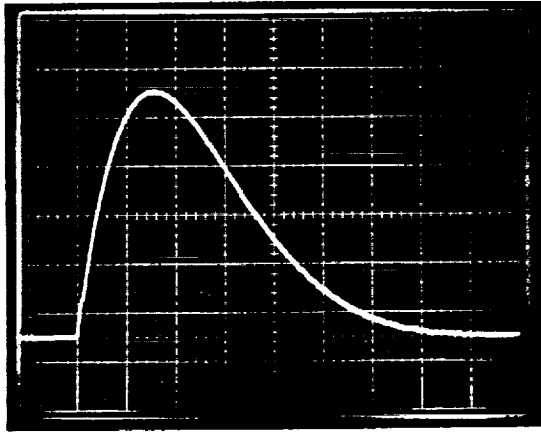


FIGURE 76 HIGH PEAK CURRENT  
COMPONENT WAVEFORM  
(KA vs t)

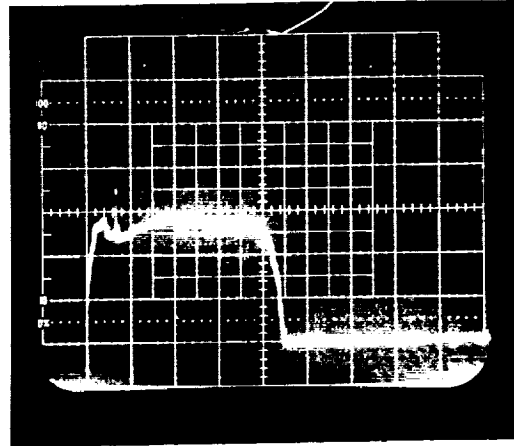


FIGURE 77 CONTINUING  
CURRENT COMPONENT  
WAVEFORM (A vs t)

It should be noted that the unpainted, unprotected calibration panel displayed less damage than the painted unprotected panel when subjected to a nearly equal lightning strike. The calibration panel displayed damage through 4-5 plies, with no through-penetration, and in fact, no visible damage to the back side.

It is suspected that the paint layer, approx. 4-6 mils, has the effect of confining the energy of the high peak current component of the strike, resulting in explosive damage. Without the paint layer, energy from the strike is more quickly dissipated.





FIGURE 78 AFTER STRIKE DAMAGE ON WIRE WOVEN PANEL (UNC-505-2)





FIGURE 80 AFTER STRIKE DAMAGE ON UNPROTECTED PANEL (UNC-509-3)

TABLE XII  
LIGHTNING DISCHARGE TEST VALUES

SPECIMEN ID	CHARGE TRANSFER (coulombs)	PEAK CURRENT (KA)	ACTION INTEGRAL ( $A^2s$ )	GENERATOR VOLTAGE (KV)	CIRCUIT RESISTANCE (OHM)
CAI-505					
-1	22	105	.275 $\times 10^6$	+37	0.23
-2	24	103	.265 $\times 10^6$	+37	0.24
-3	22	102	.26 $\times 10^6$	+36	0.23
CAI-507					
-1	21	95	.23 $\times 10^6$	+35	0.24
-2	20	103	.265 $\times 10^6$	+38	0.25
-3	17.5	102	.26 $\times 10^6$	+37	0.24
CAI-509					
-1	21	98	.24 $\times 10^6$	+40	0.30
-2*	21	---	-----	+39	---
-3	20.5	101	.255 $\times 10^6$	+39	0.28

\*Measurement signal from high peak current component was not recordable. However, voltage, charge transfer, and visual damage is similar to CAI-509-1, and CAI-509-3.

TABLE XIII  
LIGHTNING DAMAGE

SPECIMEN ID.	
Wire Woven CAI-505-1	Principle damage area .6-1.2" dia. Damage extends through top protection ply only. Top ply weave is largely intact in damage area, though fibers have no resin and are delaminated from ply below in approx. 0.4" diameter. (Photo, Fig. 78)
Nick. Coat. CAI-507-1	Principle damage area 1.75" - 2.0". Damage extends through top protection ply, with resin eliminated from .5" dia. in second ply. Top ply weave destroyed in 1.0" dia. area. Top ply delamination in 2.9" dia. area. (Photo, Fig. 79)
Un-protect. CAI-509-1	Principle damage area 2.4.3.1", principle damage area extends through 6-8 plies. 1/8" diameter hole penetrates through all 12 plies. Rear ply splintered off in a 0.2" x 6" strip. Top ply blown off in approx. 0.70 inch wide strips. (Fig. 80) Pulging of top surface, 3.00" dia., .10" high.

\*Visible damage of 3 strikes on each panel is similar; therefore, descriptions here are representative of all strikes on a given panel.

### Group B Specimens

#### Shear-T Pulloff Tests

The testing of Group B Shear-Tee pulloff specimens was initiated near the end of the reporting period and will be completed during April, 1985.

The specimens were installed in the loading fixture, as depicted in Figure 81, and load was applied at a rate of .050"/min.

Skin deflection was recorded at three locations. Deflection at the shear-tee center was recorded as cross-head travel. At the two points where the shear-tee flange terminates, deflection was measured using a caliper.

Figure 82 illustrates a specimen under 800 lb. loading.

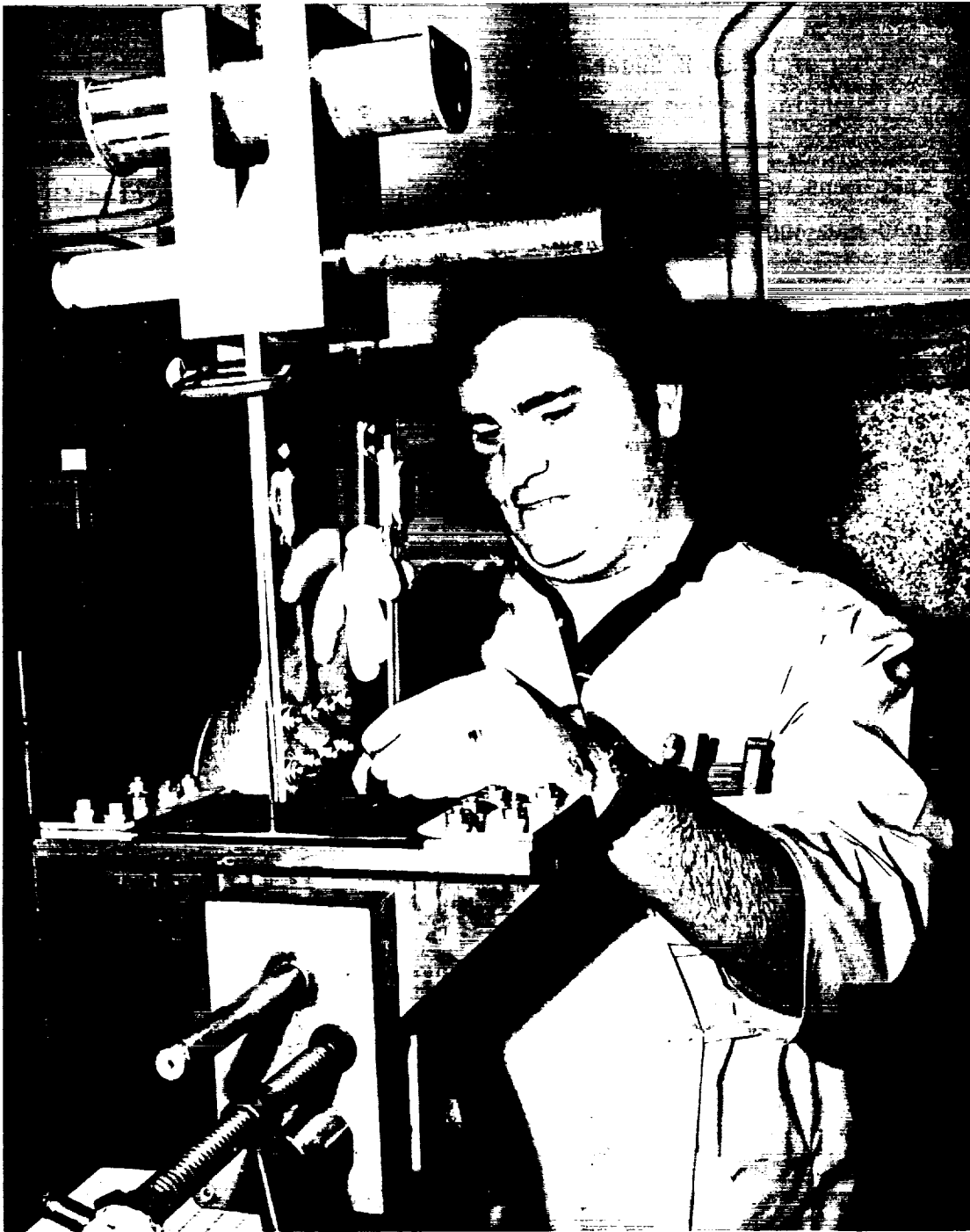


FIGURE 81 TYPICAL SHEAR-TEE SETUP

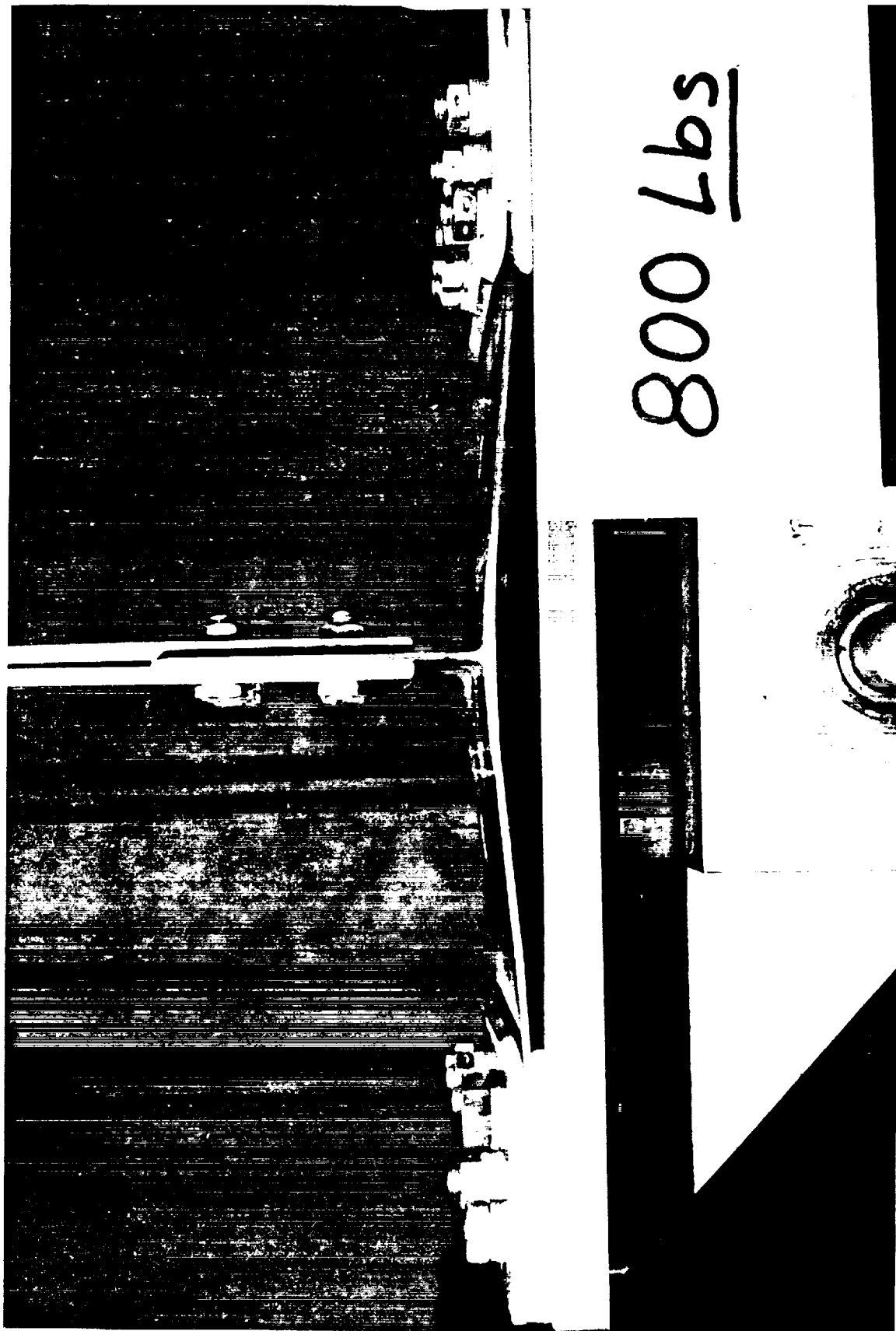


FIGURE 82 SHEAR-TEE SPECIMEN UNDER AN 800 lb. LOAD





SECTION 6

REFERENCES

1. Nelson, W.D.; Bunin, B. L.; and Hart-Smith, L. J.: Critical Joints in Large Composite Aircraft Structure. NASA CR-3710, January 1983.
2. Military Standard  
Lightning Qualification Test Techniques for Aerospace Vehicles and Hardware MIL-STD-1757A.



Douglas Aircraft Company  
Contract NAS1-17701

ACEE-34-PR-3507

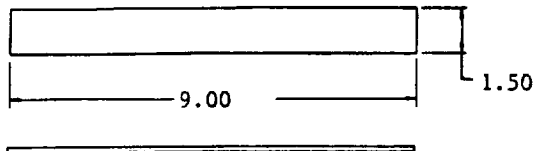
## APPENDIX A

LAYUP PATTERNS, SPECIMEN DESCRIPTIONS  
AND TEST DATA

TABLE AI

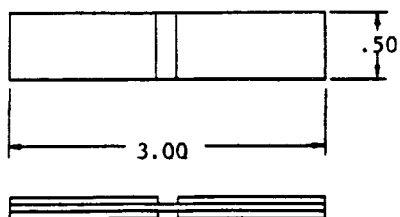
COMPOSITE FUSELAGE LAMINATES

#	Description	Layup Pattern
1	Basic Skin (All Tape) $t = .068"$	$(0, 90, 45, 0, -45, 90)_s$
2	Pad-up Skin (All Tape) $t = .091$	$(0, 90, 45, -45, 0, 45, -45, 90)_s$
3	60% $0^0$ (Cloth & Tape) $t = .147"$	$(0/90, 0, 0, \pm 45, 0, 0, 0/90)_s$
4	Longeron (All Cloth) $t = .102$	$(0/90, \pm 45, 0/90)_s$



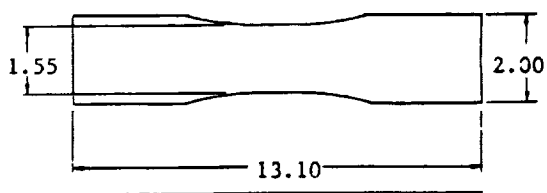
MONOLAYER SPECIMEN, TENSION (MLT)

<u>CONFIGURATION #</u>	<u>LAYUP / MAT'L</u>
-501	0/TAPE IM6
-503	90/TAPE IM6
-505	0/90/CLOTH IM6
-507	0/90/CLOTH E GLASS



MONOLAYER SPECIMEN, COMPRESSION (MLC)

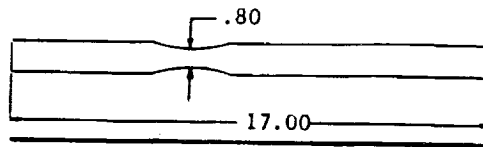
<u>CONFIGURATION #</u>	<u>LAYUP / MAT'L</u>
-501	0/TAPE IM6
-503	90/TAPE IM6
-505	0/90/CLOTH IM6
-507	0/90/CLOTH E GLASS



SHEAR SPECIMEN, 45 OFF-AXIS (MLS)

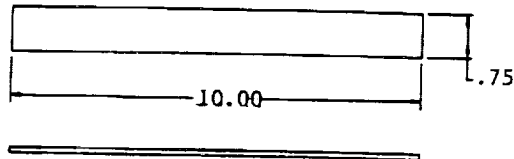
<u>CONFIGURATION #</u>	<u>LAYUP / MAT'L</u>
-501	+45,-45/TAPE IM6
-503	±45/CLOTH IM6
-505	±45/CLOTH E GLASS

FIGURE A1 - SPECIMEN DESCRIPTIONS



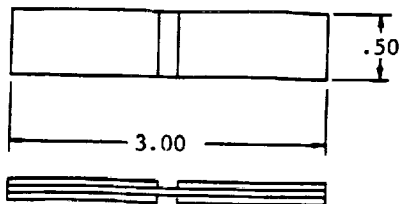
UNNOTCHED SPECIMEN, TENSION (UNT)

<u>CONFIGURATION #</u>	<u>LAYUP #</u>
-501	1
-503	2
-505	3
-511	4



UNNOTCHED SPECIMEN, TENSION (UNT)

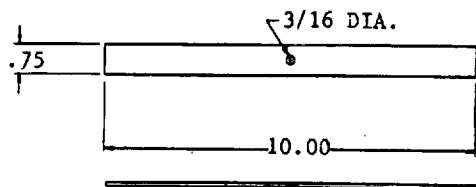
<u>CONFIGURATION #</u>	<u>LAYUP #</u>
-507	1 WITH LIGHTNING PROTECTION
-509	1 WITH LIGHTNING PROTECTION



UNNOTCHED SPECIMEN, COMPRESSION (UNC)

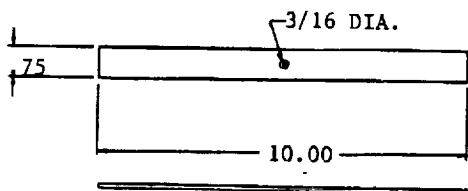
<u>CONFIGURATION #</u>	<u>LAYUP #</u>
-501	1
-503	2
-505	3
-507	4

FIGURE A1 - SPECIMEN DESCRIPTIONS (Continued)



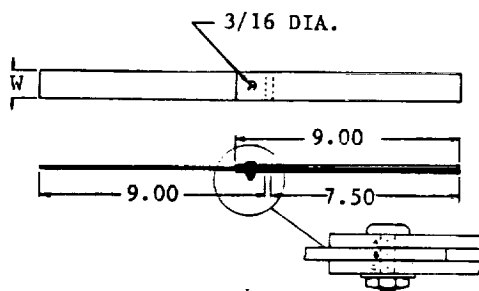
UNLOADED HOLE SPECIMEN, TENSION (ULT)

<u>CONFIGURATION #</u>	<u>LAYUP #</u>
-501	4
-503	2
-505	3
-507	2 COUNTERSUNK



UNLOADED HOLE SPECIMEN, COMPRESSION (ULC)

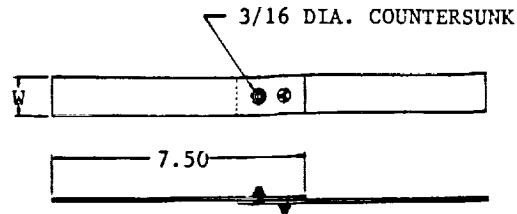
<u>CONFIGURATION #</u>	<u>LAYUP #</u>
-513	4 "LOOSE FIT" 1/8 BOLT
-515	2 "LOOSE FIT" 1/8 BOLT
-517	3 "LOOSE FIT" 1/8 BOLT
-519	4 "NET FIT" 3/16 BOLT
-521	2 "NET FIT" 3/16 BOLT
-523	3 "NET FIT" 3/16 BOLT
-525	2 COUNTERSUNK NO FASTENER
-527	2 COUNTERSUNK "NET FIT" 3/16 BOLT



DOUBLE-LAP JOINT SPECIMEN, TENSION (DLT)

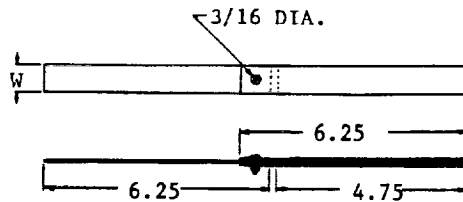
<u>CONFIGURATION #</u>	<u>WIDTH</u>	<u>LAYUP #</u>
-501	.563	4 W/D=3
-503	.563	2 W/D=3
-505	.563	3 W/D=3
-507	1.125	4 W/D=6
-509	1.125	2 W/D=6
-511	1.125	3 W/D=6
-525	.563	2 SPLICE MEMBER COUNTERSUNK W/D=3
-527	1.125	2 SPLICE MEMBER COUNTERSUNK W/D=6

FIGURE A1 - SPECIMENS DESCRIPTIONS (Continued)



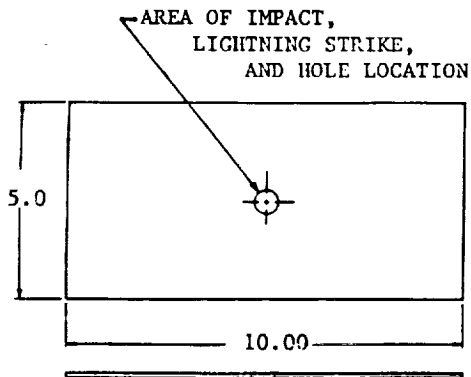
SINGLE-LAP JOINT SPECIMEN, TENSION (SLT)

CONFIGURATION #	WIDTH	LAYUP #
-501	.563	2 W/D=3
-503	1.875	2 W/D=10
-505	.563	2 W/D=3



DOUBLE-LAP JOINT SPECIMEN, COMPRESSION (DLC)

CONFIGURATION #	WIDTH	LAYUP #
-513	.563	4 W/D=3
-515	.563	2 W/D=3
-517	.563	3 W/D=3
-519	1.125	4 W/D=6
-521	1.125	2 W/D=6
-523	1.125	3 W/D=6
-529	.563	2 SPLICE MEMBER COUNTERSUNK W/D=3
-531	1.125	2 SPLICE MEMBER COUNTERSUNK W/D=6



COMPRESSION AFTER IMPACT (CAI)

CONFIGURATION #	LAYUP #
-501	1 IMPACT AT 4 FT.-LBS.
-503	1 .50 DIA. HOLE
-505	1 SUBJECTED TO LIGHTNING- NICKEL COATED PROTECTION
-507	1 SUBJECTED TO LIGHTNING- AL. WIRE WOVEN PROTECTION
-509	1 SUBJECTED TO LIGHTNING- UNPROTECTED

FIGURE A1 - SPECIMEN DESCRIPTIONS (Continued)



TABLE AII

SPECIMEN I.D.	LAYUP #	W(IN)	FAILURE LOAD (#)	FAILURE STRESS (PSI)	FAILURE MODE	AVERAGE DATA & COMMENTS
Z3941210- MLT-501-1	IM6	1.496	24150	354014	Tension	$F_L^t = 343400$
-2	Tape	1.497	22850	334734		$E_L^t = 23.0$
-3	Monolayer	1.496	23300	341554		$\nu_{LT} = .33$
MLT-503-1	IM6	1.496	443	6494	Tension	$F_T^t = 7207$
-2	Tape	1.496*	500	7329		$E_T^t = 1.25$
-3	Monolayer	1.496*	532	7798		$\nu_{LT} = .02$
MLT-505-1	IM6	1.502	13720	133545	Tension	$F_L^t = 142800$
-2	Cloth	1.504	15820	153780		$E_L^t = 10.1$
-3	Monolayer	1.504	14520	141144		$\nu_{LT} = .07$
MLT-507-1	"E Glass"	1.504	2200	29985	Tension	$F_L^t = 29199$
-2	Cloth	1.500	2210	30191		$E_L^t = 2.1$
-3	Monolayer	1.502	2010	27421		$\nu_{LT} = .18$

\* Assumed dimensions, actual data not recorded during test.

TABLE AIII

SPECIMEN I.D.	LAYUP #	W(IN)	FAILURE LOAD (#)	FAILURE STRESS (PSI)	FAILURE MODE	AVERAGE DATA & COMMENTS
Z3941211- MLC-501-1	IM6	.498	2550	112291*	Compression	$F_L^C = 202700$
	Tape	.501	4570	200038		
	Monolayer	.499	4675	205454		
MLC-503-1	IM6	.498	860	37870	Compression	$F_L^C = 37400$
	Tape	.500	870	38158		
	Monolayer	.499	820	36037		
MLC-505-1	IM6	.505	3150	91193	Compression	$F_L^C = 86300$
	Cloth	.507	2930	84489		
	Monolayer	.504	2870	83252		
MLC-507-1	"E Glass"	.502	1605	65517	Compression	$F_L^C = 65300$
	Cloth	.514	1565	62392		
	Monolayer	.504	1670	67899		

\* Data point not used in calculation of average value.

TABLE AIV					
SPECIMEN I.D.	LAYUP #	W(IN)	FAILURE LOAD (#)	FAILURE STRESS (PSI)	FAILURE MODE
Z3941212-					
MLS-501-1	IM6	1.572	2890	(Shear) 20158	
-2	Tape	1.550	2860	20232	Shear
-3	Monolayer	1.572	2880	20088	
					$F_{SH} = 20200$ $G_{LT} = .70$
MLS-503-1	IM6	1.572	3350	(Shear) 15669	
-2	Cloth	1.572	3540	16558	Shear
-3	Monolayer	1.570	3820	17890	
					$F_{SH} = 16700$ $G_{LT} = .55$
MLS-505-1	"E Glass"	1.560	2100	(Shear) 13793	
-2	Cloth	1.564	2150	14085	Shear
-3	Monolayer	1.558	2090	13745	
					$F_{SH} = 13900$

TABLE AV

SPECIMEN I.D.	LAYUP #	W(IN)	FAILURE LOAD (#)	FAILURE STRESS (PSI)	FAILURE MODE	AVERAGE DATA & COMMENTS
Z3941213- UNT-501-1	1	.800	5720	108713	Tension	$F_X^{TU} = 112998$ $E_X = 8.64$ $\nu_{XY} = .205$
-2		.802	6070	115077		
-3		.810	6360	119384		
UNT-503-1	2	.812	8360	112889	Tension	$F_X^{TU} = 118400$ $E_X = 7.95$ $\nu_{XY} = .33$
-2		.821	8060	107645		
-3		.811	8950	121006		
UNT-505-1	3	.784	18850	163560	Tension	$F_X^{TU} = 168169$ $E_X = 12.12$ $\nu_{XY} = .25$
-2		.782	19100	166153		
-3		.788	18000	155392		
UNT-507-1	#1 with Lightning Protection <sup>1</sup>	.748	5020	98117	Tension	$F_X^{TU} = 98335$ $E_X = 8.00$
-2		.747	5220	102163		
-3		.747	4840	94726		
UNT-509-1	#1 with Lightning Protection <sup>2</sup>	.750	5430	105850	Tension	$F_X^{TU} = 102532$ $E_X = 9.30$
-2		.749	5020	97986		
-3		.751	5330	103760		
UNT-511-1	4	.791	9030	111920	Tension	$F_X^{TU} = 114429$ $E_X = 8.3$ $\nu_{XY} = .180$
-2		.775	8600	108792		
-3		.770	8590	109371		

- 1 Outside 0 and 90 layers of tape replaced with 0/90 layer of aluminum wire woven carbon cloth.
- 2 Outside 0 and 90 layers of tape replaced with 0/90 layer of nickel coated carbon cloth.

TABLE AVI

SPECIMEN I.D.	LAYUP #	W(IN)	FAILURE LOAD (#)	FAILURE STRESS (PSI)	FAILURE MODE	AVERAGE DATA & COMMENTS
Z3941214- UNC-501-1	1	.505	2825	81784		
-2		.504	2960	85863	Compression	$F_X^{cu} = 83824$
-3		.505	---	---		
UNC-503-1	2	.506	3330	72160		
-2		.507	3870	83697	Compression	$F_X^{cu} = 78000$
-3		.505	3600	78165		
UNC-505-1	3	.507	7920	105835		
-2		.507	7900	105568	Compression	$F_X^{cu} = 105994$
-3		.506	7960	106580		
UNC-507-1	4	.507	4080	78895		
-2		.505	4170	80955	Compression	$F_X^{cu} = 80700$
-3		.507	4250	82182		

\* Test fixture malfunction, no data.

TABLE AVII

SPECIMEN I.D.	LAYUP #	W(IN)	FAILURE LOAD (#)	FAILURE STRESS (PSI)	FAILURE MODE	AVERAGE DATA & COMMENTS
Z3941215- ULT-501-1	4	.746 .754 .752	5130 5090 5030	(Net Section) 90457 88478 87746	Net Section Tension	$C_{uh} = .203$
ULT-503-1	2	.754 .754 .754	4100 4620 4250	(Net Section) 79709 89818 82625	Net Section Tension	$C_{uh} = -.290$
ULT-505-1	3	.745 .753 .751	13420 14100 14980	(Net Section) 163822 169678 180910	Net Section Tension	$C_{uh} = -.012$
ULT-504-1	2	.756 .754 .755	3370 3210 3530	(Net Section)* 80584 77095 84595	Net Section Tension	Countersunk

\* Net Section stress includes reduction in cross section due to countersink

TABLE AVIII

SPECIMEN I.D.	LAYUP #	W(IN)	FAILURE LOAD (#)	FAILURE STRESS (PSI)	FAILURE MODE	AVERAGE DATA & COMMENTS
Z3941215- ULC-513-1	4	.755 .755 .751	2710 2700 2710	(Net Section) 47024 46850 47024	Net Section Compression	"Loose Fit" Bolt
ULC-515-1	2	.752 .752 .751	2120 2320 1960	(Net Section) 41453 45364 38393	Net Section Compression	"Loose Fit" Bolt
ULC-517-1	3	.754 .751 .754	5880 5330 5480	(Net Section) 70922 64632 66097	Net Section Compression	"Loose Fit" Bolt
ULC-519-1	4	.758 .752 .754	2250 2890 2520	(Gross Section) 29101 37677 32766	Gross Section Compression (Front of Hole)	"Net Fit" Bolt
ULC-521-1	2	.755 .754 .754	2530 2630 2740	(Gross Section) 36824 38330 39933	Gross Section Compression (Front of Hole)	"Net Fit" Bolt
ULC-523-1	3	.751 .756 .753	6510 6190 6340	(Gross Section) 58969 55699 57277	Gross Section Compression (Front of Hole)	"Net Fit" Bolt

TABLE AIX

SPECIMEN I.D.	LAYUP #	W(IN)	FAILURE LOAD (#)	FAILURE STRESS (PSI)	FAILURE MODE	AVERAGE DATA & COMMENTS
Z3941215- ULC-525-1		.754	1630	(Net Section)* 39254		
-2	2	.754	1620	39014	Net Section Compression	Open Hole Countersunk
-3		.755	1730	41571		
ULC-527-1		.753	2100	(Gross Section) 30579		
-2	2	.753	2170	31599	Gross Section Compression	Countersunk "Net Fit" Bolt
-3		.754	2150	31266		

\* Net Section Stress includes reduction in cross section due to countersink



TABLE AX

SPECIMEN I.D.	LAYUP #	W(IN)	FAILURE LOAD (#)	FAILURE STRESS (PSI)	FAILURE MODE	AVERAGE DATA & COMMENTS
23941217- DLT-501-1	4	.563 .564 .563	2480 2500 2570	(Net Section) 65184 65534 67550	Net Section (Much Interlaminar Splitting)	$C_{LH} = .33$
DLT-503-1	2	.565 .5675 .566	2350 2340 2480	(Net Section) 68713 67968 72322	Net Section	$C_{LH} = .31$
DLT-505-1	3	.563 .564 .563	3790 3720 3780	(Bearing) 135696 133190 135338	Shearout	Fbry = 88912 Fbru = 134741
DLT-507-1	4	1.136 1.135 1.136	2880 2850 2840	(Bearing) 148606 147059 146543	Bearing (Some Evidence of Shearout)	Fbry = 91176 Fbru = 147400
DLT-509-1	2	1.134 1.132 1.136	3000 2780 3080	(Bearing) -----* 160786 173511	Bearing	Fbry = 109890 Fbru = 167149
DLT-511-1	3	1.134 1.132 1.135	3860 3840 4030	(Bearing) 138200 137500 144300	Bearing (Some Evidence of Shearout)	Fbry = 89500 Fbru = 139966

\* Test machine malfunction, no data

TABLE AXI

SPECIMEN I.D.	LAYUP #	W(IN)	FAILURE LOAD (#)	FAILURE STRESS (PSI)	FAILURE MODE	AVERAGE DATA & COMMENTS
Z3941217- DLT-525-1	2	.564	2340	(Net Section) 68754	Net Section Tension	$C_{LH} = .30$ (Countersunk)
-2		.565	2370	69451		
-3		.565	2480	72674		
DLT-527-1		1.131	2600	(Bearing) 150376	Bearing	Fbry = 100250 Fbru = 152882 (Countersunk)
-2	2	1.132	2760	159630		
-3		1.136	2570	148641		
Z3941216- SLT-501-1	2	.565	2650	(Gross Section) 51541	Net Section Tension	Pavrg = 2500 (C/S) (1250 bearing 1250 bypass)
-2		.564	2420	47151		
-3		.564	2430	47346		
SLT-503-1	2	1.880	3740	(Bearing) 108155	"Pull-Thru" Fastener Failure	Fbru = 107866 (Countersunk)
-2		1.882	3670	106130		
-3		1.882	3780	109312		
SLT-505-1	2	.564	2280	(Gross Section) 44424	Net Section Tension	Pavrg = 2314 (1157 bearing 1157 bypass)
-2		.564	2180	42475		
-3		.564	2480	48320		

TABLE AXII

SPECIMEN I.D.	LAYUP #	W(IN)	FAILURE LOAD (#)	FAILURE STRESS (PSI)	FAILURE MODE	AVERAGE DATA & COMMENTS
Z3941217- DLC-513-1	4	.563 .563 .564	2660 2500 2420	(Gross Section) 46320 43534 42066	Compression in Front of Hole	Fbry = 86000
DLC-515-1	2	.566 .566 .566	1850 2010 2120	(Gross Section) 35918 39025 41160	Section Failure Outside of Clamp- up area (Some hole deformation)	Fbry = 85800
DLC-517-1	3	.562 .565 .561	3860 3770 4150	(Gross Section) 46723 45391 50323	Compression in Front of Hole	Fbry = 82350
DLC-519-1	4	1.133 1.134 1.131	2860 4370 3450	(Bearing) 147575 225490 178019	Bearing	Fbry = 107000 Fbru = 183700
DLC-521-1	2	1.132 1.135 1.134	3110 3260 3270	(Bearing) 179873 188548 189127	Bearing	Fbry = 119000 Fbru = 185850
DLC-523-1	3	1.132 1.132 1.130	4810 4670 4700	(Bearing) 172216 167203 168278	Bearing	Fbry = 88000 Fbru = 169200

TABLE AXIII

SPECIMEN I.D.	LAYUP #	W(IN)	FAILURE LOAD (#)	FAILURE STRESS (PSI)	FAILURE MODE	AVERAGE DATA & COMMENTS
Z3941217-				(Gross Section)		
DLC-529-1		.565	2150	41816		Fbry = 94500
-2	2	.565	2380	46290	Section Failure	(Countersunk)
-3		.563	2310	45088	Outside of Clamp- up area (Some hole deformation)	
DLC-531-1		1.133	2840	(Bearing)		Fbry = 116000
-2	2	1.133	2940	164257	Bearing	Fbru = 167300
-3		1.133	2900	170040		(Countersunk)
				167727		

TABLE AXIV

SPECIMEN I.D.	LAYUP #	W(IN)	FAILURE LOAD (#)	FAILURE STRESS (PSI)	FAILURE MODE	AVERAGE DATA & COMMENTS
Z3941218- CAI-501-1	1	5.000	13900	(Gross Section) 40643	Compression	Impacted @
-2		5.003	17950	52454	thru Impact	4 FT LBS
-3		5.002	17600	51441	Damage Area	
CAI-503-1	1	-----	----- <sup>3</sup>	(Gross Section)	Compression	1/2" Hole
-2		5.010	12100	35309	thru Hole	
-3		5.000	10200	29824		
CAI-505-1	#1 with Lightning Protection <sup>1</sup>	4.996	19160	56068	Compression	Subjected to a $6A_2$ -
-2		4.996	21400	----- <sup>4</sup>	thru Damaged	100 KA @ .25x10 <sup>6</sup> A <sup>2</sup> -
-3		4.998	15040	----- <sup>4</sup>	Area	sec strike
CAI-507-1	#1 with Lightning Protection <sup>2</sup>	4.995	16660	----- <sup>4</sup>	Compression	Subjected to a $6A_2$ -
-2		4.995	17080	49991	thru Damaged	100 KA @ .25x10 <sup>6</sup> A <sup>2</sup> -
-3		4.993	16980	----- <sup>4</sup>	Area	sec strike
CAI-509-1	1	4.997	8960	26215	Compression	Subjected to a $6A_2$ -
-2		4.997	8630	25249	thru Damaged	100 KA @ .25x10 <sup>6</sup> A <sup>2</sup> -
-3		4.996	8100	23703	Area	sec strike

- 1 Outside 0 and 90 layers of tape replaced with 0/90 layer of aluminum wire woven carbon cloth
- 2 Outside 0 and 90 layers of tape replaced with 0/90 layer of nickel coated carbon cloth
- 3 Test fixture malfunction, no data.
- 4 Specimen crippled between grips and fixture.

